INFLUENCE OF HYDRODYNAMIC AND PHYSICO-CHEMICAL APPROACHES ON FOULING MITIGATION IN A MEMBRANE BIOREACTOR

by

Sher Jamal Khan

A dissertation submitted in partial fulfillment of the requirements for the degree of Doctor of Philosophy in Environmental Engineering and Management

Examination Committee:	Prof. C. Visvanathan (Chairperson) Dr. Preeda Parkpian Dr. Oleg V. Shipin Dr. Mukand S. Babel
External Examiner:	Prof. S. Vigneswaran Department of Environmental Engineering University of Technology Sydney (UTS) Sydney, Australia
Nationality:	Pakistani
Previous Degree:	Master of Science (Civil & Environmental Engineering) Portland State University (PSU) Oregon, USA Bachelor of Civil Engineering University of Engineering & Technology (UET) Taxila, Pakistan
Scholarship Donor:	Higher Education Commission (HEC), Pakistan-AIT Fellowship

Asian Institute of Technology
School of Environment, Resources and Development
Thailand
May 2008

Acknowledgements

First of all, the author would like to thank Allah, the most gracious, the most beneficent, for giving him the opportunity to achieve higher education at this level and giving him the courage and the patience during the course of his Ph.D. study at AIT.

The author would like to express his profound gratitude to his advisor Prof. C. Visvanathan for kindly giving valuable guidance, stimulating suggestions and ample encouragement during the study at AIT. The author is deeply indebted to Dr. Preeda Parkpian, Dr. Oleg V. Shipin and Dr. M.S. Babel for their valuable comments, suggestions and support and serving as members of the examination committee.

A special thank is addressed to Prof. S. Vigneswaran for kindly accepting to serve as the external examiner. His constructive and professional comments are highly appreciated.

A special note of appreciation is extended to Prof. R. Ben Aim from National Institute of Applied Science (INSA), Toulouse, France and Dr. V. Jegatheesan from James Cook University, Queensland, Australia for their help and great interest in this research including valuable comments and suggestions.

Sincere thanks are given to Prof. A.T.M Nurul Amin, Dr. Kwannate Sombatsompop, Ms. Lakhmini Halgahawaththa, Ms. Moreau Anne-Claire, Ms. Radha Adhikari, Mr. Bui Xuan Thanh, Ms. Alice Guo, Mr. Eric Thouvenot, Mr. Pradeep C. Munasinghe and Mr. Javed Anwar. The author would also like to thank all EEM staff, laboratory colleagues and technicians for their help, moral support and cooperation which contributed in various ways to the completion of this dissertation.

The author gratefully acknowledges Higher Education Commission (HEC) of Pakistan and AIT for the joint scholarship for the Ph.D. study at AIT. The author would also like to sincerely thank National University of Sciences and Technology (NUST), Pakistan for the financial assistance as part of the Faculty Development Program.

The author would like to dedicate this piece of work to his beloved grandmother who passed away during the course of this study. Her long lasting love and prayers always inspired and encouraged him to fulfill his desires.

Deepest and sincere gratitude goes to his beloved parents (Col. (R) Sher Afgan Khan and Mrs. Yasmin Sher Afgan) for their endless love, encouragement and prayers. The author wishes to express his deepest appreciation to his beloved wife (Mrs. Samina Jamal) and son (Sher Raza Khan) for their great support, patience and understanding throughout the entire period of this study.

Abstract

Membrane bioreactor (MBR), a combination of biological degradation by activated sludge and direct solid liquid separation by membrane filtration, is an attractive alternative to conventional activated sludge process (CASP) for the treatment and reuse of industrial and municipal wastewaters. Due to the higher operating costs involved in side-stream MBRs, submerged MBRs have become the preferred choice in MBR plant installations from the mid 1990s. However, the wide spread application of the submerged MBR process is constrained by membrane fouling and it is considered as the most serious problem affecting system performance. Therefore, most MBR researches aim to identify, investigate, control and model membrane fouling.

The aim of this research was to investigate hydrodynamic and physico-chemical approaches on fouling mitigation in a submerged MBR using hollow fiber membranes. Moreover, sludge characteristics and their contribution to membrane fouling under each set of mitigation approaches were examined. The thesis was structured in two parts, of which the first part focused on hydrodynamic approach and the second part on physico-chemical approach.

In the first part, the influence of shear intensity induced by mechanical mixing on activated sludge characteristics as well as membrane fouling propensity in MBRs was investigated. Four laboratory-scale MBRs were operated at different mechanical mixing conditions. The control reactor (MBR_0) was operated with aeration only supplemented by mechanical stirring at 150, 300 and 450 rpm in MBR_{150}, MBR_{300} and MBR_{450}, respectively. It was found that the MBR_{300} demonstrated prolong filtration cycle and low rate of membrane fouling. The fouling potential of the MBR_{300} mixed liquor was also low characterized by the specific cake resistance (α) and the normalized-capillary suction time (CST_N) depicting MBR_{300} condition as the optimum. Moreover, it was found that the mean particle size reduced with increase in the shear intensity. The bio-particles under high shear intensity were observed having low activity in terms of specific oxygen uptake rate (SOUR). Furthermore, the low SOUR of microbes demonstrated low biopolymer release during the biofilm simulation test due to the slow cell death rate. These results reveal that membrane fouling can be significantly mitigated by appropriate shear intensity induced by mechanical mixing condition in a MBR.

In the second part, the influence of hybrid MBRs with addition of Kaolin clay, NALCO® cationic polymer (MPE50) and powdered activated carbon (PAC) on the fouling propensity was investigated. Optimum initial dosages of clay, polymer and PAC to the MBR_{Clay}, $MBR_{Polymer}$ and MBR_{PAC}, respectively were determined using jar tests. The filtration performances and the biomass characteristics in the hybrid MBRs were compared to that in the conventional MBR ($MBR_{Control}$) from the first phase of the study. It was found that the MBR_{PAC} exhibited low fouling tendency and prolonged filtration as compared to that in the others MBRs. Improved filtration performance in MBR_{PAC} was attributed to the flocculation and adsorption phenomena. The effective flocculation of biomass by PAC was verified by the increase in mean particle size and narrow particle size distribution and the more or less rounded and firm flocs revealed by microscopic investigation. Moreover, the SOUR of microorganisms in the MBR_{PAC} was found to be lower than that in the other MBRs. The large bio-flocs with low SOUR due to PAC addition could have been the basis of improved filtration performance in the MBR_{PAC}.

Table of Contents

List of Tables

List of Figures

List of Abbreviations

ASP	Activated Sludge Process
A_m	Membrane Filtration Area
BSA	Bovine Serum Albumin
C_b	Bulk Concentration
CASP	Conventional Activated Sludge Process
COD	Chemical Oxygen Demand
CFMF	Cross Flow Microfiltration
CFV	Cross-Flow Velocity
CST	Capillary Suction Time
CST_N	Normalized Capillary Suction Time
DI	Deionized Water
DO	Dissolved Oxygen
DM	Dissolved Matter
d_p	Diameter of Particle
EPS	Extracellular Polymer Substances
eEPS	Extracted EPS
F_d	Drag Force
F_m	Lift Force
F/M	Food-to-Microorganism
G	Shear Intensity
HDO	High DO Reactor
HF	Hollow Fiber
HRT	Hydraulic Retention Time
ISM	Inner Skinned Membrane
J	Flux
J_c	Critical flux
LDO	Low DO Reactor
MBR	Membrane Bioreactor
MBR_0	MBR with aeration only
MBR_{150}	MBR supplement with mechanical stirring at 150 rpm
MBR_{300}	MBR supplement with mechanical stirring at 300 rpm
MBR_{450}	MBR supplement with mechanical stirring at 450 rpm
$MBR_{Control}$	Conventional MBR
MBR_{Clay}	Hybrid MBR with kaolin clay
$MBR_{Polymer}$	Hybrid MBR with cationic polymer
MBR_{PAC}	Hybrid MBR with PAC
MBBR	Moving Bed Biofilm Reactor
MC-MBBR	Membrane Coupled Moving Bed Biofilm Reactor
MF	Microfiltration
MFR	Membrane Fouling Reducer
MLSS	Mixed Liquor Suspended Solids
MLVSS	Mixed Liquor Volatile Suspended Solids
MPE50	Membrane Performance Enhancer
MW	Molecular Weight
MWCO	Molecular Weight Cut-Off
m_p	Mass of Deposited Particles
NF	Nanofiltration
NOM	Natural Organic Matter

OLR	Organic Loading Rate
OSM	Outer Skinned Membrane
OUR	Oxygen Uptake Rate
P_m	Mechanical Power
P_p	Pneumatic Power
P_T	Total Power
PAC	Powdered Activated Carbon
PSD	Particle Size Distribution
R_m	Intrinsic Membrane Resistance
R_c	Cake Resistance
R_{cp}	Concentration Polarization Layer Resistance
R_f	Fouling Resistance
R_t	Total Hydraulic Resistance
RO	Reverse Osmosis
SBR	Sequencing Batch Reactor
SCOD	Soluble Chemical Oxygen Demand
SMP	Soluble Microbial Product
SOUR	Specific Oxygen Uptake Rate
SRT	Solids Retention Time
SS	Suspended Solids
TMP	Trans-Membrane Pressure
dTMP/dt	Membrane Fouling Rate
TSS	Total Suspended Solids
t_{crit}	Critical Time
U	Recirculation Velocity
U_G	Aeration Velocity
UF	Ultrafiltration
V	Volume
VSS	Volatile Suspended Solids
α	Specific Cake Resistance
μ	Dynamic Viscosity
ε	Void Volume
ρ	Density
ΔP	Trans-Membrane Pressure (TMP)

Chapter 1

Introduction

1.1 Background

In biological wastewater treatment, conventional activated sludge process (CASP) is one of the most important and popular systems that has been used for domestic and industrial wastewater treatment. However, the CASP not only requires large aeration and sedimentation tanks, but also generates large quantities of excess sludge. In addition, the process suffers from solid-liquid separation problems, such as bulking and foaming. An alternative technology is the membrane bioreactor (MBR), a combination of biological degradation by activated sludge and direct solid liquid separation by membrane filtration. The concept is technically similar to that of a traditional wastewater treatment plant, except for the separation of activated sludge and treated wastewater. In a MBR installation, this separation is not done by sedimentation in a secondary clarification tank, but by filtration using microfiltration (MF) or ultrafiltration (UF) membrane technology. Compared with conventional wastewater treatment processes, MBRs offer several advantages including high biodegradation efficiency, excellent effluent quality, smaller sludge production and compactness. As a result, MBR offers an attractive option for the treatment and reuse of industrial and municipal wastewaters. Because of further technical developments and significant cost reductions, the interest in MBR technology for municipal as well as industrial wastewater treatment has sharply increased. Besides its current application in municipal and industrial wastewater treatment, potential application areas include nitrate removal in drinking water, removal of endocrine disrupting compounds from water and wastewater streams, enhancing biofuels production via membrane assisted fermentation and gas deliver or extraction.

The first generation MBRs introduced in the late 1960s combined the activated sludge bioreactor with external cross-flow membrane filtration loop known as side-stream MBRs. Due to the higher operating costs involved in side-stream MBRs (of the order 10 kWh/m^3 product), submerged MBRs introduced by Yamamoto in 1989 have become the preferred choice in MBR plant installations from the mid 1990s. Submerged MBRs consume much lower power than external side-stream MBRs (typically less than 1 kWh/m^3 product) due to absence of high-flow recirculation pump. External MBR are considered more suitable for the treatment of industrial wastewater characterized by high temperature, high organic strength, extreme pH, high toxicity and low filterability while submerged systems are utilized mostly for the treatment of municipal wastewater. The membrane configurations applied in submerged systems are mainly flat sheet (FS) and hollow fiber (HF) membranes. The main manufacturers of FS membranes are Kubota (Japan) and of HF are Zenon (Canada) and Mitsubishi-Rayon (Japan). Both these two types of membrane configurations have their advantages and disadvantages.

Currently, over 1000 MBRs are in operation world wide, with many more proposed or currently under construction. MBRs have proliferated in Japan, which has approximately 66% of the world's total installations. The remainder can be found mainly in North America or Europe (Roest et al., 2002). Over 98% of the systems couple the membrane separation with aerobic biological process rather than with an anaerobic bioreactor. Approximately 55% of the systems have the membranes submerged in the bioreactor while the remaining has the membranes external to the biological process (Stephenson et al.,

2000). A significant increase in MBR application is anticipated due to more stringent effluent regulations and water reuse initiatives.

However, the wide spread application of the MBR process is constrained by challenges including membrane fouling, pretreatment, membrane lifespan, cost and plant capacity. Membrane fouling in MBR is considered as a major limitation to faster commercialization of MBR technology and is considered as the most serious problem affecting system performance. Fouling results in permeate flux decline leading to more frequent membrane cleaning and necessary replacement consequently increasing operating costs. Therefore, most of the MBR studies aim to investigate causes, characteristics, mechanisms of fouling and methods to mitigate membrane fouling.

Membrane fouling is a complex phenomenon and it is affected by the membrane properties and configuration, wastewater quality and operating conditions. It can be due to cake layer formation on membrane surface, progressive pore blockage, or adsorption of soluble compounds on membrane surface, inside pores or interaction with other elements in suspension. The deposition of cake layer on the membrane surface, known as reversible fouling, is largely readily removable by applying various techniques. On the other hand, internal fouling caused by adsorption of dissolved matter and colloidal pore closure is considered irreversible and is of more serious concern in fouling control. The irreversible fouling is generally removed either by chemical cleaning or by aggregation or enmeshment using flocculation–coagulation agents.

Some of the techniques that have been attempted to control membrane fouling include: a) modification of membrane module design by optimizing the flat sheets or packing density of hollow fibers, b) controlling the filtration process below the critical flux by air-sparging and by operating in intermittent mode, c) improvement of the filtration characteristics of the mixed liquor by adding powdered activated carbon (PAC) and d) restoration of permeability by backwashing, by back-pulsing and/or by chemical cleaning (Yang et al., 2006). The specific design of airflow patterns and location of aerators are also considered as crucial parameters in fouling mitigation. Most of the studies on membrane fouling control have been conducted to reduce cake formation. More efficient fouling mitigation methods can be implemented only when the fouling mechanisms are fully understood.

However, the complexity and heterogeneity of membrane fouling is further enhanced by the phenomenon ‘biofouling’ which is the adhesion and growth of microorganisms on membrane surface resulting in biofilm formation. Although biofouling in MBR has been widely studied and characterized, it still remains a black box which requires further attention. In this context, the aim of the present study was to investigate the influence of hydrodynamic and physico-chemical approaches on fouling mitigation in submerged MBRs. Moreover, sludge characteristics and their contribution to membrane fouling were examined.

1.2 Objectives of Study

The main objectives of this research study were:

1. To investigate the influence of mechanical mixing rates in submerged hollow fiber MBRs on membrane filtration performance and sludge characteristics.

2. To determine optimum mechanical mixing condition based on filtration performance and sludge filterability characteristics.

3. To develop hybrid MBRs by the addition of kaolin clay, powdered activated carbon (PAC) and NALCO® polymer (MPE50) to MBR systems. Investigate the fouling propensity among the hybrid MBRs and compare with conventional MBR.

4. To analyze modified sludge characteristics in hybrid MBRs and determine the most suitable hybrid MBR system which achieves low fouling rates.

1.3 Scope of Study

The scope of study can be divided into two phases:

1) Mechanically mixed MBR phase;
2) Hybrid MBR phase

1) Mechanically mixed MBR Phase

- Synthetic wastewater was prepared in the laboratory and the seed sludge was taken from sequencing batch reactor (SBR) process of municipal wastewater treatment plant (Yannawa wastewater treatment plant, Bangkok, Thailand);
- Four laboratory scale MBRs were setup and operated at similar operating conditions such as airflow rate, organic loading rate (OLR) and sludge retention time (SRT) whereas the mechanical mixing rates were varied;
- MBRs were operated for long term to examine membrane fouling behaviors in terms of trans-membrane pressure (TMP) rise under constant flux operation;
- Sludge filterability was characterized by the specific cake resistance (α) and the normalized capillary suction time (CST_N) of the MBR samples;
- Optimum mixing intensity in MBR was determined based on enhanced membrane filtration performance and improved fouling rates.

2) Hybrid MBR Phase

- Three conventional MBRs were converted to hybrid MBRs by the addition of optimized dosages of kaolin clay, PAC and NALCO® Polymer;
- Optimum dosages for the flocculent/adsorbent agents were determined by jar tests;
- Long term filtration performances and sludge characteristics of the hybrid MBR systems were compared to that of the conventional MBR system;
- Optimum hybrid system was determined based on the sludge characteristics and the fouling tendencies.

Chapter 2

Literature Review

2.1 Membrane processes

Since 1960s, the interest in membrane processes in water and wastewater treatment has grown and since then are the object of substantial research, development and full scale applications. The recent increase in use of membranes in environmental engineering applications can be due to the increased potable and wastewater treatment regulations, increased demand for water requiring use of lower quality water resources and emphasis on wastewater reuse and recycling. Membrane processes appear to be well suited to satisfy the stringent drinking water requirements. New developments in membrane technology are continually resulting in improved performance and reduced costs. Figure 2.1 shows the trend of membrane cost over the past 15 years and there is a clear exponential decrease in the membrane cost which has enhanced its application world wide. Due to its greater application and use nowadays, the membrane cost tends to reduce even further.

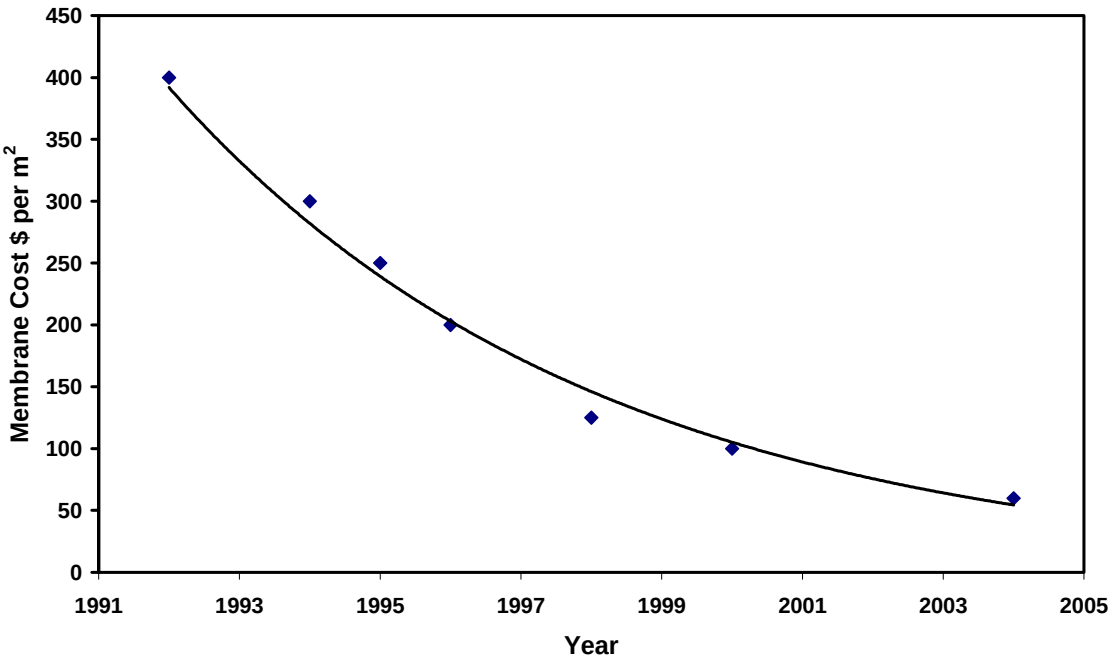

Figure 2.1: Reduction in membrane replacement cost per m^2 (Churchouse and Wildgoose, 1999)

Based on the advantages offered by membrane processes, they are able to achieve separation for certain types of materials which have been difficult and expensive to separate in the past such as:

- Dispersive colloids and fine particles, especially those which are compressible, have density close to that of liquid phase, have high viscosity or are gelatinous;
- Biological materials in the range of colloidal size and sensitive to their physical and chemical environment;
- Low molecular weight, non-volatile organics and dissolved salts.

2.1.1 Membrane

A membrane can be defined as a thin film that is capable of separating materials as a function of their physical and chemical properties when a driving force is applied across it. A good membrane should have high porosity and should sustain mechanical, chemical and thermal stability. Operating conditions such as temperature, pressure, pH, and chemical compatibility should be considered for the selection of a membrane type.

Membranes can be classified according to different view points. Classification can be based according to the following:

- Membrane material (polymeric, ceramic, metallic);
- Membrane structure (porous, dense);
- Membrane thickness (thick, thin);
- Membrane texture (symmetrical, asymmetrical, composite);
- Separation mechanism (sieve, diffusion, evaporation, ion exchange);
- Driving force (pressure, activity, electric potential);
- Phases in contact (liquid-liquid, liquid-gas);
- Type of pressure driven membranes ((MF, UF, NF, RO).

A membrane of reasonable mechanical strength and one that can maintain a high throughput of a desired permeate with high degree of selectivity depends on the combination of membrane properties considered based on the classification mentioned above.

2.1.2 Membrane operation

A membrane process can be defined as an operation where a feed stream is divided into two streams: a permeate, containing material which has passed through the membrane, and a retentate, containing the non-permeating species, as shown in Figure 2.2.

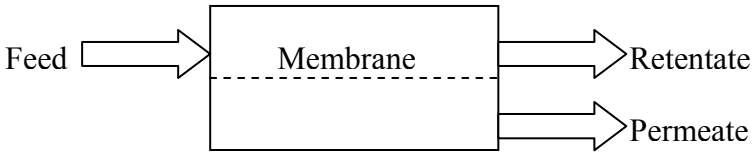

Figure 2.2: Principle of membrane operation

In the operation of a membrane process, the feed solution is pumped through the module and a valve is used to control the pressure of retentate. The permeate is withdrawn at atmospheric pressure. During operation, the constituents in the feed stream accumulate on the membrane. This deposition on the membrane is termed as fouling. Due to membrane fouling, the pressure builds up on the feed side and flux through the membrane starts to decrease. Membrane fouling is important in the design and operation of membrane systems as it affects pretreatment needs, cleaning requirements, operating conditions, cost, and performance. When the performance of membrane deteriorates to a given level, the membrane modules are back washed and/or chemically cleaned. Membrane fouling will be discussed in detail later on in this review.

According to AWWARF et al. (1996), the main membrane processes in water and wastewater treatment are categorized into three parts:

- Pressure-driven membrane operations
- Permeation operations
- Dialysis operations

The pressure driven membrane operations are the most frequently used. These are membrane operations in which the driving force is a pressure difference across the membrane which include the following:

- Microfiltration (MF)
- Ultrafiltration (UF)
- Nanofiltration (NF)
- Reverse Osmosis (RO)

Table 2.1: Comparison of various pressure driven membrane processes

	Microfiltration (MF)	Ultrafiltration (UF)	Nanofiltration (NF)/ Reverse Osmosis (RO)
Membrane	Symmetric/ Asymmetric porous	Asymmetric porous	Asymmetric/ composite dense
Pore size	Macropores (0.05-10 μm)	Mesopores (2-50 nm)	Micropores (<2 nm)
Applied Pressure	Low (<2 bar)	Low (1-10 bar)	High (10-60 bar)
Separation principle	Sieving mechanism	Sieving mechanism	Solution-diffusion
Application	Removal of particles including bacteria, yeasts etc.	Removal of colloids including virus, proteins etc.	Removal of low MW solutes including aqueous salts, metal ions, sugar etc.

Source: Modified from Mulder (1996)

Table 2.1 presents the comparison of various pressure driven membrane processes. Microfiltration (MF) and ultrafiltration (UF) processes achieve separation by sieving. UF is able to remove colloidal and dissolved species and their ability to reject material is defined by the molecular weight cut-off (MWCO) in daltons of the solute. On the other hand, MF is capable of removing suspended solids to about 0.05μm in size. Nanofiltration (NF) and reverse osmosis (RO) processes are able to separate ions from water. NF, also called low-pressure reverse osmosis, is effective to reject multivalent ions (Ca^{+}, Mg^{+}) and allow water to pass through as compared to monovalent ions (Na^{+}, Cl^{-}) rejected in RO or hyperfiltration.

MF and UF membranes are most commonly made of polymeric materials such as polyamide, polysulphone, cellular-acetate, polycarbonate and other advanced polymers. However recent developments of inorganic membranes composed of materials such as ceramic, aluminium-oxide or silca-glass show higher temperature stability, increased resistance to fouling and narrower pore size distribution as compared to polymeric types. These advantages can balance out by their high capital cost.

2.1.3 Membrane module configurations

The single operational unit into which membranes are packed is called a module. The optimum configuration for a module is one having the following characteristics:

- Maximum packing density i.e. provides maximum exchange surface per unit volume;
- Avoids leakage between the feed and the permeate compartments;
- High degree of turbulence on the feed side for mass transfer promotion i.e. sufficient circulation of the fluid to be treated or air bubbling near membrane surface in order to limit the phenomenon of membrane fouling;
- Low cost per unit membrane area;
- Low energy expenditure per product volume of water or wastewater;
- Ease of cleaning and maintenance;
- Ease of operation;
- Possibility of membrane replacement.

There are five principal modules currently employed in membrane processes: 1) Pleated cartridge; 2) Plate-and-frame; 3) Spiral-wound; 4) Tubular; 5) Hollow fiber. At present, hollow fiber and plate and frame are the most popular and extensively used modules in membrane bioreactor (MBR) processes. A general overview of the module configurations is presented in Table 2.2.

Table 2.2: Membrane configurations

Configuration	Packing density (m^2/m^3)	Cost	Replacement	Advantages	Disadvantages	Applications
Pleated cartridge	800-1000	Low	Cartridge	Robust and compact	Easily fouled, cannot be cleaned, disposal unit	Dead-end MF
Plate-and-frame	400-600	High	Sheet	Dismantled for cleaning	Complicated design, cannot be backflushed	ED, UF, RO
Spiral-wound	800-1000	Low	Element	Low energy cost, robust and compact	Not easily cleaned-cannot be backflushed	RO, UF
Tubular	20-30	Very high	Tubes	Easy mechanical cleaning and tolerates high TSS levels	High capital and replacement cost	Cross-flow MF
Hollow fiber	5000-40000	Very low	Bundle	Compact, backflushed cleaning and tolerates high colloidal levels	Sensitive to pressure shocks	MF, UF, RO

Source: Modified from Stephenson et al., 2000

2.1.4 Membrane operational modes

In general, there are two modes of membrane operations: (a) Dead end filtration; (b) Cross flow filtration.

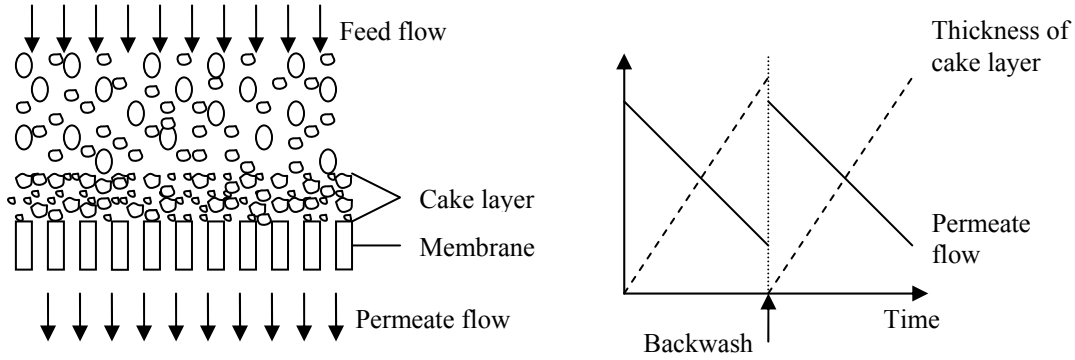

Figure 2.3: Dead-end Filtration

In dead end filtration or direct filtration, the flow direction is perpendicular to the filter medium as shown in Figure 2.3. The retained material or retentate builds up a layer on the membrane surface known as cake formation. With the passage of time, the thickness of the cake layer increases and consequently the flux through the membrane decreases at constant trans-membrane pressure (TMP). Similarly, the TMP increases with increase in cake layer thickness at constant flux operation. Thus, depending on the nature and thickness of cake layer, the filtration process must be interrupted to clean the membrane. The other option is to replace the membrane with a new one. Such operation is normally restricted to either low solids water or cyclic operation with frequent backwashing.

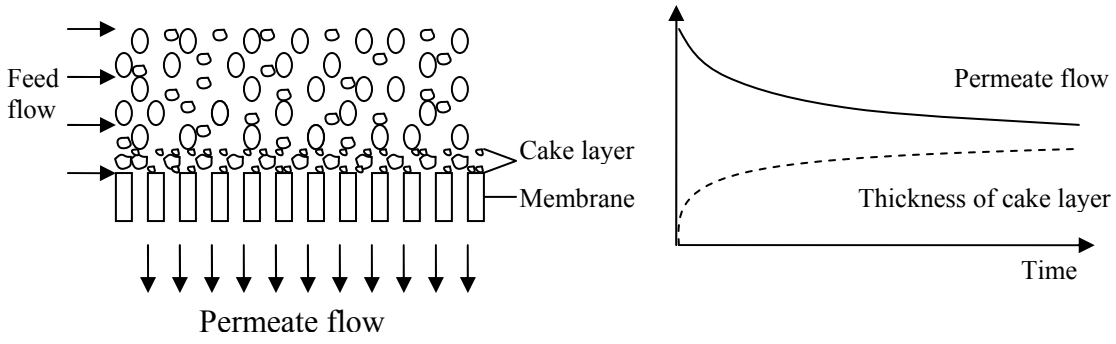

Figure 2.4: Cross-flow Filtration

In cross flow filtration, the flow direction is parallel to the membrane surface as shown in Figure 2.4. In microfiltration, when the feed is perpendicular to permeate flow direction, the process is called cross-flow microfiltration (CFMF). Cross flow generates turbulence near the filter medium and expedites the removal of accumulated materials from the membrane surface, opposing cake layer formation. The permeate flow decreases in the initial phase due to unavoidable fouling and achieves steady state in the equilibrium phase. At steady state, the cake layer thickness becomes constant which enables consistent operation of the membrane system.

2.2 Membrane bioreactor (MBR)

Membrane bioreactor (MBR), an innovative technology, is a combination of activated sludge and membrane separation processes into a single process where suspended solids and microorganisms are separated from the treated water by membrane filtration. The entire biomass is confined within the system, providing both perfect control of the sludge age for the microorganisms in the reactor and the disinfection of the influent.

The optimum design of MBR process is very complex since it is dependent on many factors including feed characteristics, mixed liquor suspended solids (MLSS) concentration, sludge retention time (SRT), hydraulic retention time (HRT), operational flux, membrane material cost, energy consumption, and sludge treatment and disposal and their interrelation (Stephenson et al., 2000). Some of the advantages and disadvantages of aerobic MBR process are discussed here.

2.2.1 Advantages and disadvantages of MBR process

Advantages

MBR technology is becoming more attractive due to its advantages that include superior effluent quality, absolute control of hydraulic and solids retention times, smaller volume and foot print, and reduced sludge production and better process reliability (Visvanathan et al., 2000).

i) Biomass separation

In a conventional secondary clarifier only the fraction of the activated sludge that settles as flocs can be retained. In an MBR, all components of the biomass including bacteria and viruses that are larger than membrane cutoff are retained. As a result, the separation of biomass from treated wastewater is independent of biomass sedimentation qualities. Organic removal is often greater than 95% even with relatively short HRTs. Consequently the system is easy to operate and maintain. The superior effluent quality from MBR process enables the direct discharge into the surface water bodies and reuse of effluent for cooling, toilet flushing, lawn watering or with further treatment, as process water (Visvanathan et al., 2000).

ii) Independence of SRT and HRT

SRT and HRT being completely independent of each other, allow MBRs to be operated at HRTs and SRTs without washout of biomass common in activated sludge process. Sludge age is particularly important to allow the development of slow-growing microorganism such as methanogenic or nitrifying bacteria. The membrane avoids problem of filamentous sludge growth and degassing sludges, enabling optimal control of residence time of the microorganisms (Stephenson et al., 2000).

iii) High MLSS concentration

High MLSS concentration and low F/M ratio, due to long SRT, results in systems that can be very compact. Space saving is also achieved because there is no need for final clarifiers or post-treatment devices. The combination of high biomass concentrations and the

complete retention of solids allow the MBR process to be operated at higher organic loading rate (OLR) as compared to conventional activated sludge process. The high MLSS also reduces excess sludge production and consequently reduces cost of treatment and disposal.

iv) Small floc size

The floc size in MBR sludge is very much smaller than 100 μm and the floc size distribution is concentrated within a small range. In contrast, the floc size from conventional activated sludge processes varies from 0.5 to 1000 μm (Visvanathan et al., 2000). Zhang et al. (1997) compared four MBRs with four conventional activated sludge processes and found that the size distribution of flocs were smaller in the MBRs i.e. 7-40 μm as compared with 70-300 μm in activated sludge. Ng and Hermanowicz (2005) found that the smaller flocs in MBR could stimulate higher microbial activity in the system because of greater microorganism exposure to substrate concentration and most probably contributes to better organic removal.

Disadvantages

Disadvantages of MBRs include high capital and operating costs, limited experience in membrane use, membrane fouling limiting the maximum flux obtainable, high biomass concentrations result in aeration problems and potential high cost of periodic membrane chemical cleaning and replacement. The current effluent standards can be achieved with conventional treatment processes, therefore limiting the wide spread use of MBR. Membrane component costs are approximately proportional to plant size which imposes a limit to the maximum size of an economically viable MBR plant.

2.2.2 Types of MBRs

Membrane applications for wastewater treatment have led to the development of three membrane bioreactors (Stephenson et al., 2000) that include:

i) Biomass separation membrane bioreactors;
ii) Membrane aeration bioreactors;
iii) Extractive membrane bioreactors.

Biomass separation MBRs, simply known as MBRs, are the most widely studied and have been applied extensively at full scale while aeration bioreactors and extractive membrane bioreactors have only been operated up to pilot scale.

2.2.3 MBR configurations

Biomass separation MBR employs MF or UF modules for biomass retention. The membrane module can either be placed in external circuit to the bioreactor or submerged into the bioreactor as shown in Figure 2.5 (a) and (b), respectively.

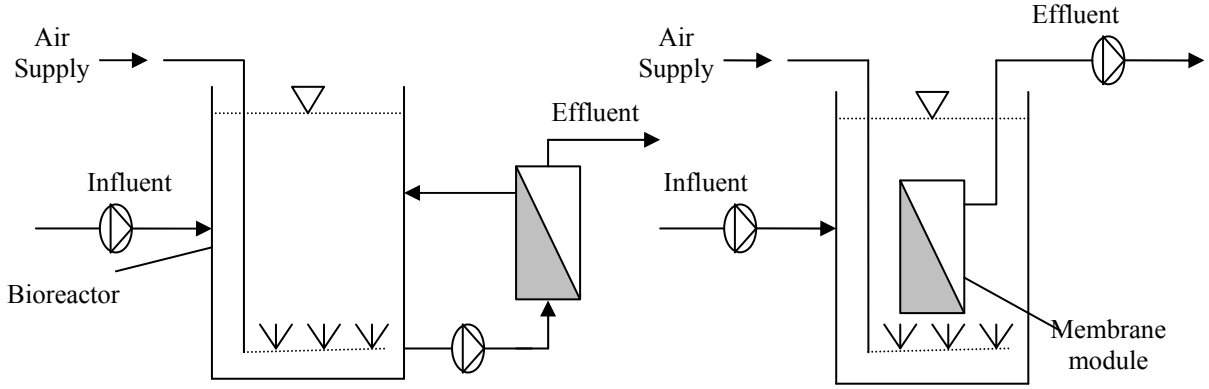

(a) Membrane in external circuit (b) Submerged membrane

Figure 2.5: Biomass separation MBR (a) Membrane in external circuit and (b) Submerged membrane

The membranes used in biomass separation MBRs are asymmetric with a dense top layer or skin of 0.1 to 0.5 μm thickness and a supporting thick sub-layer (Visvanathan et al., 2000). The skin can be placed either on the outside of the membrane called outer skinned membrane (OSM) or inside the membrane called inner skinned membrane (ISM) (AWWARF et al., 1996). This top layer eventually defines the characteristics of membrane separation.

Membrane in external circuit system, also known as recirculated MBR, is independent of the bioreactor. It can be operated with either outer or inner skinned membranes. In this system, the feed enters the bioreactor where it contacts biomass. This mixture is then pumped around a recirculation loop containing the membrane module where the permeate is discharged and the retentate is returned to the bioreactor. The TMP and the cross-flow velocity for membrane operation are both generated from a pump.

Submerged membrane system, also known as integrated MBR, requires outer skinned membranes and is independent of recirculation loop as the separation occurs within the bioreactor itself. In this system, the pressure across the membrane can only be applied by suction through the membrane or by TMP derived from the hydraulic head of the water above the membrane. Therefore the power requirement for operation is generally lower than the membrane in external circuit system which requires cross-flow membrane filtration. Fouling control is achieved by scouring of the membrane surface with aeration. The movement of bubbles close to the membrane surface generates the necessary liquid shear intensity. The comparison of key features in side-stream and submerged MBR configurations are summarized in Table 2.3.

Table 2.3: Comparison of sidestream and submerged MBR configurations

Sidestream	Submerged
Long history (since 1970)	Recent development (since 1990)
Membrane placed external to bioreactor	Membrane placed in bioreactor
Pumped systems with permeation rate determined by TMP and cross-flow	Permeate removed under hydrostatic head, with or without permeate suction, at rate partly determined by aeration
Higher flux and hydraulic resistance; lower aeration and membrane area requirement	Lower flux and hydraulic resistance; greater aeration and membrane area requirements
Stabilized flux with periodic chemical cleaning	Stabilized flux with periodic chemical cleaning for flat plate membrane configuration; short backwash cycle with periodic chemical cleaning for hollow fiber configuration
Greater overall energy demand; greater hydrodynamic control	Low overall energy demand; reduced hydrodynamic control

Source: Judd (2004)

Sidestream membrane configuration has been employed at full scale domestic and industrial wastewater treatment plants worldwide. Since early 1990s, the submerged membrane configuration due to its lower energy demand has emerged as a more suitable option to serve small populations. Judd et al. (2001) found that the energy demand for a submerged system permeate product was twice as energy efficient (2 kWh/m^3) as the side-stream system (3.9 kWh/m^3). Its application from lab scale to full scale setup has progressed very rapidly due to the demand for decentralized treatment and high energy efficient units. Kubota (flat sheet) and Zenon (hollow fiber) are both commercially available submerged systems and the most significant manufacturers in terms of growth and total installed area. Table 2.4 presents the difference in energy consumption and other operational parameters for the two MBR configurations.

Table 2.4: Membrane configuration, operating parameters and energy consumption for MBR systems

Process	Submerged				Side-stream			
Membrane[a]	P&F	P&F	HF	HF	T	T	HF	HF
Material[b]	PS	PE	PE	PE	PS	C	C	PS
Pore size (μm)/ MWCO (KDa)	0.4	0.4	0.1	0.1	50	300	0.1	0.1
Surface area (m^2)	0.24	0.96	2	4	2.6	0.08	1.1	0.39
TMP (bar)	0.1	0.3	0.13	0.15	5	2	2	2.75
Permeate flux (L/m^2/h)	7.9	20.8	8	12	170	175	77	8.3
Crossflow velocity (m/sec)	0.5	0.3-0.5	-	-	1-2	3	1.5-3.5	-
Energy, permeate (kWh/m^3)	-	0.013	0.005	0.23	0.17	9.9	32	0.045
Energy, aeration (kWh/m^3)	4.0	0.009	0.140	70.00	0.52	2.8	9.1	10
Total energy consumption,(kWh/m^3)	4.0	0.022	0.145	70.23	0.69	12.7	41.1	10.045

[a] P&F, plate and frame; HF, hollow fiber; T, tubular
[b] PS, polysulphone; PE, polyethylene; C, ceramic
Source: Gander et al. (2000)

Energy consumption arises from power requirements for pumping feed water, recycling retentate, permeate suction and aeration. According to Table 2.4, there is a substantial difference between energy consumption of the two MBR operating systems. For example, submerged systems do not require retentate recycle and some do not require permeate suction (operated under hydraulic head). Aeration is utilized in significantly different ways for the two MBR configurations. In the side-stream configuration, aeration is supplied to the bioreactor by fine bubble aerators which are highly efficient for supplying oxygen to the biomass. On the other hand, course bubble aeration is used in submerged systems generating the cross-flow as well as scouring the membrane and providing oxygen to the biomass. Coarse bubble aerators are less efficient than fine bubble aerators for supplying oxygen to the biomass but have the advantage of lower cost. It is due this low cost of aeration and low pumping costs that the total energy consumption tends to be lower in submerged as compared to side-stream systems. In some operations, coarse and fine bubble aerators are used in combination (Le-Clech et al., 2003a; Germain et al., 2005).

2.2.4 MBR performance

The membrane performance in a MBR system is characterized by the rejection, normally expressed as removal efficiency, of the respective concentrations of the target contaminants in the feed and by the permeability i.e., flux per unit pressure. Removal of particles, including biological and non-biological colloids and macromolecules, is achieved by sieving and adsorption. One of the main advantages of MF and UF membranes is the significant ability to disinfect, by rejection of both bacteria and viruses, resulting in an effluent free from pathogenic microorganisms. The rejection is further improved with time due to the build up of the dynamic membrane.

It has been reported that the membrane in an MBR contributes approximately 30% to the removal of organic matter, mostly insoluble fraction with soluble fraction being removed via active biomass (Urbain et al, 1997 cited in Gander et. al., 2000). Organic loading rates are restricted by the permeate flux but are generally higher than conventional activated sludge process (ASP). It has been shown that nitrification is greater in MBR as compared to ASP due to the longer retention times of nitrifying bacteria at high SRT and low F/M ratio.

Cicek et al. (1999) cited in Stephenson et al. (2000) compared the performance of an ASP with a side-stream MBR at SRTs of 20 and 30 days, respectively. On the contrary, Ng and Hermanowicz (2005) compared submerged MBR with ASP system at short SRTs. Both these studies were carried out for synthetic sewage and the performance results are presented in Table 2.5.

Table 2.5: Performance comparison between ASP and MBR

Process	SRT (d)	HRT (h)	COD Removal (%)	TSS Removal (%)	Ammonia N Removal (%)	Reference
Side-stream MBR	30	-	99	99.9	99.2	Stephenson et al. (2000)
Submerged MBR	0.25	3	97.3	99.9	40.9	Ng and Hermanowicz, (2005)
	0.5	3	97.5	99.9	44.6	
	2.5	3	98.4	99.9	40.9	
	5	6	98.2	99.9	99.9	
ASP	20	-	94.5	60.9	98.9	Stephenson et al. (2000)
ASP	0.25	3	77.5	75.7	41.1	Ng and Hermanowicz, (2005)
	0.5	3	78.7	76.0	34.4	
	2.5	6	83.0	81.7	34.4	
	5	6	93.8	94.7	99.5	

According to Table 2.5, at similar operational conditions, organic removal efficiency of MBR is higher than ASP with almost complete retention of suspended solids. However, removal efficiencies were observed to be lower at short SRTs for both systems. At extremely short SRT of 0.25 d, the MBR maintained high COD removal while that of ASP deteriorated. Nevertheless, nitrification was a concern at SRT less than 2.5 d. Moreover, high biomass production from sludge wasting may allow more biogas production for energy recovery, and potentially more carbon dioxide extraction for commercial benefit.

2.3 Membrane fouling in MBR

The flux of clean water across a membrane without materials deposition on its surface or within its pores is described by Darcy's law:

$$J = \frac{\Delta P}{\mu R_m} \qquad \text{Equation 2.1}$$

where ΔP is the trans-membrane pressure (TMP), μ is the absolute viscosity of permeate water and R_m is the hydraulic resistance of clean membrane.

The clean water flux should increase proportionally with increase in TMP. However, the presence of dissolved and colloidal materials in water can produce deviations from linear behavior of permeate flux versus TMP due to the accumulation of materials on the membrane. Materials accumulation near, on and within the membrane resulting in flux reduction with time is referred to as 'membrane fouling'. Membrane fouling in MBRs may be physical, inorganic, organic or biological. Physical fouling refers to the plugging of membrane pores by colloids also known as colloidal pore clogging. Inorganic and organic fouling usually refers to scaling and macromolecular compounds adsorption, respectively.

Membrane fouling in MBRs is attributed to the physico-chemical interactions between the activated sludge and the membrane. Deposition of cake layer on membrane surface is largely readily removable by employing physical washing and is known as reversible

fouling. On the contrary, internal fouling caused by the adsorption of solutes and colloids on membrane surface and inside pores (pore narrowing) is considered irreversible and is generally removed by chemical cleaning or a combination of physical/chemical cleaning protocol. Fouling by adsorption may be partially reversible depending on the strength of adhesion and cleaning protocol. Both reversible and irreversible permeate flux declines or TMP rises are known as fouling and the materials responsible are known as foulants. A loss in permeate that is truly irreversible, usually requiring replacement of the membrane is termed as 'membrane poisoning'.

The simplest theoretical model that describes the membrane fouling phenomena is the resistance in series model:

$$J = \frac{\Delta P}{\mu R_t} \qquad \text{Equation 2.2}$$

$$R_t = R_m + R_c + R_f \qquad \text{Equation 2.3}$$

where R_t is the total hydraulic resistance, R_c is the reversible cake resistance caused by the cake layer deposited over the membrane surface and R_f is the irreversible fouling resistance caused by adsorption of dissolved matter and/or colloidal pore blockage within the membrane.

In most water and wastewater treatment, concentration polarization layer resistance, R_{cp} contributes negligible resistance to permeate flux; i.e., $R_{cp} << R_c$ and therefore, may be neglected. Nonetheless, concentration polarization plays an important role in the formation of cake and gel layers. Gel layer formation over a membrane surface is most often irreversible although seems like in the form of reversible cake layer.

2.3.1 Gel Polarization

Investigators (Blatt et al., 1970; Porter, 1972 cited in Bowen and Jenner, 1995) found that, for flux versus applied pressure of macromolecular solution and colloidal dispersion, the steady state flux reaches a limiting value where further increase in applied pressure results in minimal increase in permeate flux, known as limiting flux. This flux plateau behavior was explained by gel polarization phenomenon. According to this phenomenon, the concentration at the membrane surface increases as the macro-solutes reaches its solubility limit and precipitates on the membrane surface to form solid gels. While for colloids, the gel layer resembles a layer of closely packed spheres.

2.3.2 Cake Formation

According to cake filtration theory, the cake resistance is expressed as (Bowen and Jenner, 1995):

$$R_c = \alpha \frac{m_p}{A_m} \qquad \text{Equation 2.4}$$

where m_p is the mass of deposited particles, A_m is the membrane filtration area and α is the specific cake resistance, which can be approximately related to the properties for spherical particles by Carmen Kozeny relationship:

$$\alpha = \frac{180(1-\varepsilon_c)}{\rho.d_p^2.\varepsilon_c^3} \qquad \text{Equation 2.5}$$

where ε is the void volume of the cake layer and d_p is the mean diameter of the particles.

This relationship implies that smaller the particles, greater the specific cake resistance (α). According to Bowen and Jenner (1995), for dead-end unstirred filtration under constant pressure conditions and without any particle back transport, R_c increases with time because:

$$m_p \cong V.C_b \qquad \text{Equation 2.6}$$

Substituting this relationship in Equation 2.4 implies that:

$$R_c = \frac{\alpha.V.C_b}{A_m} \qquad \text{Equation 2.7}$$

where V is the total volume filtered and C_b is the bulk concentration.

The combination of Equation 2.2, 2.3 (excluding R_f fraction) and 2.7 with $J = A_m^{-1}$ dV/dt gives by integration the constant pressure filtration equation:

$$\frac{t}{V} = \frac{\mu R_m}{A_m|\Delta P|} + \frac{\mu.\alpha.C_b}{2A_m^2|\Delta P|}V \qquad \text{Equation 2.8}$$

Equation 2.8 yields a straight line on plotting experimental data of t/V versus t which allows determination of the specific cake resistance (α) and the membrane resistance R_m. Cake layer begins to form on the membrane surface, when the rate of convective transport of the material to the membrane is greater than the back transport, increasing the particle concentration on the membrane. Under cross-flow mode operation, permeate flux decreases until transport of particles to the cake layer is balanced by particle transport from the cake and permeate flux attains an approximately constant value.

2.3.3 Macromolecule Adsorptive Fouling

Adsorption of humic acids and other naturally occurring organic materials (NOMs) on membrane can have a much greater effect on permeate flux than pore clogging due to clays or other inorganic colloids, even at lower concentration (Lahoussine-Turcaud et al., 1990 cited in AWWARF et al., 1996). The characteristics of organic materials that determine their relative tendency to foul membranes include membrane affinity, molecular weight, functionality and confrontation. Hydrophobic interactions may increase the accumulation of NOMs on membranes, leading to more adsorptive fouling. Grozes et al. (1993) cited in AWWARF et al. (1996) investigated permeate flux decline due to the adsorption of tannic acid (MW 700) and dextran (MW 10,400) on different UF membranes. It was found that

dextran solution had little effect on permeate flux of a 100,000-MWCO membrane while tannic acid solution having lower MW produced significant fouling of the membrane. Dextran adsorption was found to be ten times lower than that for tannic acid.

Ognier et al. (2002) investigated adsorptive fouling during filtration of a MBR mixed liquor suspensions in a Sartorius filtration module using plane organic membrane. It was found that the initial fouling, before cake build-up, was irreversible mainly due to adsorption of soluble fraction of the suspension and is independent of the filtration time and the hydrodynamic conditions. Moreover, the irreversible adsorptive fouling was insignificant in comparison with the total resistance and the major part of the resistance in frontal filtration mode was the reversible part that could be removed by back-flushing. The specific cake resistance of 3×10^{15} m/kg, obtained for the raw suspension, was ten times higher than the values observed for protein solution, indicating the heterogeneous composition of activated sludge in terms of dissolved material. Experimental results for the sludge supernatant showed that the value of the slope of t/V versus t (2.76×10^{12} s/m^6) was similar to that obtained for 1 g/L protein solution (2.4×10^{12} s/m^6) although, the protein concentration was far lower in the supernatant. This confirmed the presence of macromolecular compounds other than proteins in the soluble part of the activated sludge.

2.4 Membrane fouling factors in MBR

All the parameters involved in the design and operation of a MBR system influence the fouling behavior. Three main categories of fouling factors are defined which include:

a. Feed and biomass characteristics
b. Operating conditions
c. Membrane and module characteristics

The three categories and the parameters that fall within each category are illustrated in Figure 2.6.

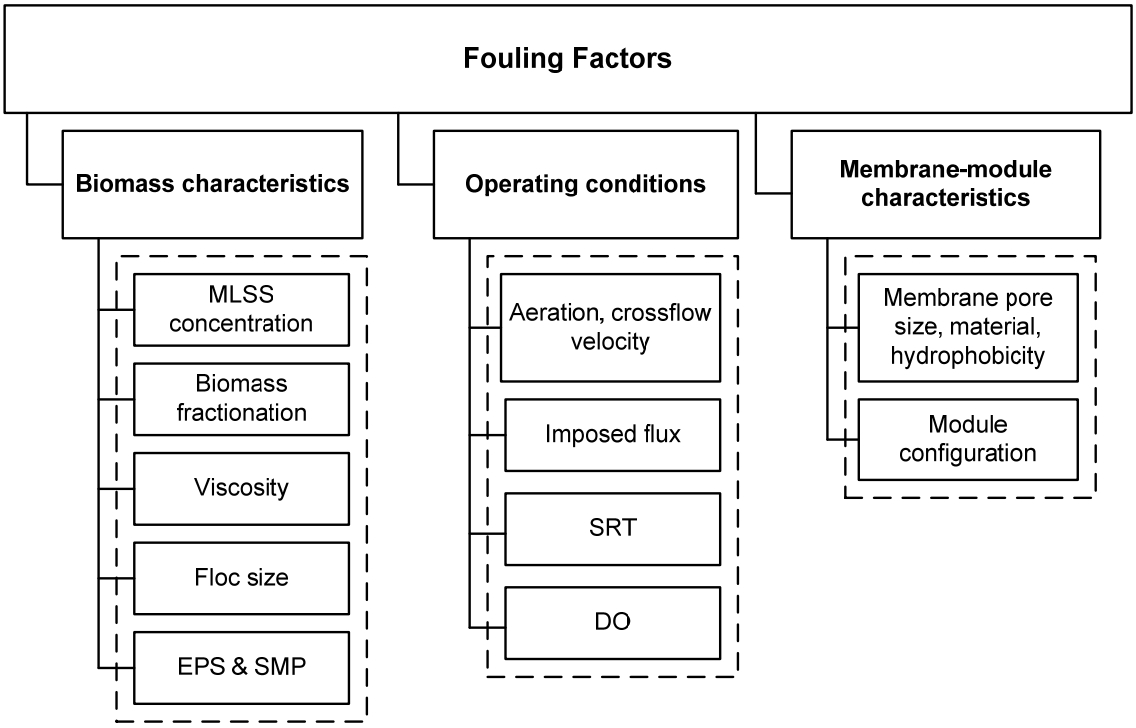

Figure 2.6: Membrane fouling factors in MBR (adapted from Zhang et al., 2006; Le-Clech et al., 2006)

These fouling factors may act independently or in combination to influence membrane filtration cycle and fouling propensity. As membrane fouling is a complex phenomenon it is difficult to single out one major contributor. The fouling parameters within the categories of biomass characteristics and operating conditions that are pertinent to this study are discussed in detail in the following sections.

2.4.1 Biomass characteristics

Activated sludge is a complex and heterogeneous suspension containing both feed components and metabolites produced during the biological reactions as well as biomass itself. Biofouling behavior in MBR depends on the structure of the biofouling layer formed on the membrane surface during filtration period. The two terms commonly encountered in literature representing biofouling layer are "cake layer" and "biofilm". The term "cake layer" is defined as layer comprised of rejected particulate and soluble biomass materials accumulated on the retentate side of a membrane surface while the other term "biofilm" can be broadly defined as microbial communities associated with a membrane surface encased in an extra-polymeric substance (EPS) matrix. The biofilm communities, although consisting of rejected microbial flocs, are active to secrete EPS. To represent the biofouling layer in MBR under the context of both cake layer and biofilm notions, an appropriate term "biocake" was recently introduced which could represent both rejected material and growing microorganisms on the membrane surface in a MBR (Lee et al., 2007a).

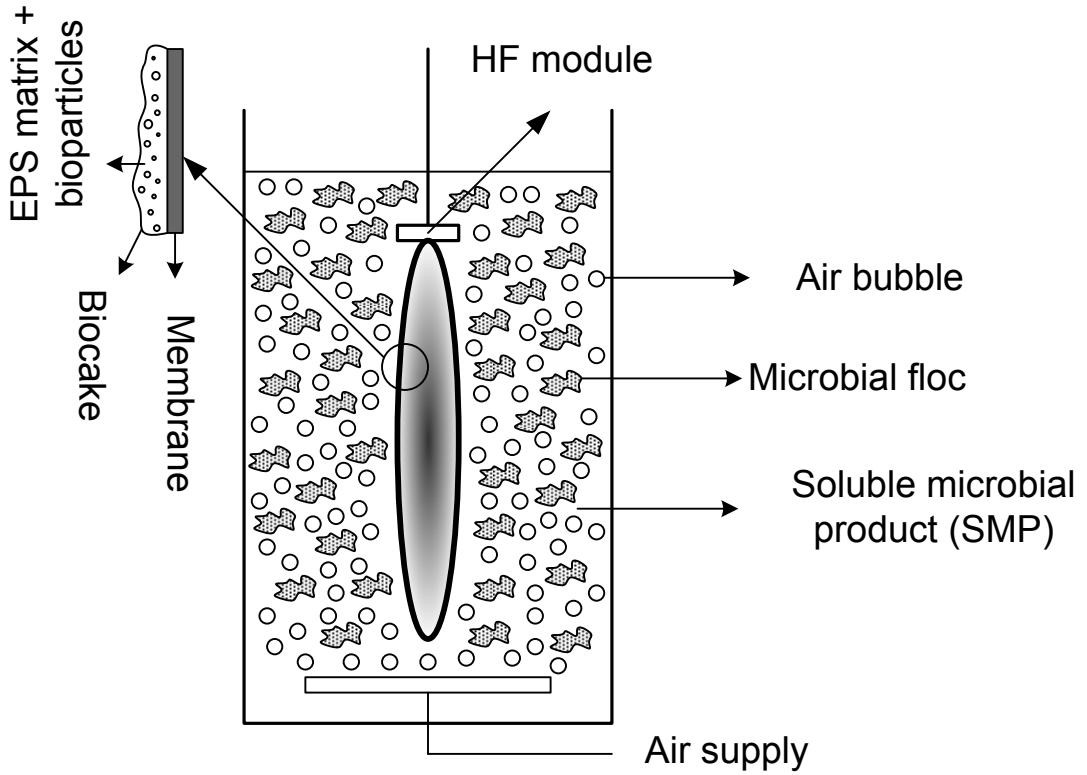

Figure 2.7: Biofouling concept in MBR

The factors effecting biocake permeability include the biofloc morphology and activity, EPS within the biofloc periphery (eEPS) and soluble microbial product (SMP) in the suspension as shown in Figure 2.7.

2.4.1.1 MLSS concentration

According to cake filtration theory, MLSS (bulk concentration, C_b) is considered to directly impact the cake layer resistance. Yamamoto et al. (1989) found that for a submerged MBR, a sharp decrease in flux was observed when MLSS concentration reached 19,200 mg/L. However, considerable decrease in flux was observed even at low MLSS of 5,200 mg/L. The reduction in permeate flux observed due to increase in MLSS concentration is contributed to the heterogeneous nature of MLSS composition including microbial flocs, colloids and solutes. The colloidal and solute fraction in activated sludge is mostly attributed to the EPS produced during the biological process and reported as key membrane foulants in MBR.

When a membrane is first placed into service, pores can be blocked partially or completely by the retained particles because of a direct contact of the particles with the membrane pore surface as shown in Figure 2.8 (a). Therefore, generally a slight decrease in membrane permeability occurs at the very beginning of the filtration operation before cake formation. This initial fouling known as 'membrane conditioning' induces irreversible resistance and can be caused due to solute adsorption and colloidal pore blockage (Zhang et al., 2006). Recent studies have revealed that the initial fouling phenomenon is of prime importance in determining membrane performance.

The biomass cake layer may itself remove smaller particles as it compacts over time as shown in Figure 2.8 (b). The cake or gel layer essentially acts as a second membrane through which permeate must pass. Lee et al. (2001), for an attached and suspended growth MBRs, found that MLSS of 3,000 mg/L in suspended growth MBR could form a dynamic membrane on the membrane surface resulting in better filtration performance as compared to that in attached growth MBR with only 100 mg/L of MLSS in suspension. The increase in rate of the TMP for attached growth was 7 times higher than that for the suspended growth system. Small particles like soluble organics can rapidly deteriorate the permeability of membrane by directly adsorbing onto the surface or inside the membrane pores without such dynamic membrane or layer interruption.

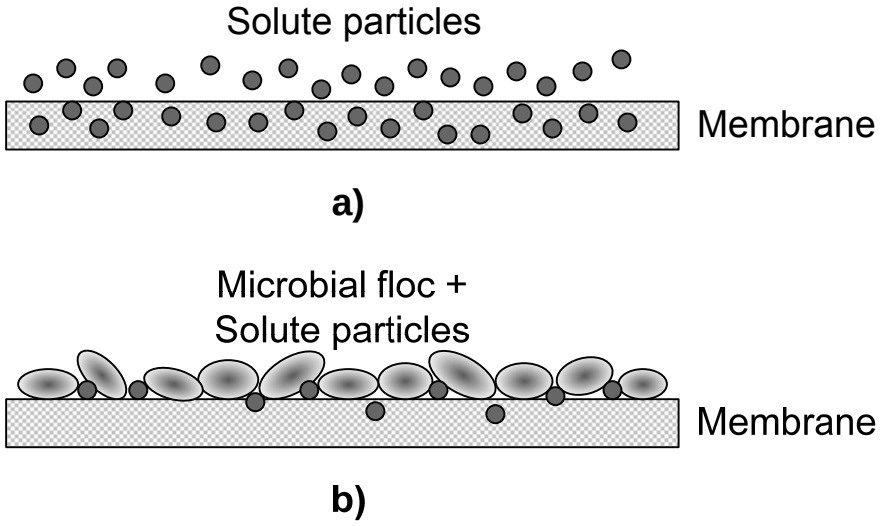

Figure 2.8: Concept of membrane fouling a) without and b) with dynamic membrane (adapted from Lee at al., 2001)

Table 2.6 presents the resistance analysis performed after filtration run for attached and suspended growth MBR systems (Lee et al., 2001).

Table 2.6: Effect of growth pattern on each resistance in the submerged MBR

Submerged MBR	Attached growth[a]		Suspended growth[b]	
	10^{12} /m	%	10^{12} /m	%
Intrinsic membrane resistance, R_m	0.49	12	0.50	12
Cake resistance, R_c	2.94	69	3.39	80
Fouling resistance, R_f	0.81	19	0.35	8
Total membrane resistance, R_t	4.24	100	4.24	100

[a] MLSS: 100 mg/L, attached biomass: 2000 mg/L; [b] MLSS: 3000 mg/L
Source: Lee at al. (2001)

The attached and suspended growth systems took 20 and 140 h, respectively to obtain the same total membrane resistance (R_t) of 4.24 x 10^{12} 1/m. A small decrease in R_c was observed in attached growth which was compensated with an increase in R_f, eventually leading to a more severe loss of permeability. This result shows that in the absence of dynamic membrane, the impact of internal fouling due to soluble and colloidal particles is severer while R_c still holds a larger part of R_t. This study infers that MBRs should be operated at an adequate MLSS concentration (≥ 3,000 mg/L) to avoid direct solute adsorption and allow cake layer formation providing some protection to the membrane as it serves as a more selective barrier than the membrane itself.

However, Sombatsompop et al. (2006) found that membrane fouling increased with increase in MLSS concentration in a suspended as well as attached growth MBRs operated at MLSS concentrations of 6, 10 and 15 g/L. In this study, the attached growth MBR having moving media demonstrated much improved filtration performance as compared to that in the attached growth MBR for a given MLSS concentration condition. The low fouling tendency in the attached growth MBR was associated with retarded biomass deposition and consequent less cake formation due to high shear intensity induced by the moving media. In another study, membrane fouling was observed to decrease at low MLSS concentrations (< 6 g/L) while more fouling occurred as the concentration increased above 15 g/L (Rosenberger et al. 2005 cited in Le-Clech et al., 2006). The MLSS concentration between 8 and 12 g/L did not appear to have significant effect on membrane fouling. Overall, lack of clear correlation between MLSS concentration and fouling behavior indicates that MLSS concentration alone is a not a strong indicator of fouling propensity in a MBR operation.

2.4.1.2 Biomass fractionation

Activated sludge can be fractionated into three components, namely: suspended solids, colloids and solutes. The affect of each of these components on MBR fouling is necessary for fouling characterization. The methodology applied to separate these three components has not been standardized and varies from one study to another. In this regard, a comparison of methods to fractionate the activated sludge from recent studies is reported in Table 2.7.

Table 2.7: Methods for fractionation of activated sludge

Supernatant (Colloids + Solutes)	Supernatant (Solutes only)	Source
Settling (4 h)	Filtering the settled sample through MF membrane (Millipore) of nominal pore size of 0.45 μm	Bae and Tak (2005)
Filtering through filter paper of nominal pore size of 0.45 μm; Direct centrifugation at 366 rad/s (3500 rpm) for 5 min		Lee et al. (2003)
Settling (1 h)	Filtering the settled sample through filter paper of nominal pore size of 0.2 μm	Bai and Leow (2002)
Direct centrifugation at 4500 rpm for 1 min	Flocculation of supernatant with $Al_2(SO_4)_3$ at 250 mg/L and second centrifugation (4500 rpm for 10 min)	Bouhabila et al. (2001)
Filtering through filter paper of nominal pore size of 0.45 μm; a) Centrifugation at 2000g (3340 rpm) for 10 minutes	b) Again centrifugation at 10,000g (7470 rpm) for 10 minutes	Lee et al. (2001)
Settling	Flocculation of supernatant with $FeCl_3$ at 400 mg/L	Defrance et al. (2000)
Settling (2 h)	Filtering the supernatent through filter paper of nominal pore size of 0.05 μm	Wisniewski and Grasmick (1998)

Wisniewski and Grasmick (1998) fractionated the activated sludge suspension from a side-stream MBR into settleable particles (particle size above 100 μm), supracolloidal-colloidal (non-settleable particle with size ranging from 0.05 μm to 100 μm) and soluble (particle size below 0.05 μm). The hydraulic resistances induced by these different fractions were simply additional and no interaction between these fractions occurred. The resistance analysis revealed that 52% of the total resistance could be due to soluble compounds. This soluble fraction is composed essentially of bacterial residual compounds initially present and also of bacterial products released by the cells during recirculation. However, the significance of supracolloidal and colloidal fraction towards hydraulic resistance could change for different conditions of filtration.

Defrance et al. (2000) investigated filtration variation with individual concentration of each activated sludge fraction in side-stream MBR. It was found that shear stresses generated by the pump and the recirculation along the membrane decreased the mean size of bacterial flocs as was noted in Wisniewski and Grasmick (1998). It was reported that the relative contributions of suspended solids, colloids and dissolved matter to the total hydraulic resistance were 65, 30 and 5%, respectively. However, the sum of resistances of the three fractions (calculated total resistance) was found to be 50% higher than the measured total resistance, indicating that fouling resistances caused by each constituent were not additional. The other important result was that the permeate flux did not decrease much when the biomass concentration was increased from 2 to 6 g/L.

Furthermore, Bouhabila et al. (2001) determined the influence on membrane fouling of the three fractions of submerged MBR sludge. The experimental study was performed in three hollow-fiber submerged MBRs treating synthetic wastewater and operated at SRTs of 10, 20 and 30 d corresponding to MLSS concentrations of approx. 17, 23 and 27 g/L,

respectively. It was found that the specific resistance (α) of the supernatants (colloids and solutes only) were 20 to 30 times higher than that of the sludge, which is representative of high fouling potential of this fraction due to pore clogging and adsorption phenomena as shown in Figure 2.9. However for MBR operated at 30 d SRT, a strong decrease of the specific resistance of the supernatant can be observed after 40 days operational period probably due to better biodegradation of polymers. The resistance analysis of this study revealed that colloidal fraction was an important factor in membrane fouling contributing 50% of the total hydraulic resistance (R_t).

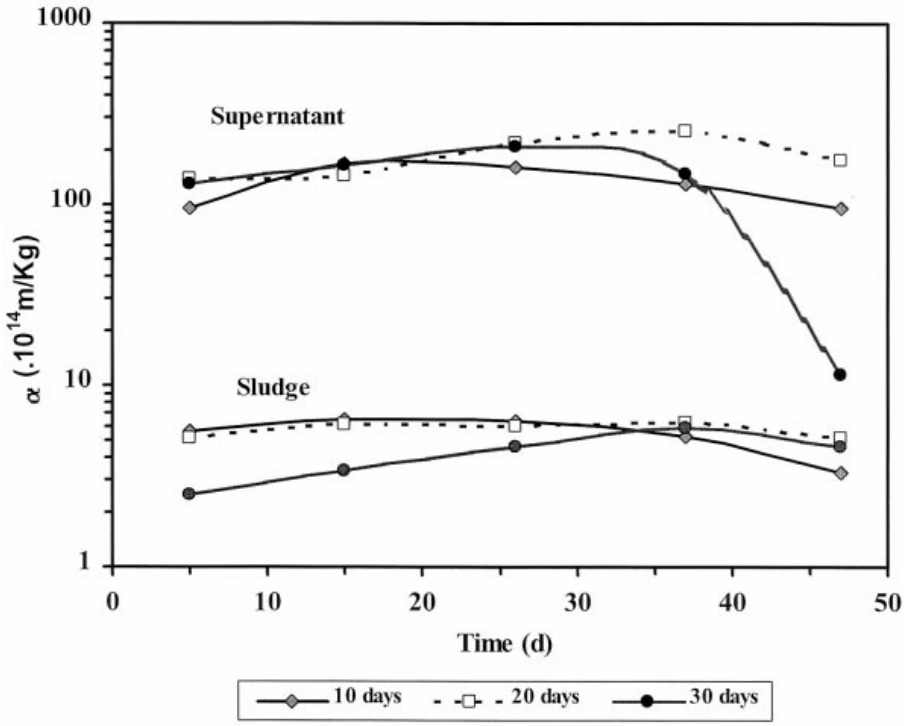

Figure 2.9: Comparison between specific resistance of supernatant and sludge for various SRTs (Bouhabila et al., 2001)

Table 2.8 presents a comparison of the relative contribution of SS, colloids and dissolved matter to the total resistance caused by fouling reported by recent studies.

Table 2.8: Relative role of different sludge fractions in membrane fouling

Configuration	Suspended solids (%)	Colloids (%)	Solutes (%)	Source
Submerged	63-71	29-37 (colloids + solutes)		Lee et al. (2003)
Submerged	24	50	26	Bouhabila et al. (2001)
Side-stream	65	30	5	Defrance et al. (2000)
Side-stream	23	25	52	Wisniewski and Grasmick (1998)

The differences in relative contribution for each of the factions can be due to the following reasons:

- Feed conditions
- Physiological state of the biomass e.g. biomass characteristics at different SRT
- Membranes used
- Methods used for fractionation

Thus, it is futile to compare relative fouling contributions from one study to another because varying experimental conditions produce discrepant results. However, series of experiments with controlled conditions could result in a uniform and relevant set of results.

2.4.2 Operating conditions

2.4.2.1 Aeration/cross-flow velocity

The two main hydrodynamic approaches taken into consideration in MBR operation include cross-flow velocity and aeration. The cross-flow velocity approach is mainly applicable to side-stream MBR while bubbling has been the strategy of choice for submerged-MBRs to induce flow circulation and shear stress on the membrane surface. Aeration used in submerged-MBR systems has three major roles: providing oxygen to the biomass, maintaining the activated sludge in suspension and mitigating fouling by constant scouring of the membrane surface (Le-Clech et al., 2006). The effect of bubbling can help overcome issues related to high packing density in hollow fiber bundles. However, to achieve effective aeration throughout the population of fibers in a bundle is a challenge due to the uneven distribution of the aeration shear intensity (Yeo et al., 2006).

Ueda et al. (1997) reported that an optimum aeration rate exists beyond which a further increase has no significant effect on membrane fouling suppression. However, other researches have found that the membrane fouling mitigation keeps improving with increase in aeration intensity (Le-Clech et al., 2003a; Germain et al., 2005; Ji and Zhou, 2006). For a pilot scale MBR system with submerged tubular module, it was found that increasing approach velocity always increased the critical flux (J_c) across the entire range of conditions tested (Le-Clech et al., 2003a). However, the influence of increasing the MLSS concentration from 4 to 12 g/L emphasized its predominant role on J_c while the effect of aeration intensity appeared less significant. Similarly, Germain et al. (2005) found that increasing the aeration velocity (U_G) in a pilot scale submerged-MBR always reduced the fouling rate for range of MLSS concentrations and permeate fluxes (J) tested. For J above 22 L/m^2/h and MLSS concentration above 11 g/L, the influence of changes in U_G on fouling rates were more marked. Moreover, Ji and Zhou (2006) found that the number of membrane operation cycles in MBR doubled by reducing the aeration rate from 2.0 to 0.7 L/min. The improved membrane filtration with increased aeration was observed despite reduction in floc size. With intense aeration rate, high shear stress was exerted on bio-flocs leading to the breakage of flocs, decrease in floc size and release of EPS into the supernatant. Apparently, the turbulence induced by the high aeration rate offset the influence of small bio-particle and relatively high EPS content on membrane filtration performance.

In side-stream MBR configuration, the extent of membrane fouling has been investigated by increasing the circulation velocity across the membrane surface. Wisniewski and Grasmick (1998) and Defrance et al. (2000) found that high circulation velocity modified the composition and characteristics of biological suspension. It was reported that high shear stress exerted on microbial flocs during recirculation resulted in reduced particle size, de-structured flocs and increase in non-settleable fraction (Wisniewski and Grasmick, 1998). The high non-settleable fraction, comprising mostly of colloidal matter and various polymers, caused significant decrease in the permeate flux and consequently high hydraulic resistance at the beginning of filtration in dead-end filtration test as shown in shown in Figure 2.10.

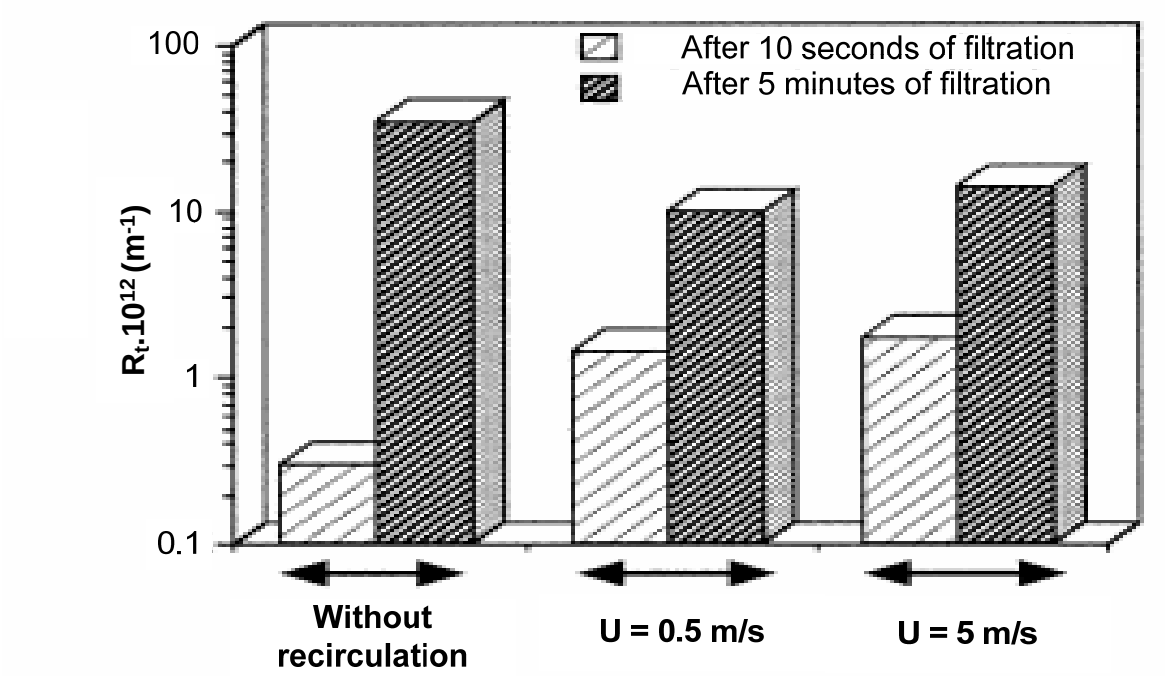

Figure 2.10: Hydraulic resistances for three types of biological suspensions measured after 10 s and 5 min of filtration (Wisniewski and Grasmick, 1998)

Bai and Leow (2002) investigated the role of operational parameters in a side-stream MBR by varying airflow rate and mechanical mixing (stirrer speed) in an activated sludge tank and wastewater circulation velocity through a hollow fiber MF module. The turbulent environment induced by high mechanical mixing speed, high aeration rate or high circulation velocity always broke the bioflocs into smaller ones. Particles of size larger than 100 μm were most easily broken, while particles small than 50 μm were not affected significantly. Moreover, the permeation fluxes always reduced when the particle size in the feed wastewater to the MF unit became smaller for a constant MLSS concentration of 2 g/L. Further evaluation of the different fractions of the activated sludge revealed higher permeation fluxes for solute fraction followed by colloid + solute fraction and lastly by original wastewater feed. The difference in the fluxes for the three types of suspensions was attributed to the suspended solid concentration in the feed which reduced for colloid + solute fraction followed by solute only.

2.4.2.2 Imposed flux

The recent technique that has been employed to control fouling and minimize chemical cleaning frequency is operation of MF system under sub-critical flux conditions. It is very important to identify the optimum operational flux of a MBR since it permits to approach the required compromise between high fluxes and long term operation without chemical cleaning.

a. Concept of critical flux

The concept of critical flux for MF fouling was originally proposed by Field et al. (1995). The critical flux hypothesis is that "on start-up there exists a flux below which a decline of flux with time does not occur; above it fouling is observed". This flux is referred to as the critical flux. Below critical flux, there will be little or even no irreversible membrane fouling. The strong form of the hypothesis is that a flux exists which is equivalent to the

corresponding clean water flux at the same TMP. The weak form is that on start-up a constant flux is rapidly established and maintained. The strong and weak forms of critical flux are graphically shown in Figure 2.11.

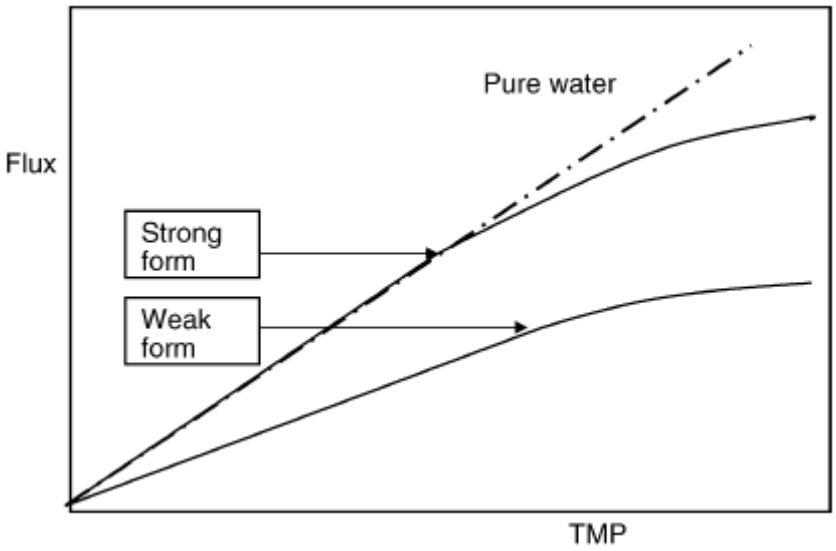

Figure 2.11: Forms of critical flux (Bacchin et al., 2006)

When the permeation is below critical flux value, referred to as sub-critical flux, no particle deposition should occur in the region of the membrane.

Critical flux value depends on:

- Characteristics of the membrane (pore diameter, porosity, material);
- Characteristics of the suspension (nature, particle size distribution in relation to pore size distribution and concentration);
- Hydrodynamic conditions.

MBRs can be operated in two modes-constant pressure or constant flux. In constant pressure operation mode, constant flux can be achieved if the TMP is maintained below the critical TMP whereas in constant flux operation mode, constant pressure can be realized if the flux is maintained below the critical flux.

In general, constant flux operation is shown to have some advantages over normal constant pressure operation because it provides constant convective flow towards the membrane and avoid possibility of over fouling by monitoring the increase in TMP. Moreover, the interpretation of data from constant pressure experiments often causes problems since flux variation produce changes in concentration, rheology, solubility etc. in the boundary layer during any experiment. Therefore, it is recommended to have membrane filtration at constant flux. By selecting the initial flux less than critical flux, the rate of fouling can be greatly reduced because of minimum cake thickness.

b. Limiting flux

The critical flux should not be confused with limiting flux although they may be equivalent is some cases. Limiting flux is a common feature in membrane operations when the flux becomes independent of the driving force and an increase in TMP yields no flux increase exhibiting a flux plateau. Unlike the limiting flux, the critical flux is a criterion for the

transition between concentration polarization and fouling. The critical flux is reached when irreversible fouling occurs locally on the membrane, whereas the limiting flux is reached when the whole membrane surface operates above the critical flux: i.e. when a further increase in flux at any point on the membrane surface lead to another layer deposit fully compensating the increased pressure drop. (Bacchin, 2004) developed a simple model suggesting that the limiting and critical fluxes can be theoretically linked. With certain assumptions, it was shown that the critical flux is equal to 2/3 of the limiting flux.

c. Hysteresis effect

It was found for a constant-pressure MF that as TMP is increased the flux increases linearly and provided a critical flux value is not exceeded the behavior is reversible i.e. pressure can be reduced and the same fluxes are again observed (Benkahla et al., 1993 cited in Field et al., 1995). However, when the critical flux value is exceeded then reducing TMP does not restore the original flux but a lower one. This cycling of TMP leads to an effect known as "hysteresis effect".

Le-Clech et al. (2003b) determined critical flux employing constant-flux in submerged MBR and incrementally increasing the flux for a fixed duration for each increment. Such operation gave a stable TMP at low flux but an increasing rate of TMP at fluxes beyond critical value. Moreover, it was found that when flux was increased incrementally the TMP increased linearly and provided a critical flux value was not exceeded, flux could be reduced and the same pressures were again observed. However, when the critical flux value was exceeded then reducing flux did not restore the original TMP but a higher one, exhibiting hysteresis effect as shown in Figure 2.12. The value of the critical flux below which no hysteresis is observed can be increased by increasing cross-flow velocity in sidestream MBR or aeration rate in submerged MBR.

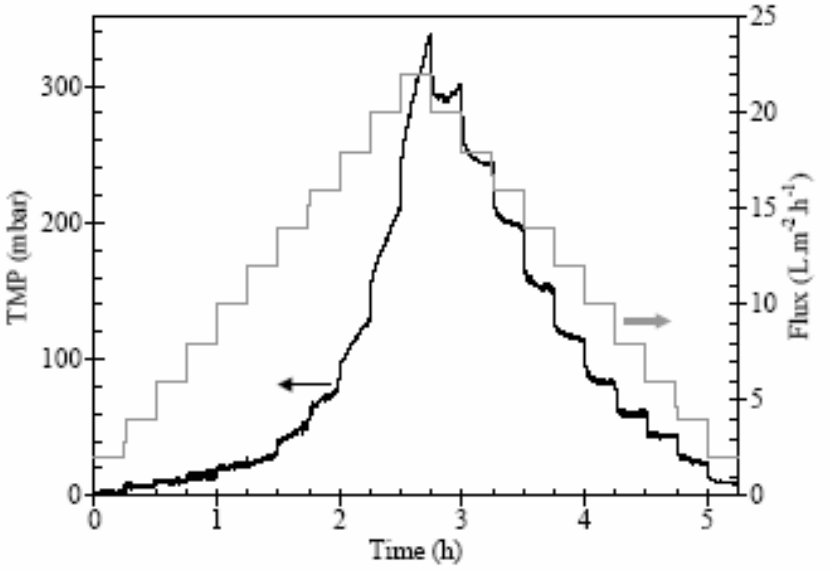

Figure 2.12: Critical flux determination for synthetic sewage (Le-Clech et al., 2003b)

d. Critical flux measurement in microfiltration

The critical flux concept is based on the balance of convection towards a membrane and back transport. It is generally considered that back-flux of particles from the membrane

towards the bulk of solution is a function of particle size and back-flux increases with increase in particle size. Thus, if the critical flux is higher for larger particles, finer particles become part of the cake layer sooner as compared to larger particles. Therefore, measurement of the critical flux for a range of particles is highly desirable.

At start-up of a MF experiment, if the initial flux is greater than the critical flux for all components of suspension, all particle sizes in the vicinity of the membrane will experience a net force towards the membrane. One will observe that initial deposition does not favor any particular size of particle but as flux declines, the critical flux of each size of particle will progressively pass and the percentage of larger particles in cake layer will decline. On the other hand, initial flux below the critical flux of all particles should lead to a cake with a different structure or possibly no cake at all. Defrance and Jaffrin (1999) found that the role of dissolved matter in critical flux phenomenon is probably small since it accounted for 5% of fouling resistance.

The force perpendicular to the membrane surface acting on a particle in the retentate is the drag force F_d due to the filtration flux and a lift force F_m arising from different pressure forces on the top and bottom of the particle due to the shear intensity (G) and causes the particle to migrate away from the membrane (Defrance and Jaffrin, 1999). Since the Reynolds number is based on the particle diameter and permeate flux is very small, the drag force on a spherical particle can be estimated by:

$$F_d = 3\pi\mu d_p J_f \qquad \text{Equation 2.9}$$

While the lift force can be calculated as:

$$F_m = \frac{183}{8\times 576}\pi\frac{\rho_s}{\mu_s^2} d_p^4 \tau_w^2 \qquad \text{Equation 2.10}$$

Particle will deposit on the membrane when $F_d \geq F_m$. Equality leads to a critical particle diameter d_{p_c} given by

$$d_{p_c} = 5.326\mu_s\left(\frac{J_f}{\rho_s \tau_w^2}\right)^{1/3} \qquad \text{Equation 2.11}$$

According to the Equation 2.11, the d_{p_c} increases as $J_f^{1/3}$ is increased.

According to Ognier et al. (2004), the first step to determine critical flux value is to step wise increase the permeate flux value while monitoring changes in TMP. If no changes are observed in TMP during this time, the flux value J tested is regarded as below critical flux (J_c) and the operation is repeated at higher flux value. When TMP does not stabilize for given flux value, the flux is considered as above critical flux.

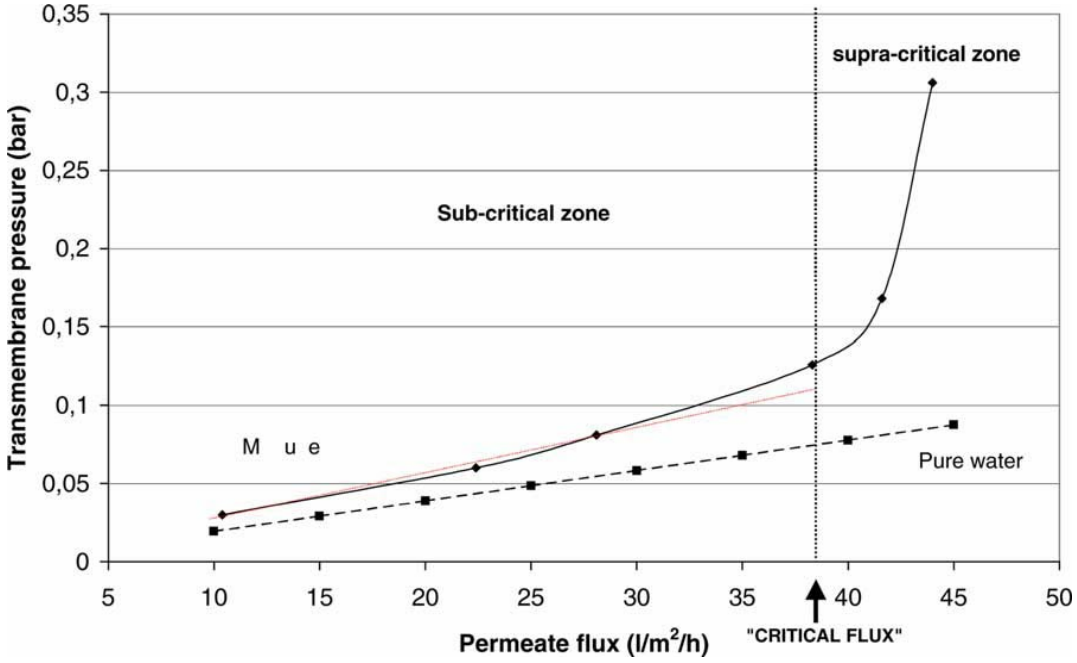

Figure 2.13: Experimental determination of critical flux (Ognier et. al, 2004)

Figure 2.13 shows the experimental results obtained for different levels of imposed permeate flow for a sidestream MBR (Ognier et. al, 2004). It is found that above a flux value of approximately 40 L/m^2/h, a clear break occurred in the curve with a significant change in pressure. This shift in TMP trend is characteristic of biological floc deposition on the membrane and thus of supra-critical condition.

Wu et al. (1999) determined the critical flux for two colloidal silica suspensions namely: Bovine serum albumin (BSA) solution and Baker yeast suspension with a hydrophilic flat sheet membrane operated at constant permeate flux. For the experiments carried out, the strong form of critical flux was defined as the flux when the membrane resistance does not change from the one observed with clean water. Whereas, the weak from was defined as the flux when the membrane resistance changes with the onset of colloidal fouling but does not change with increasing flux until the critical flux is reached. It was found that for two different membranes and three feed fluids, the critical flux decreased with increasing membrane pore size. The difference in observed critical flux values could be due to a change in local porosity and hence local convective velocities as opposed to average flux across the entire membrane surface. This implies that membranes with larger pore size are susceptible to greater fouling.

Variables which significantly affect the critical flux measurement are incremental flux step, duration at each flux step, initial state of membrane (new, backwashed and/or chemically cleaned), feed characteristics and system hydraulics (sidestream or submerged MBR configurations) (Le-Clech et al., 2003b). According to few researches, the methods used to determine critical flux at constant-flux operation mode are presented in Table 2.9.

Table 2.9: Methods for critical flux measurement

Membrane configuration	Flux range ($L/m^2/h$)	Flux step ($L/m^2/h$)	Membrane area (m^2)	Time duration at each step (min)	Reference
Flat-sheet	10-70	5	0.00672	5	Wu et al. (1999)
Submerged tubular MBR	2-22	2	0.19	15	Le-Clech et al. (2003)
Side-stream tubular MBR	50-100	10	0.24	60	Defrance and Jaffrin (1999); Ognier et al. (2004)

Table 2.9 presents that there is clear difference in the protocols used to determine critical flux for different systems and at present any of the given protocols cannot be considered as a standard.

2.4.2.3 Sludge retention time (SRT)

SRT which consequently controls the food-to-microorganism (F/M) ratio is probably the most important biological parameter in controlling membrane fouling in MBRs. Researches have carried out extensive investigation in depicting membrane fouling at various SRTs. Currently, MBRs tend to be operated at long SRTs to maintain high biomass concentration, reduce sludge production and minimize reactor volume.

Trussell et al. (2007) investigated membrane fouling by operating a pilot scale submerged membrane bioreactor at 10, 20 and 30 d SRT. It was found that MBRs operation at 20-30 d SRT contributed relatively lower to membrane fouling than that of 10 d SRT at MLSS concentration of approximately 15 g/L. The poor filterability of sludge at 10 d SRT was attributed to higher colloidal material, total SMP and soluble COD concentrations which resulted in more viscous sludge than that of the 20 and 30 d sludges. The poor mixed liquor filterability at 10 SRT required longer aeration period to restore the original permeability, indicating the formation of "stickier" cake layer. Furthermore, researches determined that relatively high SRT operation (20-60 d) was able to reduce the fouling potential due to low SMP generation (Lee et al., 2003; Liang et al., 2007). These two studies found that the metabolic activity of sludge, characterized by specific oxygen uptake rate (SOUR) slightly decreased as SRT lengthened. This can be attributed to the increase of inert biomass which are metabolic products from endogenous respiration and possibly to the potential inhibition of SMP (Liang et al., 2007). However, the filtration resistance due to microbial floc increased with increase in MLSS concentration at extended SRT, resulting in overall increase in fouling resistance (Lee et al., 2003). The same study revealed that the mean colloid size enlarged as SRT increased as the proportions of the particles smaller than the nominal pore size of the membrane (0.4 μm) were 68, 62 and 54% of the total colloids at SRT 20, 40 and 60 days, respectively. It was depicted that lower microbial concentration under given aeration intensity might enhance floc breakage, favoring cell debris and macromolecules (i.e. colloids). However, the influence of solutes and colloids on membrane fouling resistance appeared to be insignificant regardless of SRT.

Operating MBRs at prolong SRT with high biomass concentration frequently create problems such as keeping high MLSS levels in suspension and properly oxygenated as well as membrane filtration deterioration due to ineffective membrane scouring (Le-Clech

et al., 2006; Ng and Hermanowicz, 2005). In this regard, Ng and Hermanowicz, (2005) investigated the performance of MBR operation at extremely short SRT (0.25-5 d). It was demonstrated that when nitrification is not a concern, it is possible to operate a MBR at short SRT producing effluent of excellent quality or achieving excellent organic removal efficiency. However, the sludge settling was found to be poor at short SRT related to non-flocculating microorganisms.

There is no substantial rationale to operate MBRs at extremely short or long SRT. Generally, it is suggested that MBRs should be operated at SRTs from 20 up to 40 d for SMP fouling control (Lee et al., 2003; Liang et al., 2007; Trussell et al., 2007) and adequate MLSS levels. MLSS concentration recommended by the membrane suppliers and OLR desired is more prone to define the working SRT.

2.4.2.4 Dissolved oxygen (DO)

The effect of dissolved oxygen (DO) concentration on membrane fouling has not been extensively investigated since all aerobic biological reactors are maintained above 2 mg/L and depends on the aeration intensity requirements of the MBR system. However, recently Jin et al. (2006) investigated the influence of DO concentration on biofilm structure and membrane filterability in submerged MBR. It was determined that the rate of membrane fouling for the low DO (LDO) reactor (<0.1 mg/L) was 7.5 times faster than that for the high DO (HDO) reactor (>3 mg/L). The MLSS concentrations in LDO and HDO reactors were kept at 1-2 g/L and 7-12 g/L due to different growth conditions for the microorganisms. Both reactors were operated at similar tangential shear intensity by supplying air at 1 L/min in the HDO reactor whereas 0.1 L/min of air and 0.9 L/min of nitrogen was supplied to the LDO reactor. Even though the biofilm deposited on the membrane surface in the HDO was thicker than that in the LDO at the terminating TMP of 30 kPa, the biofilm resistances in both the reactors were similar. The short filtration period at low DO concentration was attributed to reduced porosity of the LDO biofilm by the presence of high number of small particles (2-5 μm) in the LDO biofilm.

2.5 Fouling mechanism in MBR

The current trend in MBR is to operate at constant flux and monitor TMP rise. Since fouling rate and cleaning frequency increases with increase in imposed flux, it is favorable to operate MBR at modest flux i.e. sub-critical flux. Ognier et al. (2004) analyzed long-term variation in membrane permeability under sub-critical flux conditions with no intermediate membrane regeneration in side-stream MBR. During prolonged runs, two distinct periods were identified as shown in Figure 2.14.

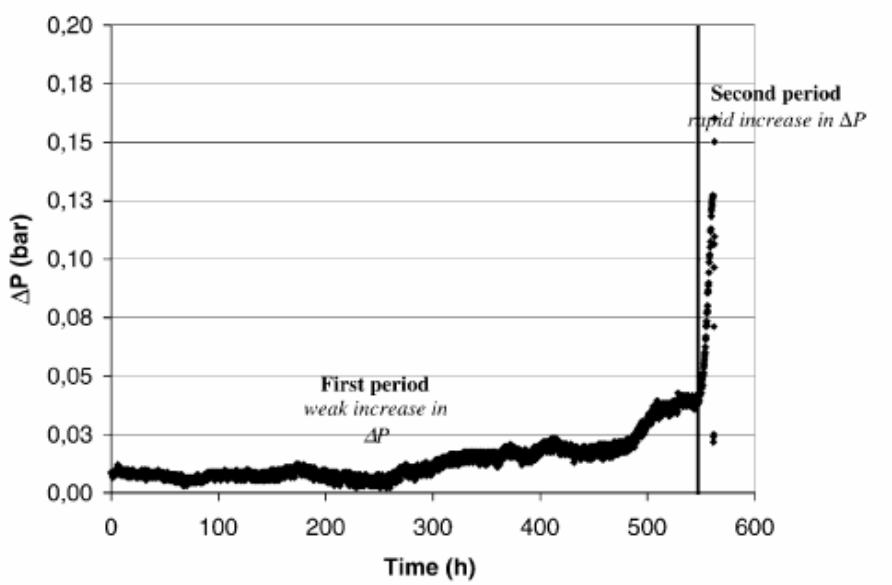

Figure 2.14: TMP change during long term constant sub-critical flux conditions (Ognier et. al, 2004)

In the first period, it was noticed that the initial choice of sub-critical condition in a long run does not prevent the gradual fouling of the membrane. Moreover, the period during which fouling gradually occurred appeared to be irreversible due to adsorption or colloidal fouling. In the second period, a marked increase in fouling rate was observed which reflected supra-critical condition with cake layer formation and hydraulically reversible.

During the first period, solute-membrane or colloids-membrane interactions provoke a reduction in the number of pores open to the filtrate flow. This reduction of the area open to the flow is expressed as gradual increase in local flux in the pores remaining open. In the absence of regular membrane regeneration, the local flux increase slowly intensifies as the pores close and may lead to the local flux reaching a level equal to critical flux value and leading to a steep rise in the TMP as observed in Figure 2.14. A deposit then forms on the membrane initiating a very high hydraulic resistance which marks the onset of cake formation. This fouling mechanism known as 'local filtration flux concept' is depicted in Figure 2.15.

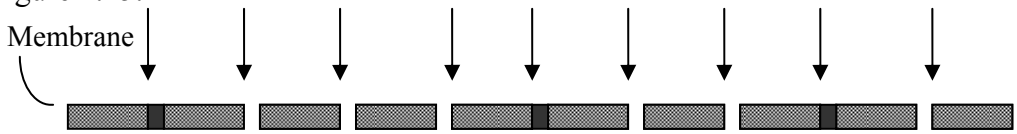

(a) Progressive decrease of open pore number and progressive increase of local filtration flux

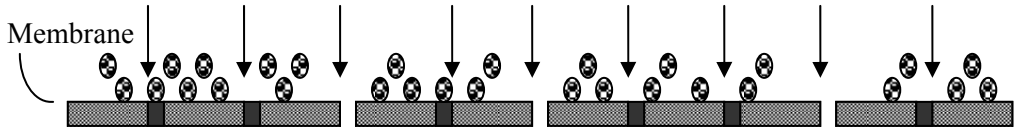

(b) Progressive cake layer formation as local filtration flux reaches critical flux

Figure 2.15: Fouling mechanism in sub-critical flux conditions (adapted from Ognier et al., 2004)

Tony Fane research group on membrane fouling has extensively investigated the fouling behavior pattern. In one of their earlier studies, long term experiments in anaerobic side-stream MBR revealed two step pattern (Cho and Fane, 2002) as shown in Figure 2.16.

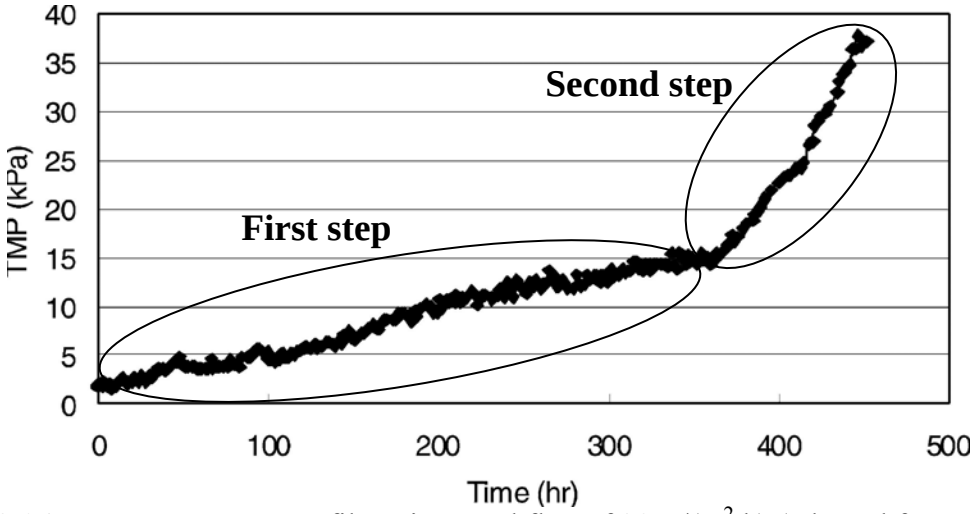

Figure 2.16: Long term TMP profile at imposed flux of 30 L/(m^2.h) (adapted from Cho and Fane, 2002)

Prior to these two filtration steps, a conditioning step was reported in of their recent publications referred to as Stage 1 (Zhang et al., 2006). This study by Zhang et al. (2006) reported a detailed mechanism involved in the three fouling stages summarized in Figure 2.17.

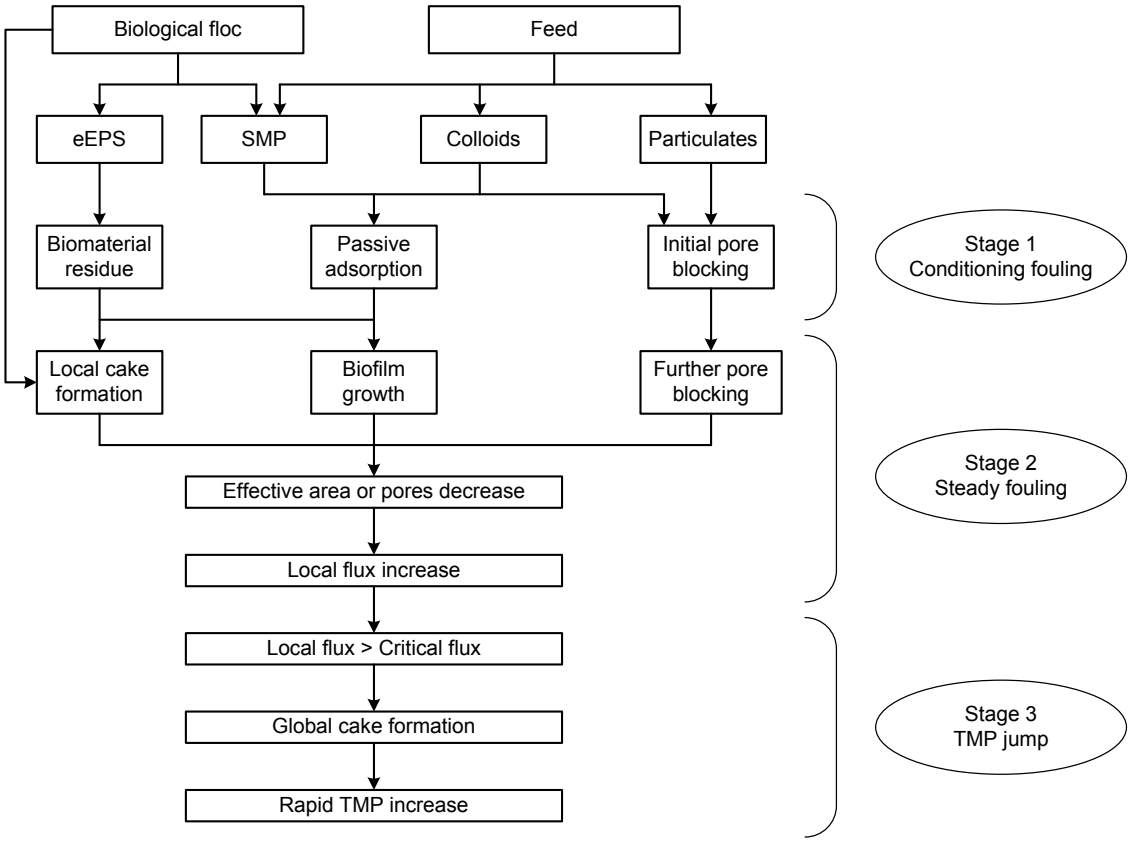

Figure 2.17: Fouling mechanisms in MBR at constant flux (adapted from Le-Clech et al., 2006; Zhang et al., 2006)

The three fouling stages are discussed as follows:

2.5.1 Stage 1-conditioning fouling

At the early stage of MBR operation, there is strong interaction between virgin membrane and colloids and solute, mostly SMP present in the mixed liquor resulting in adsorption as well as colloidal pore narrowing or blocking which is mostly irreversible. This initial irreversible resistance is referred to as 'conditioning fouling' (Le-Clech et al., 2006). Passive adsorption of colloids and organics has been observed even for zero-flux operation, before any deposition initiates (Zhang et al., 2006). The conditioning fouling has been reported to be independent of the shear intensity exerted on the membrane surface in the MBR while it is dependent on the membrane pore size distribution and surface chemistry. However, its contribution to the overall hydraulic resistance at the end of the membrane filtration cycle is negligible.

2.5.2 Stage 2-Steady fouling

Operating MBRs even below the critical flux causes the small bio-flocs and SMP to gradually deposit on the membrane surface. Moreover, biofilm growth can initiate on the irreversibly attached biofloc residues on the membrane surface from Stage 1. The biomass deposition and/or biofilm growth tendency increases leading to steady rise in TMP. Over time, this phenomenon worsens. This gradual fouling is dependent on the shear intensity and its distribution on the membrane surface induced by the aeration rate in a submerged MBR. The biomass may intend to deposit earlier in low shear stress regions of the membrane module due to irregular scouring of membranes via aeration.

2.5.3 Stage 3-TMP jump

At the end of stage 2, with some regions or pores of the membrane more fouled than others, the filtration through these specific locations is expected to decrease. As a result, permeate productivity redistributes to the less fouled membrane areas or pores, for which the local flux exceeds the critical flux. At this stage one observes rapid TMP rise known as 'TMP jump'. Zhang et al. (2006) found that the sudden rise in TMP can also be caused by sudden changes in the biofilm or cake layer structure. It was demonstrated that under low DO concentration and substrate conditions in the biofilm sub-layers, the biomass could release large amount of polysaccharides and block the membrane pores, resulting in sharp decrease in the membrane permeability. Another study revealed that according to 'percolation theory', the porosity of the fouling layer gradually reduces during filtration by material deposition. At critical condition, the cake layer losses connectivity and there is sharp increase in the TMP (Hermanowicz, 2004 cited in Le-Clech et al., 2006).

2.5.4 Fouling mechanism in submerged HF bundle

Lee et al. (2007a) investigated the biofim porosity along the length of submerged hollow fibers. It was found that the biofilm porosity near the potted ends was lower than those at the free moving ends because the biofilm formed on potted ends was more easily compressed by the reduced local shear intensity condition. Yeo et al. (2006) reported that for fiber bundle, the permeate flows became less evenly distributed among the fibers over time and the standard deviation of fluxes from individual fibers increased. Consequently TMP rose to maintain average flux across the fiber bundle and at some point, both TMP

and flow standard deviation sharply increased. This is believed to be due to uneven flow distribution within the bundle initiated by local blockages between fibers. The flow standard deviation profile and TMP was able to be steady under high turbulent condition around the fibers.

Alain Grasmick research group has recently reported the fouling mechanism in submerged HF bundle at the mesoscopic and macroscopic scale (Lebegue et al., 2007) while fouling mechanism at the microscopic scale was reported in their earlier studies. At microscopic scale, the interaction between the membrane pores and the material in the mixed liquor is taken into consideration and the decrease in the number of pores remaining open to filtration over time is analyzed. At mesoscopic scale, the filtration performance of individual fibers is investigated while at macroscopic scale, an average behavior at the bundle level is considered. However, with high packing density of HF bundle leading to uneven distribution of fluid turbulence within the bundle, the macroscopic hypothesis may cause large discrepancy. The macro-scale level of fouling observation may be feasible for filtration control in industrial membrane systems.

In closely packed HF bundle it is very difficult to maintain homogenous flow distribution or regular shear intensity throughout the fiber network. This difficulty of low shear intensity at the center of a bundle may cause large accumulation of sludge inside the bundle leading to bundle clogging and consequent rapid fouling behavior. The conventional aeration applied in an outside mode does not allow significant water circulation inside the bundle and the center part can appear as a dead zone as shown in Figure 2.18 (a). However, air distribution practiced directly inside the bundle can allow some local flow in the center of the bundle. In case of HF with low packing density, external aeration allows a high liquid circulation throughout the bundle avoiding dead zones as shown in Figure 2.18 (b).

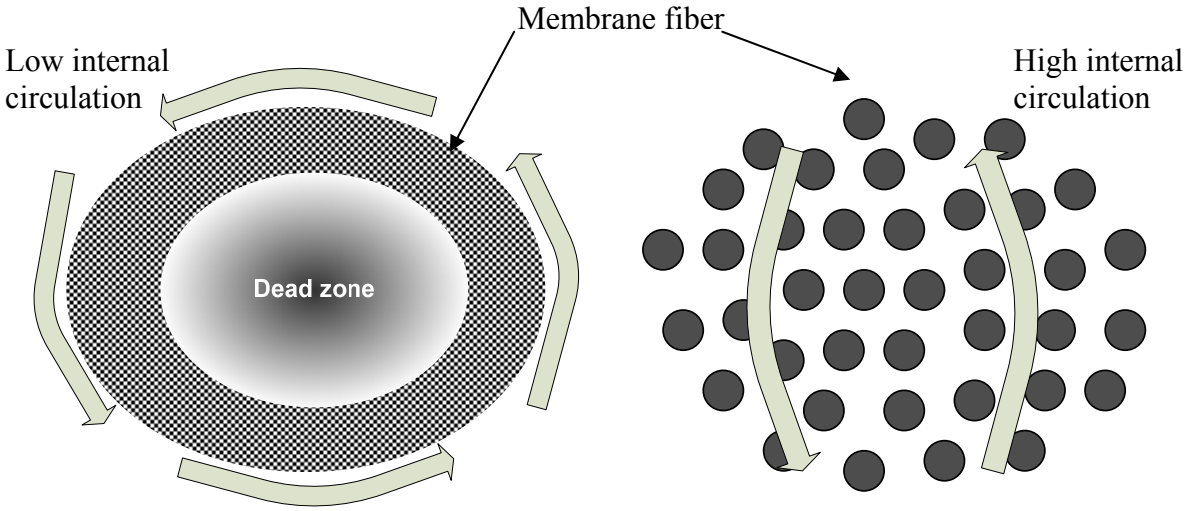

Figure 2.18 Influence of packing density on bundle fouling (a) High packing density (b) Low packing density (adapted from Lebegue et al., 2007)

During filtration through closely packed HF bundle with external aeration, one can observe a progressive radial concentration of the biomass suspension moving towards the inner fibers and consequent increase in the suspension viscosity resulting in intensified local

accumulation of compounds within the inner fibers. As the filtration condition worsens at the inner fibers, the global flux condition is held constant by flux redistribution to the outer (active) fibers only. This increase in the local flux of the outer fibers intensifies over time reaching a level equal to the critical flux. Under supra-critical conditions, the TMP rises rapidly which induces sharp increase in the total hydraulic resistance requiring the need of membrane chemical cleaning. The accumulation of biomass within the inner fibers can progressively induce gelatinous mucilage if the biomass recirculation becomes very low or allow anaerobic fermentation due to very low DO condition.

For a given external aeration intensity, the bundle diameter, the packing density and the sludge concentration are determining criteria of membrane fouling propensity in submerged HF bundle (Lebegue et al., 2007). The occurrence of sludge accumulation within the bundle known as 'sludging phenomenon' which can initiate the TMP jump appears to be a critical point in submerged MBR operation.

Chung-Hak Lee research group has recently investigated the relationship between biofouling and biofilm architecture in submerged MBR. They investigated the influence of the temporal changes in biofilm or biocake characteristics along its depth on the membrane fouling propensity in MBR. They also observed the classical two stages of fouling under sub-critical flux operation, i.e. slow and gradual TMP rise followed by rapid TMP rise (Lee et al., 2007a) as shown in Figure 2.19.

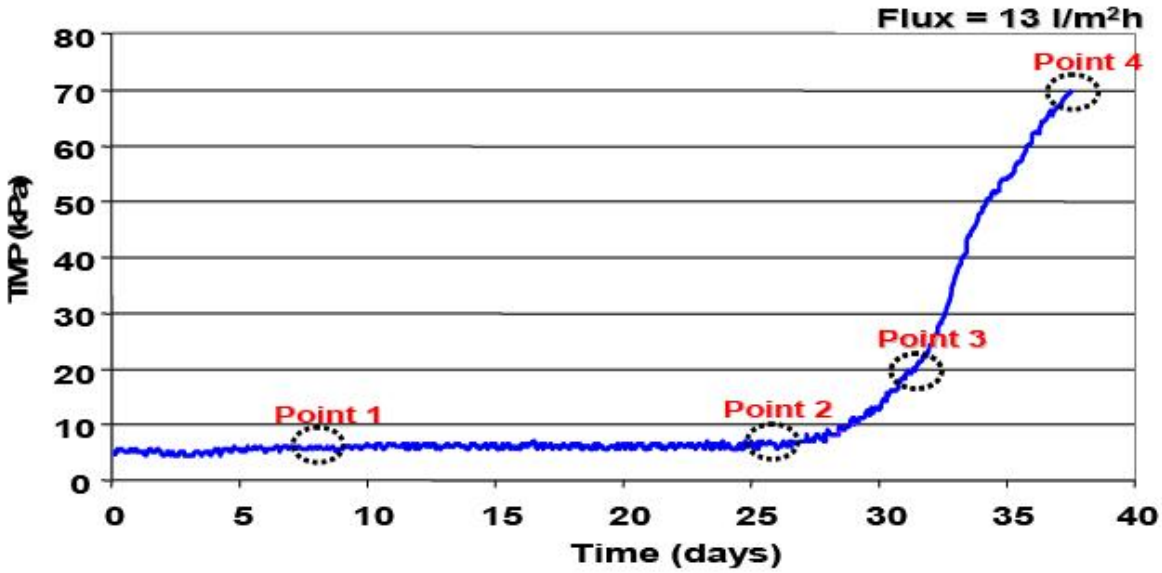

Figure 2.19: Profile of TMP rise at constant flux in MBR (Lee et al., 2007a)

The biological effect on the membrane biocake with temporal variation was correlated with the TMP profile. In this context, the ratio of live to dead cells was monitored along the depth of the biocake as a function of operating time as shown in Figure 2.20.

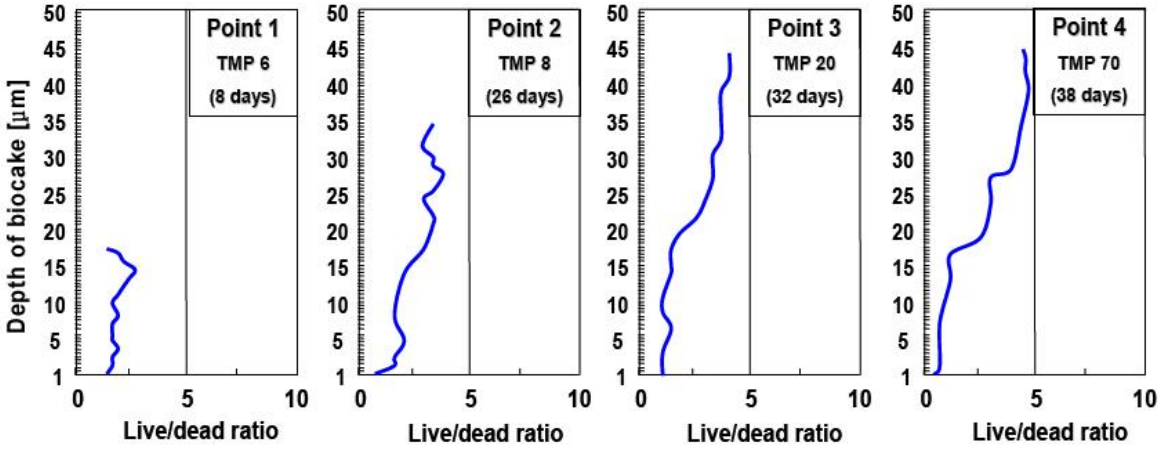

Figure 2.20: Distribution of live/dead cell ratio along the depth of biocake in MBR (Lee et al, 2007a)

Figure 2.20 shows that the live/dead ratios became smaller, especially at lower sub-layers of biocake corresponding to points 3 (20 TMP; 32 days) and 4 (70 TMP; 38 days) than those corresponding to points 1 (6 TMP; 8 days) and 2 (8 TMP; 26 days) in the TMP profile (Figure 2.19). As the biocake accumulates on the surface of membrane, endogenous decay or cell-lysis at the bottom layer would be expected to occur due to poor oxygen and substrate transfer. This biocake accumulation gave rise to the excretion of EPS (polysaccharides & proteins) which could reduce the porosity of the biocake. The EPS concentration jump in the biocake between points 2 & 3 coincided with the reduction in live/dead cell ratio (Figure 2.20). Thus, temporal changes in the biological properties at the bottom layers of a biocake can be considered to be in close association with the change in membrane fouling rates (dTMP/dt) in a submerged MBR.

2.6 Fouling mitigation approaches in MBR

During filtration process, permeate flux decline reaches a point where it is no longer economical to continue filtration, necessitating membrane cleaning. A number of cleaning options exist, with backwashing and/or chemical cleaning being the most common. Backwash and chemical cleaning incur additional operating costs with extended operating cycle due to the reversal of permeate flow for backwash and chemical usage. In submerged MBRs, the permeate flux is relatively low and can be maintained for extended periods without decline. On the contrary, in side-stream MBRs, the flux decline and fouling rate is much higher. Conventionally, fouling in a submerged MBR is reduced by operation under turbulent aeration conditions. Turbulent aeration promotes scouring of the membrane surface to suppress fouling layer formation and flux decline. The specific design of airflow patterns and location of aerators can also be considered as crucial parameters in fouling mitigation (Le-Clech et al., 2006).

Apart from aeration intensity, researches have investigated alternative hydrodynamic approaches such as intermittent flux (Sombatsompop et al., 2006; Wang et al., 2007), two phase bubbling (Le-Clech et al., 2003; Germain et al., 2005) and backwash (Bouhabila et al., 2001). Moreover, intermittent bubbling has also been investigated as a fouling control technique. Some of these techniques have been recommended by the membrane suppliers for better filtration performance.

2.6.1 Sustainable flux

To maintain reasonable flux rate without significant fouling in MBRs, the concept of 'sustainable flux' has been postulated which is similar to the notion of sub-critical flux. Sustainable flux has been defined as the flux for which the TMP increases gradually at an acceptable rate such that chemical cleaning is not necessary (Le-Clech et al., 2006). Sustainable flux can only be assessed through long term filtration periods as compared to short term experiments for the determination of critical flux. The sustainable flux value in MBR can be determined on the basis of the filtration period at which there is a distinction between a low fouling rate and a high fouling rate. In MBR operation, not only the value of sustainable flux is of important but the strategies used to maintain this flux as well. Moreover, the sustainable flux determination is dependent on the filtration timeframe in the application field. Operating at a small time scale, there can be very low or non-detection of changes is fouling rate whereas fouling rate becomes unacceptable for long filtration periods (Bacchin et al., 2006).

2.6.2 Modification of biomass characteristics-Hybrid MBRs

The addition of adsorbents into biological system improves the removal of pollutants particularly, organic compounds. Recently, addition of powdered activated carbon (PAC) has been investigated to mitigate the membrane fouling in membrane hybrid systems. When PAC was mixed with MBR sludge, biologically activated carbon formed and was responsible for removal of low molecular organics and thus reduced the membrane fouling (Ying and Ping, 2006; Munz et al., 2007). These studies show that adsorption of EPS on PAC improves with increase in PAC concentration and consequently resulting in low fouling of the membranes. Ying and Ping (2006) investigated the effect of PAC concentrations of 0, 0.75 and 1.5 g/L in three MBRs on sludge characteristics and membrane fouling behavior. It was found that 0.75 g/L of PAC concentration was the optimum as it resulted in minimum bound EPS as well as lowest total resistance. Aerobic granular sludge has also been developed and used in MBR for membrane fouling mitigation due to its large size, shape regularity and high settling ability (Li et al., 2005).

Recently, a novel cationic polymer called Membrane Performance Enhancer (MPE50) has been developed by NALCO® and applied to MBRs to control membrane fouling (Yoon et al., 2005; Yoon and Collins, 2006). Lee et al. (2007b) investigated the influence of MPE50 on membrane fouling mitigation in MBR with particular focus on changes in biofilm structure. 50 mg/L of the polymer dosage was found to be the optimum as it resulted in long filtration time to reach 30 kPa and beyond this dosage, the filtration time abruptly shortened. The long filtration time observed coincided with maximum bio-particle size. Moreover, the soluble COD and soluble EPS in the MPE50 added MBR were found to be lower than that in the control MBR (without MPE50). The biofilm structure investigation at the same TMP revealed that the biofilm porosity in the MPE50 added MBR was higher and amount of attached biomass was lower than that in the control MBR.

Another attractive membrane hybrid system for fouling control is moving bed biofilm reactor (MBBR) coupled with MBR system. MBBR exhibit several advantages over ASP including better oxygen transfer, higher nitrification and organic removal rate, higher biomass concentration and relatively shorter HRT (Sombatsompop et al., 2006). Moreover, biofilms enable maintenance of high biomass age promoting the development of slow-growing microorganisms such as nitrifiers as it reduces their washout from the system (Lee

et al., 2006). However, MBBR similar to ASP requires sedimentation tank and the settling characteristics effects both treatment efficiency and surface of settling tank. In this context, membrane coupled moving bed biofilm reactor (MC-MBBR) can be an attractive system which achieves complete solid-liquid separation independent of the characteristics of mixed liquor. The fouling of the membrane has been found to be retarded due to the biofilm carriers (media) circulation by aeration in MC-MBBR as compared to conventional MBRs due to modification in the physical characteristics of the activated sludge (Sombatsompop et al., 2006). Lee et al. (2006) compared the membrane fouling propensities by varying the media volume fraction and revealed that the TMP rise was slower with increase in media volume fraction. The low fouling behavior was found to be associated with the collision frequency of the media and the membrane surface causing biofilm detachment despite decrease in floc size. The moving media compartment was separated from the membrane module in one study (Sombatsompop et al., 2006) while the system in another study (Lee et al., 2006) permitted the collision of moving media with the membrane surface. These two researches suggest that moving media introduction to MBR system can improve membrane fouling mitigation with or without its interaction with the membrane surface.

The fouling mitigation approaches and its influence on fouling factors indicate there is no precise fouling factor that can singled out which influences membrane fouling the most. Similarly, it is difficult to select a single approach/technique for membrane fouling mitigation considering it the most effective. However, a combination of approaches can be attractive solution to the membrane fouling problem. Moreover, hybrid membrane systems are being investigated intensively due to the combined positive effects of two or more technologies on membrane system performance as well as membrane fouling propensity. The quest for novel fouling control strategies/techniques is being undertaken by recent researches.

Chapter 3

Methodology

3.1 Phases of research

The research was carried out in two phases discussed as follows:

Phase I: Mechanically mixed MBR
Phase II: Hybrid MBR

3.1.1 Phase I: Mechanically mixed MBR

The aim of this research phase was to investigate hollow fiber membrane fouling mitigation and activated sludge modification under the influence of variable mechanical mixing conditions in submerged MBR. The 'roadmap' to investigate the influence of mechanical mixing on the biological as well as the hydrodynamic environments in submerged-MBR is summarized in Figure 3.1.

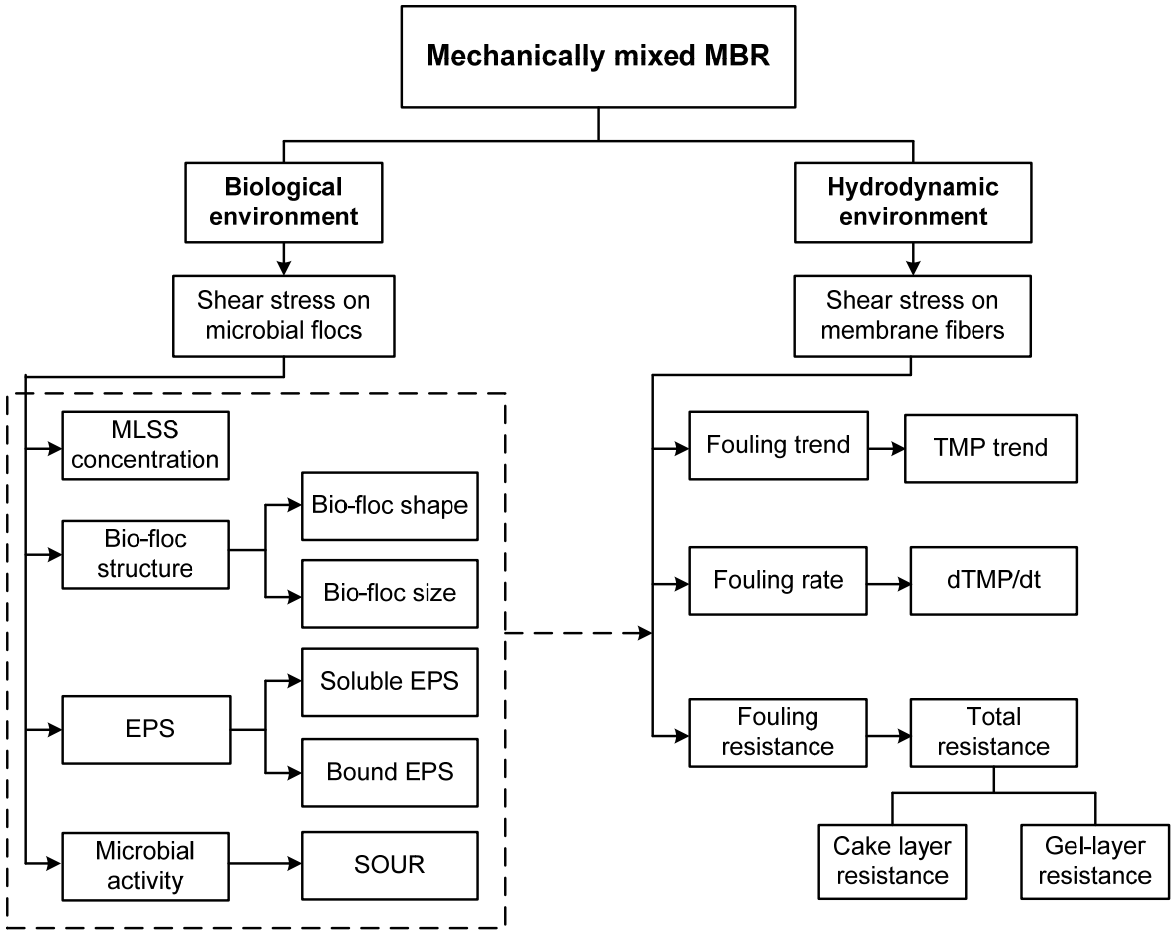

Figure 3.1: Influence of mechanical mixing on biological and hydrodynamic environments in a MBR

The methodology implemented towards Phase I is illustrated in Figure 3.2.

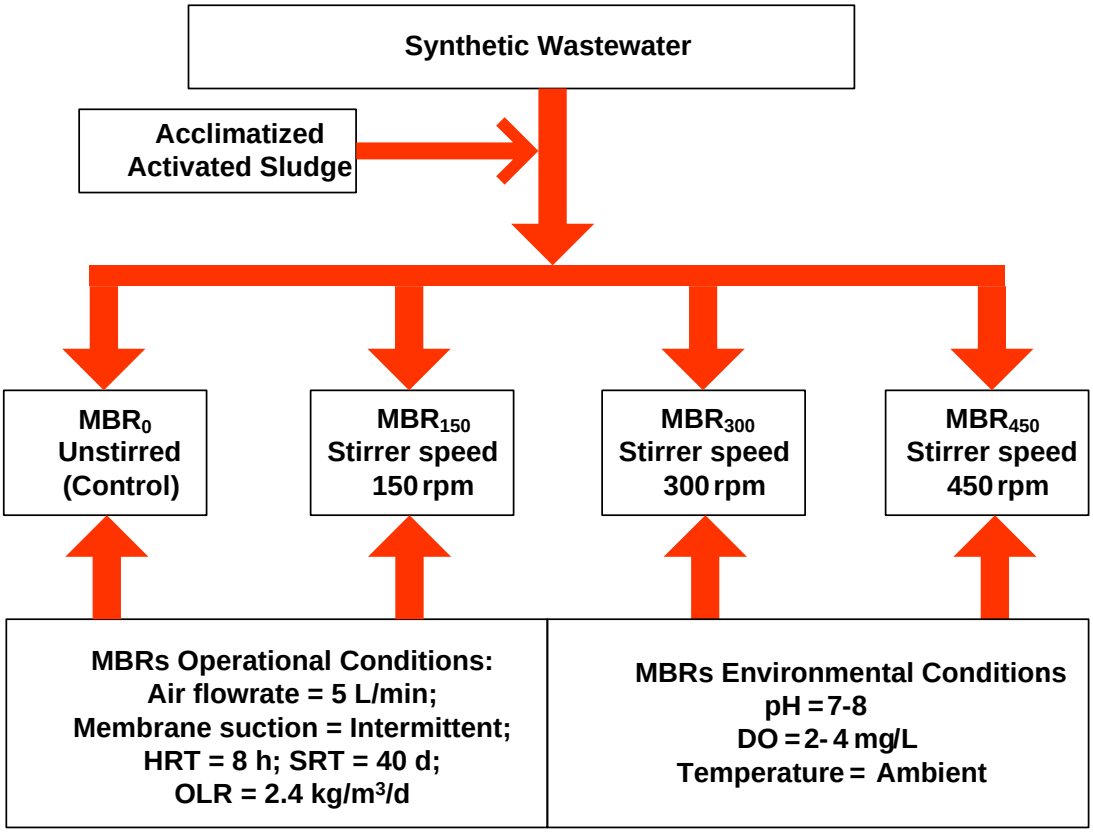

Figure 3.2: Phase I methodology

According to Figure 3.2, four MBRs were operated in an intermittent mode (10 min on, 2 min off) at a constant flux under similar HRT of 8 h. Each MBR consisted of a bioreactor with 10 L working volume and was supplied with air through air diffusers maintained at a flow rate of 5 L/min. HF membrane modules were submerged in the bioreactors with characteristics reported in Table 3.1.

Table 3.1: Hollow-fiber (HF) membrane characteristics

Item	Characteristic
Model	SteraporeSUR Series hollow-fiber micro-filtration membrane
Membrane material	Polyethylene
Pore size	0.1 µm
Filtration area	0.42 m^2
MLSS	5,000-12,000 mg/L recommended (minimum: 3,000 mg/L; maximum: 15,000 mg/L)
Temperature	15-35^oC
Filtration flow rate	Constant
Suction pressure	5-30 kPa
Intermittent suction	Operating time ≤ 13 min; relaxing time ≥ 2 min
Manufacturer	Mitsubishi Rayon Engineering Co. Ltd., Japan

Source: Mitsubishi Rayon (2004)

The schematic of the four laboratory-scale MBRs is shown in Figure 3.3.

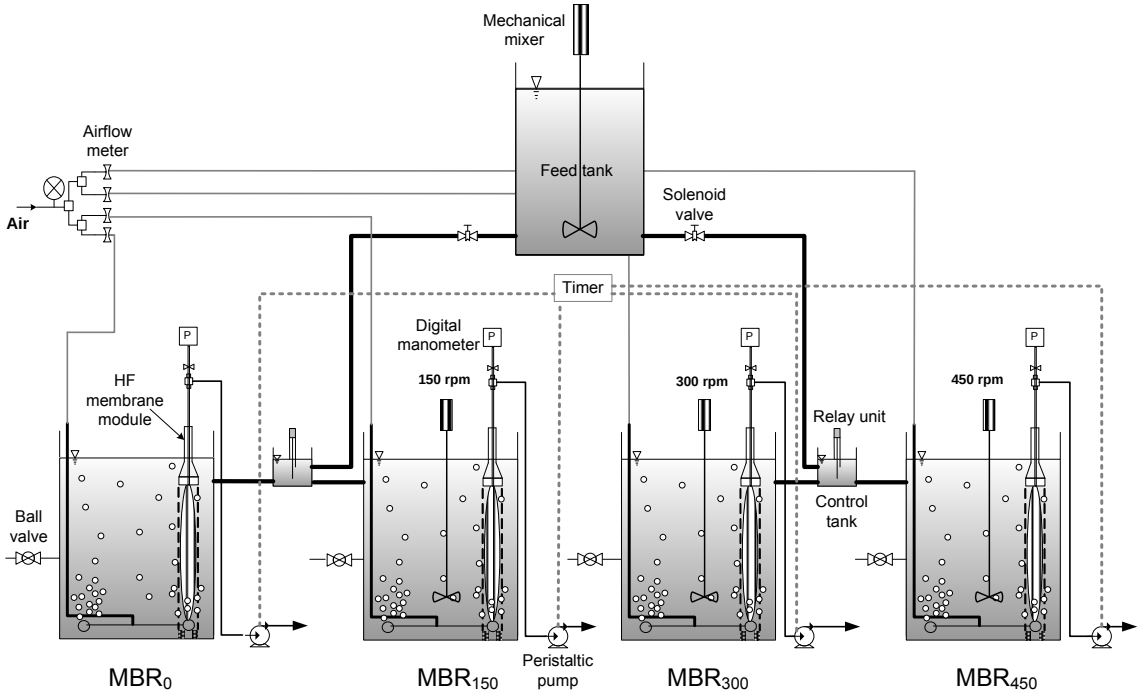

Figure 3.3: Schematic of the laboratory scale submerged-MBR systems

Based on cross-sectional area of bioreactor, the air flow rate was equivalent to an aeration intensity of 10.6 $m^3/m^2.h$ (m/h). The varying condition among the four MBRs was mechanical mixing with no stirring in control reactor (MBR_0) followed by stirring speeds at 150, 300 and 450 rpm in the MBR_{150}, MBR_{300} and MBR_{450}, respectively.

The shear intensities (G) corresponding to the mechanical stirring speeds in the MBRs were determined using expressions presented in Table 3.2 (Metcalf and Eddy, 2003) and values reported in Table 3.3. Detailed calculations of shear intensities (G) in the MBRs are reported in Appendix-A.

Table 3.2: Power requirement and shear intensity expressions

Expression	Unit	Formula	Remarks
Mechanical power (P_m)	W	$P_m = N_p \rho\, n^3 D^5$ $(N_R \geq 10{,}000)$ $N_R = \frac{D^2 n \rho}{\mu}$	ρ = density of mixed liquor (1000 kg/m^3); n = mixing speed (rev/s) ; D = diameter of impeller (0.1 m); N_p= Power number for impeller (N_p=1.1); N_R = Reynolds number
Pneumatic power (P_p)	kW	$P_p = p_a V_a \ln \frac{p_c}{p_a}$	p_a = atmospheric pressure (kPa); V_a = air flow rate (m^3/s); p_c = air pressure at the point of discharge (kPa)
Total power (P_T)	W	$P_T = P_m + P_p$	
Shear intensity (G)	1/s	$G = \sqrt{\frac{P_T}{\mu V}}$	V = reactor volume (0.01 m^3); μ = dynamic viscosity (N-s/m^2)

Source: Metcalf and Eddy (2003)

Table 3.3: Shear intensity (G) in the MBRs

MBR	Mechanical mixing (rev/s)	Pneumatic mixing (m^3/h)	Reynolds Number (N_R)	P_p (W)	P_m (W)	P_T (W)	G (1/s)
MBR_0	0.0	0.3	0	0.17	0.00	0.17	83
MBR_{150}	2.5	0.3	10,000	0.17	0.17	0.34	117
MBR_{300}	5.0	0.3	20,000	0.17	1.38	1.55	249
MBR_{450}	7.5	0.3	30,000	0.17	4.64	4.81	439

According to Table 3.3, the pneumatic mixing due to air supply and the corresponding power dissipated (P_P) remained constant while the mechanical mixing due to stirring and the corresponding power requirements (P_m) varied resulting in G variation among the MBRs. The shear intensity (G) was found to be 83, 117, 249 and 439 s^{-1} in the MBR_0, MBR_{150}, MBR_{300} and $MBR_{450,}$ respectively.

Synthetic wastewater and seed sludge

Synthetic wastewater simulating municipal wastewater was used as a substrate in the biological process with COD:N:P ratio of 100:10:2 and an OLR of 2.4 $kg/m^3.d$. The composition of the synthetic wastewater is reported in Table 3.4.

Table 3.4: Composition of synthetic wastewater

Component	Concentration (mg/L)
Anhydrous dextrose (Glucose)	516
Soya protein	250
NH_4Cl	229
KH_2PO_4	70
$MgSO_4.7H_2O$	10
$CaCl_2.2H_2O$	10
$FeCl_3$	3
$NaHCO_3$	750

Source: Adapted from Sombatsompop et al. (2006)

Commercial soya protein (SUPRO EX-33) from Food Equipment Co. Ltd., Thailand was utilized in the composition of synthetic wastewater. pH in the bioreactors was maintained between 7.0-7.5 using $NaHCO_3$ (750 mg/L). Seed sludge was taken from sequencing batch reactor (SBR) process of municipal wastewater treatment plant (Yannawa wastewater treatment plant, Bangkok, Thailand). The activated sludge was acclimatized with synthetic wastewater over a period of two months before seeding of the MBRs.

3.1.2 Phase II: Hybrid MBR

The aim of Phase II was to investigate membrane fouling mitigation in flocculent/adsorbent added hybrid MBRs by modifying the sludge properties. The 'roadmap' to achieve Phase II objectives is outlined in Figure 3.4.

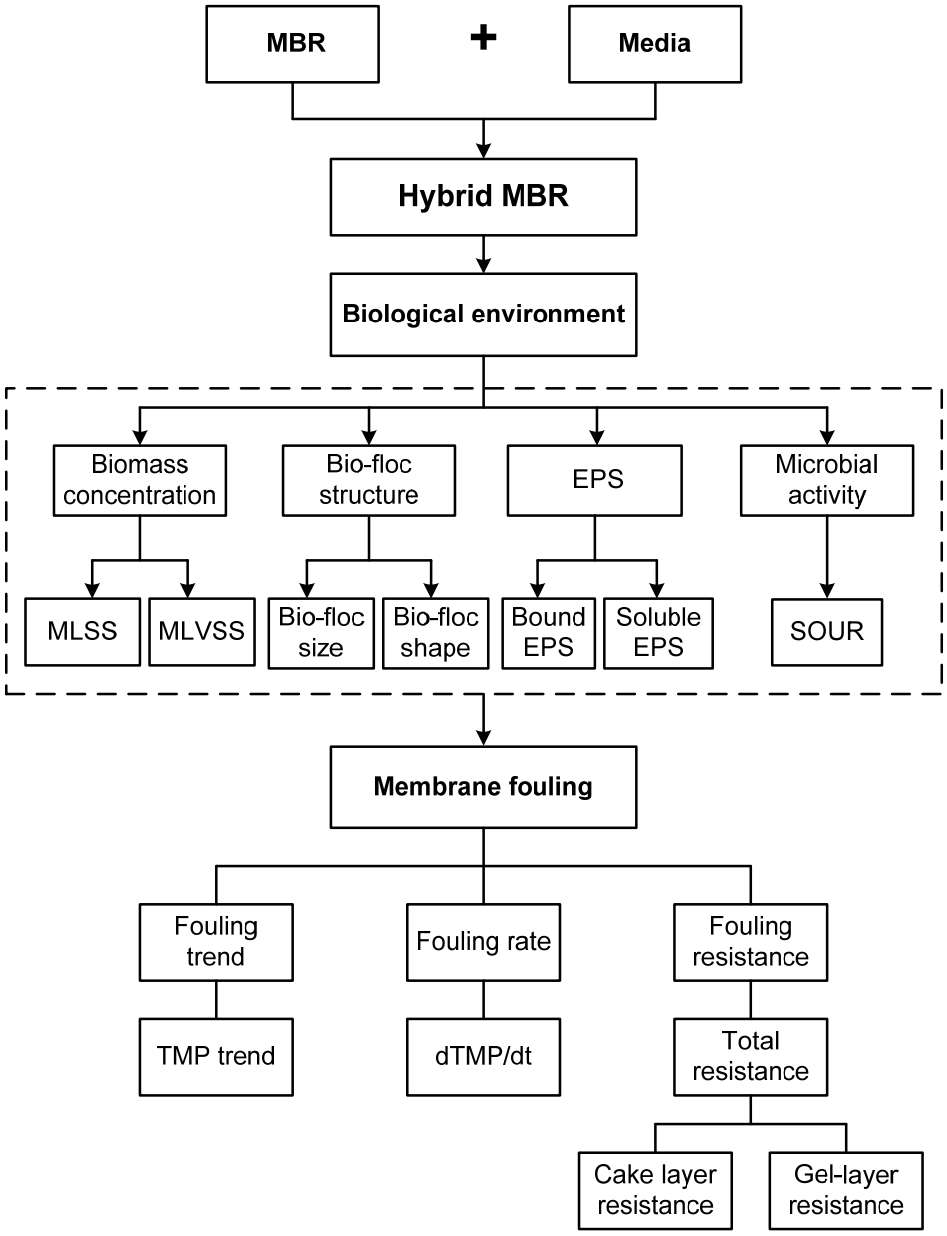

Figure 3.4: Influence of flocculent/adsorbent addition on biological environment and membrane fouling in a hybrid MBR

In Phase II, three laboratory-scale hybrid MBRs were developed with the addition flocculent/adsorbent for membrane fouling mitigation by physico-chemical approach and compared to conventional MBR ($MBR_{Control}$). Kaolin clay, NALCO® cationic polymer (MPE50) and powdered activated carbon (PAC) were added to MBR_{Clay}, $MBR_{Polymer}$ and MBR_{PAC}, respectively. The composition of synthetic wastewater as well as the operational conditions of the MBRs including OLR, SRT and aeration rate were similar to the one in Phase I. The methodology implemented towards Phase II is illustrated in Figure 3.5.

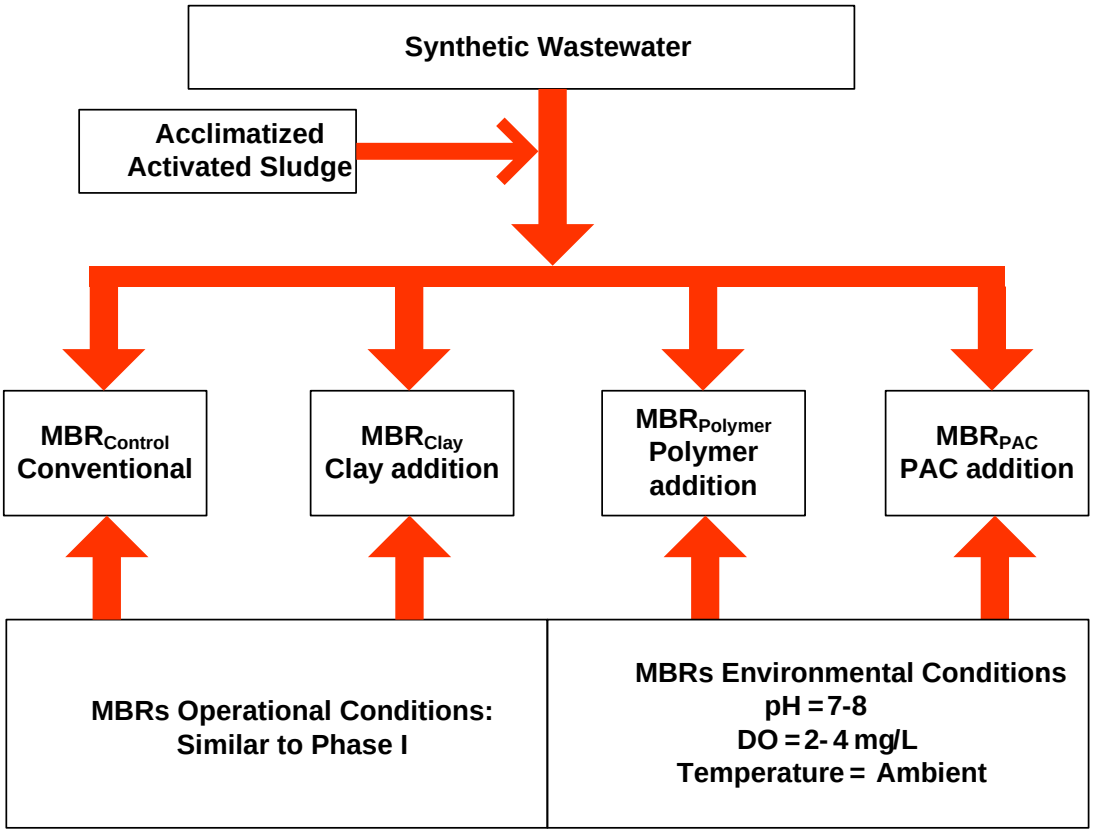

Figure 3.5: Phase II methodology

The condition of flocculent/adsorbent added to the MBRs is reported in Table 3.5.

Table 3.5: Condition of adsorbents/flocculants

Type of solution/suspension	Size range/solution condition
Cationic polymer (MPE50)	Soluble in water
Kaolin clay	Sieved (100-325 mesh)
Powder activated carbon (PAC)	Sieved (100-325 mesh)

The optimum initial dosages of clay, polymer and PAC in the MBR_{clay}, $MBR_{polymer}$ and MBR_{PAC}, respectively were determined using jar test.

Jar test procedure

The following classical jar test procedure was used:

1. Mixed liquor sample volume of 500 mL
2. Rapid mixing at 120-150 rpm for 2 min
3. Slow mixing at 30-40 rpm for 20 min
4. Settling for 30 min

The optimum initial concentration of flocculent/adsorbent was determined based on the visual inspection of sludge settling, the settled sludge volume after 30 min and the soluble

COD (SCOD) concentration in the supernatant of settled sludge. The daily addition of the flocculent/adsorbent to the MBRs was calculated based on 40 d SRT.

3.2 Analytical methods

The list of parameters that were analyzed, method adopted to determine each parameter and equipment/material used is reported in Table 3.6.

Table 3.6: Analytical parameters, methods and equipment/material

Parameter	Method	Equipment/Material	Reference
MLSS-MLVSS	Filtration-Evaporation	1.2 µm glass microfiber filter (GF/C, Whatman); 105^{o}C oven (MLSS); 550^{o}C oven (MLVSS)	APHA (2005)
COD	Close reflux	COD tube; 150^{o}C oven	APHA (2005)
Specific cake resistance (α)	Dead-end filtration at constant pressure	Filtration cell (Amicon, Model 8400, USA); 0.22-µm flat-sheet cellulose membrane filter (Millipore, GVWP 09050, USA)	Rosenberger et al. (2006); Foley (2006);
Capillary suction time (CST)	Rate of water release	CST apparatus (Triton electronic Ltd, UK); CST filter	APHA (2005)
Specific oxygen uptake rate (SOUR)	Rate of DO depletion	DO meter (YSI, Model 52, USA)	Xing et al. (2001); Mathieu and Etienne (2000); APHA (2005)
Soluble EPS	Centrifugation at 4,000 g followed by 20,000 g	Centrifuge with 4000 g capacity (Hettich Universal 320R, UK); Centrifuge with 20,000 g capacity (Hettich Mikro 22R, UK);	Zhang et al. (2006)
Bound EPS	Cation exchange resin (CER) extraction method	CER (DOWEX HCR-S/S, Dow Chemical Company, USA)	Frolund et al. (1996)
Carbohydrate concentration	Colorimetric method	Spectrophotometer (U-2001, Hitachi, Japan)	Dubois et al. (1956)
Protein concentration	Colorimetric method	Spectrophotometer (U-2001, Hitachi, Japan)	Lowry et al (1951)
Sludge morphology	Microscopic observation	Microscope (OLYMPUS CX 40, Japan)	Bai and Leow (2002)

The detailed protocols for the measurement of the analytical parameters are discussed in the following sections.

3.2.1 Specific cake resistance (α)

Batch filtration tests were performed to determine the specific cake resistance (α) of the sludge samples. The test was conducted in a 400 mL unstirred filtration cell (Model 8400, Amicon, USA) using a 0.22-μm flat-sheet cellulose membrane filter (GVWP 09050, Millipore, USA) as shown in Figure 3.6.

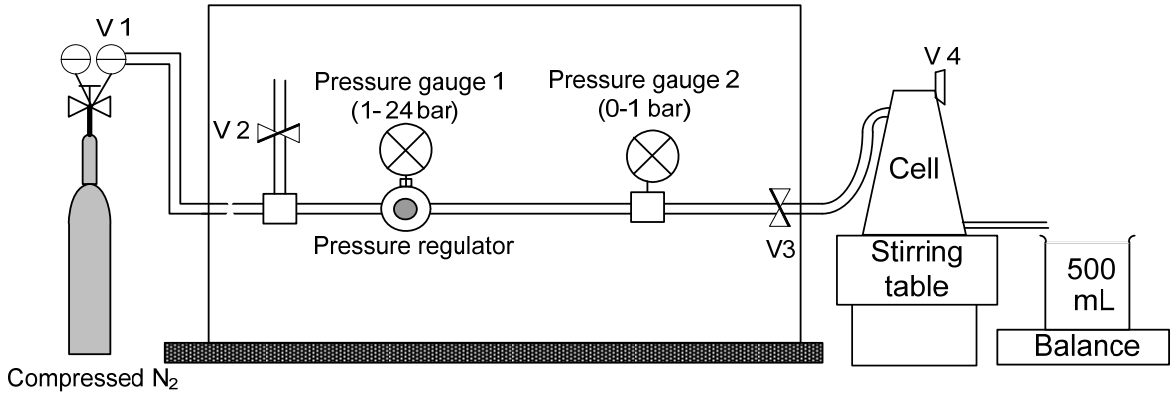

Figure 3.6: Specific cake resistance experimental setup

The cell was filled with 200 mL of mixed liquor sample and a constant pressure of 30 kPa was applied by pressurized nitrogen from a gas cylinder. The filtrate was continuously recorded by an electronic balance connected to a notebook using WINWEDGE software. The specific cake resistance (α) (m/kg) was calculated (Wang et al., 2007) by

$$\alpha = \frac{2000 A^2 \Delta P}{\mu C} \frac{t/V}{V} \qquad \text{Equation 3.1}$$

where ΔP is the applied pressure (kPa), A is the filtration area (0.00418 m^2), C is the MLSS concentration (kg/m^3), μ is the viscosity of permeate (N-s/m^2) and [(t/V)/V] (s/m^6) is the slope of the straight portion of the curve that is obtained by plotting the time of filtration to volume of filtrate (t/V) versus the filtrate volume (V).

3.2.2 Normalized capillary suction time (CST_N)

The capillary suction time (CST) of the sludge samples from the MBRs was determined using the CST apparatus (Triton electronic Ltd, UK). However, the CST measurement which reflects the dewatering rate of sludge in units of time (seconds) does not take into account the suspended solids (SS) concentration due to which comparative evaluation of sludge dewaterability among different MBR systems becomes imprecise. In order to minimize the effect of SS on CST, the CST values were normalized by dividing with the SS concentration for each MBR sludge sample. Thus the expression used to determine CST_N was as follows:

$$CST_N[s/(g/L)] = \frac{CST(s)}{SS(g/L)} \qquad \text{Equation 3.2}$$

3.2.3 Specific oxygen uptake rate (SOUR)

The following protocol used for SOUR measurement was modified from Standard Methods (APHA, 2005):

1. Preparation of DO meter (YSI, Model 52) by switching it on 20 minute prior to usage.
2. 300 mL activated sludge was aerated for 2 hours (Xing et al., 2001) to reach endogenous respiration phase, that is, all the available substrate was consumed reaching DO saturation (> 6 mg/L).
3. Once endogenous respiration rate was reached, the biomass sample was transferred to 300 mL BOD bottle and substrate sample was injected with S/X ratio of 0.02 gCOD/gVSS (Mathieu and Etienne, 2000).
4. After substrate addition, the decrease in DO was recorded every 10 seconds.
5. Recording was stopped once DO dropped below 1 mg/L.

Concentration of substrate sample

The concentration of substrate test sample was determined using the following expression:

$$C = \frac{aXV}{v} \qquad \text{Equation 3.3}$$

where C = substrate concentration in 1mL injected sample
a = S/X ratio = 0.02
X = biomass concentration ≈ 6,000 mg/L
S = substrate concentration
V = respirometer vessel = 300 mL (BOD bottle)
v = injection volume = 1 mL

$$C = \frac{0.02 \times 6000 \times 300}{1} = 36{,}000\, mg/L$$

Oxygen uptake rate (OUR) calculation

The oxygen uptake rate (OUR) was determined by the slope of the linear curve that is obtained by plotting the observed DO (mg/L) readings versus time (minutes) and using the following expression:

$$OUR\ (mg/L)/h = \frac{DO_{start} - DO_{end}}{t_{elapsed}} \times \frac{60\,\text{min}}{h} \qquad \text{Equation 3.4}$$

Where DO_{start} = DO at start of test interval
DO_{end} = DO at end of test interval
$t_{elapsed}$ = Elapsed time in minutes between two consecutive DO readings

Specific oxygen uptake rate (SOUR) calculation

The specific oxygen uptake rate (SOUR) was calculated by normalizing the OUR with the active biomass (MLVSS) concentration using the following expression:

$$SOUR\ (mg/g)/h = \frac{OUR\ (mg/L/h)}{MLVSS(g/L)} \qquad \text{Equation 3.5}$$

3.2.4 Extracellular polymeric substance (EPS) analysis

Mixed liquor samples of 50 mL from the four MBRs were taken and cooled immediately at 4^{o}C to minimize microbial activity. Soluble EPS was obtained by centrifugation of the mixed liquor at 4000 g for 20 min followed by high speed centrifugation at 20,000 g for 20 min and separation of the supernatant (Zhang et al., 2006). Bound EPS was extracted from the mixed liquor using cation exchange resin (CER) extraction method (Frolund et al., 1996). The CER (DOWEX HCR-S/S, Dow Chemical Company, USA) used was in Na^{+} form with bead size distribution range between 16-50 mesh. The centrifuged sludge was re-suspended in a phosphate buffer solution and the CER (70 g CER/g MLVSS) was added and mixed at 600 rpm for 1 h. Then the mixture was centrifuged twice at 4000 g for 10 and 20 min, respectively, to obtain the supernatant as bound EPS. Carbohydrate and protein fractions of the soluble and bound EPS were measured by the colorimetric methods of Dubois et al. (1956) and Lowry et al. (1951), respectively using spectrophotometer (U-2001, Hitachi, Japan). D-Glucose and Bovine serum albumin (BSA) were used as carbohydrate and protein standards, respectively. Further details on the soluble and bound EPS measurement in terms of carbohydrate and protein concentrations and the carbohydrate and protein standard curves are discussed in Appendix-B.

3.2.5 Soluble and colloidal COD concentration

Soluble COD concentration representing dissolved and colloidal matter was measured in the supernatant of centrifuged sludge sample at 4000 g for 20 min. The effluent COD concentration was measured in the effluent from the HF membrane module having pore size of 0.1 μm. Thus, the colloidal COD concentration of each sludge sample was determined by subtracting the effluent COD from the soluble COD concentration.

3.2.6 Particle and colloidal size distribution

Particle and colloidal size distribution in sludge samples were determined by equipments reported in Table 3.7.

Table 3.7: Determination of particle and colloidal size distribution

Item	Equipment	Size range	Sample
Particle size distribution	Mastersizer S (Malvern, UK)	0.05-900 μm	Original mixed liquor
Colloidal size distribution	Zetasizer Nano ZS (Malvern, UK)	0.6-6000 nm	Supernatant

Colloidal distribution was measured in the supernatant of activated sludge sample centrifuged at 4500 rpm for 1 min.

3.2.7 Sludge morphology

The microbial sludge morphology was determined using microscope (Olympus, CX40, Japan) equipped with digital camera (Moticam 1000, China) producing images of 1.3 mega pixels. The images were captured and edited on computer using Motic Images Plus 2.0 software.

3.2.8 Membrane fouling characterization

Membrane fouling propensity

The behavior of membrane fouling in the MBRs was monitored in terms of rise in TMP with operational time. In this regard, flux and TMP were recorded on regular basis. The operation was stopped when TMP reached 30 kPa and chemical cleaning procedure was carried out. The membrane fouling rates (dTMP/dt) were determined from profiles of the TMP versus operational duration. At the end of the membrane operational cycles, the resistance analysis was carried out to evaluate the membrane fouling characteristics under each set of MBR conditions.

Membrane fouling resistances

The resistance-in-series model was applied to evaluate the filtration characteristics using following equations (Lee et al., 2001; Rosenberger et al., 2006):

$$J = \frac{\Delta P}{\mu . R_t . f_t}, \quad f_t = e^{-0.0239(T-20)} \qquad \text{Equation 3.6}$$

$$R_t = R_m + R_c + R_f \qquad \text{Equation 3.7}$$

where J is the operational flux, ΔP is the TMP, μ is the viscosity of permeate, f_t is the temperature correction to 20^{o}C to account for the dependence of permeate viscosity (μ) on temperature, R_t is the total hydraulic resistance, R_m is the intrinsic membrane resistance, R_c is the reversible cake resistance formed by the cake layer deposited over the membrane surface and R_f is the irreversible fouling or gel layer resistance caused by adsorption of dissolved and colloidal matter onto the membrane surface and into the pores.

R_m was measured by filtering de-ionized (DI) water through a chemically cleaned membrane and R_t was measured from the final flux and TMP values at the end of each operation cycle. R_m + R_f was measured by filtering DI water through the membrane after removing the cake layer with tap water. Each of the R_t, R_m, R_c and R_f values were obtained using the following equations.

$$R_t = \frac{\Delta P_{MBR}}{\mu . J} \quad \text{Equation 3.8}$$

$$R_m + R_f = \frac{\Delta P'_w}{\mu . J} \quad \text{Equation 3.9}$$

$$R_m = \frac{\Delta P_w}{\mu . J} \quad \text{Equation 3.10}$$

$$R_f = \left(R_m + R_f\right) - R_m \quad \text{Equation 3.11}$$

$$R_c = R_t - \left(R_m + R_f\right) \quad \text{Equation 3.12}$$

where J is the constant flux, P_{MBR} is the final TMP at the end of the MBR operational cycle, $P^{/}_{w}$ is the TMP at filtering DI water through the membrane after removing the cake layer and P_w is the TMP at filtering DI water through the chemically cleaned membrane.

Membrane cleaning

The HF membrane module cleaning process known as 'out-of-system immersion cleaning' (Mitsubishi Rayon, 2004) was implemented that involved two main stages. In the first stage, the membrane was physically cleaned to remove all visible cake layer deposited on the membrane fibers and within adjacent fibers. In the second stage, the membrane was chemically cleaned to decompose organic matter deposited on the membrane surface and inside pores restoring the intrinsic TMP. The protocol for out-of-system immersion cleaning and membrane resistance measurement is represented in Figure 3.7.

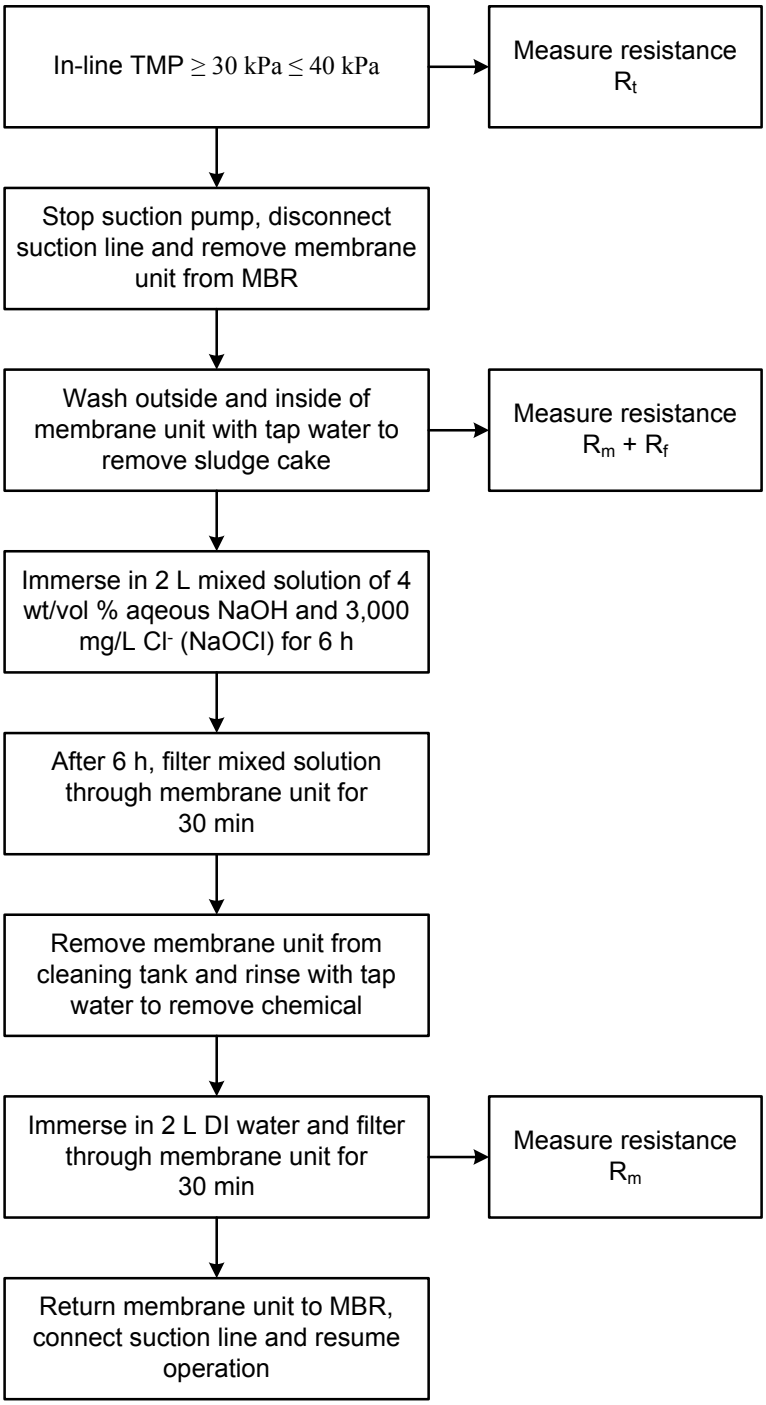

Figure 3.7: Protocol for membrane cleaning and membrane resistance measurement

Chapter 4

Results and Discussion

The results and discussion section is divided into two parts as per the two phases of the research work. In the first part, the hydrodynamic approach towards fouling mitigation in terms of mechanical mixing intensities is discussed. In this part, a comparative study of the fouling behaviors and sludge characteristics among four MBRs was carried out with aeration only in MBR_0 supplemented by mechanical stirring at 150, 300 and 450 rpm in MBR_{150}, MBR_{300} and MBR_{450}, respectively. In the second part, physico-chemcial approach towards fouling mitigation by the development of hybrid MBRs with the addition of flocculent/adsorbent agents to MBRs is discussed. In this section, a comparative evaluation of the fouling propensities and modified sludge properties among three hybrid MBRs was conducted with the addition of clay suspensions, NALCO® cationic polymer (MPE50) and powdered activated carbon (PAC) to MBR_{Clay}, $MBR_{Polymer}$ and MBR_{PAC}, respectively. The analytical results of the three hybrid MBRs were compared to that of the conventional MBR ($MBR_{Control}$) from Phase I.

4.1 Phase I: Mechanically mixed MBRs

The MBRs were run in a steady-state condition over a period of 120 days and the values of all the experimental parameters were averaged along with standard deviation as reported in Appendix-C. The MLSS concentration was maintained between 6-8 g/L with MLVSS/MLSS ratio of approximately 90% at SRT of 40 d for the 120 days of MBRs operation (Appendix-C; Table C-3). The COD removal efficiency of the MBRs was above 95% representative of effective biodegradation and physical separation by the HF membranes.

4.1.1 Filtration behavior in the MBRs

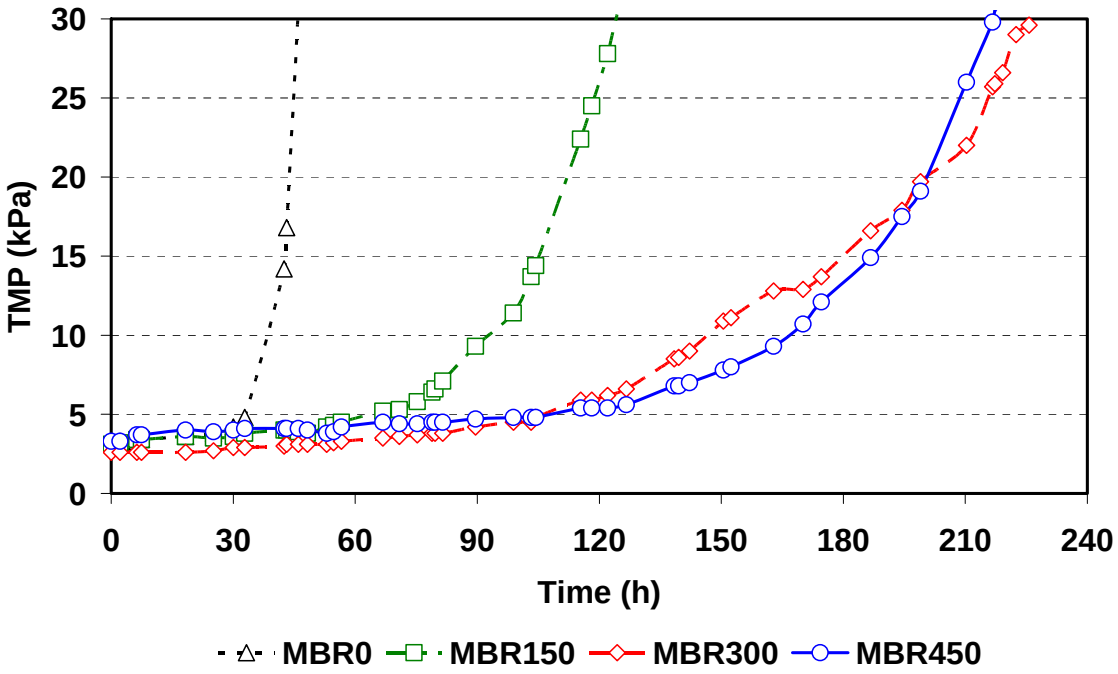

Figure 4.1: TMP profile at constant flux during the MBRs operation

Typical TMP trend in each of the four MBRs during filtration period is shown in Figure 4.1 and TMP and flux data versus time for this typical filtration run is reported in Appendix-C (Table C-1). During this phase of the mechanically mixed MBR study, accurate reproducibility of the TMP trends was problematic due to the complexities of the MBR design which included covering of the HF membrane module with plastic net. In order to avoid damage of the moving hollow fibers during aeration by the mechanical impeller, the fibers movement was confined within the proximity of the net as shown in Figure 3.3. The plastic net at times behaved as a barrier for free movement of the bio-particles across the HF bundle and also the net experienced clogging before actual membrane fouling took place on several occasions.

Figure 4.1 shows that the membrane in MBR_0 fouled rapidly followed by the one in MBR_{150}. However, membrane filtration in MBR_{300} and MBR_{450} could be achieved up to five times the filtration period of MBR_0. Taking into consideration the relatively similar biomass concentrations among the MBRs, MBR_{300} and MBR_{450} demonstrated lower fouling tendency in terms of the filtration duration. Moreover, filtration duration could not be further increased in MBR_{450} with a higher G as compared to the one in MBR_{300}. In Figure 4.1, all the TMP profiles exhibited two-stage process. Initially, linear gradual TMP rise was observed followed by sudden increase in the rate of TMP rise leading to need for membrane chemical cleaning.

There are two significant parameters during the first stage: the critical time (t_{crit}) over which the first stage is maintained and the fouling rate (dTMP/dt) during this stage (Pollice et al., 2005). Figure 4.1 shows that the first stage of fouling was maintained until TMP reached 7 kPa in the four MBRs operation. The TMP profile data (Appendix-C; Table C-1) revealed that the t_{crit} was observed at approximately 30, 80, 130 and 140 h during operation of MBR_0, MBR_{150}, MBR_{300} and MBR_{450}, respectively. The longer duration maintained in the MBR_{300} and MBR_{450} for the first fouling stage can be mainly attributed to the high shear intensity on membrane fibers induced by mechanical stirring.

4.1.2 Membrane fouling rates

Based on the membrane filtration performances in the MBRs (Figure 4.1), the membrane fouling rates (dTMP/dt) during the first and second fouling stages were determined. The first stage ranged from the start-up TMP of 3 to 7 kPa and the second stage ranged from 10 kPa to the terminating TMP of 30 kPa. TMP between 7 and 10 kPa was considered as a transition phase. The fouling rates of the two phases as shown in Figure 4.2 were determined by the slope of the linear curve from the TMP versus time plot. The TMP versus time plots for the two fouling stages are reported in Appendix-C (Figures C-1 and C-2).

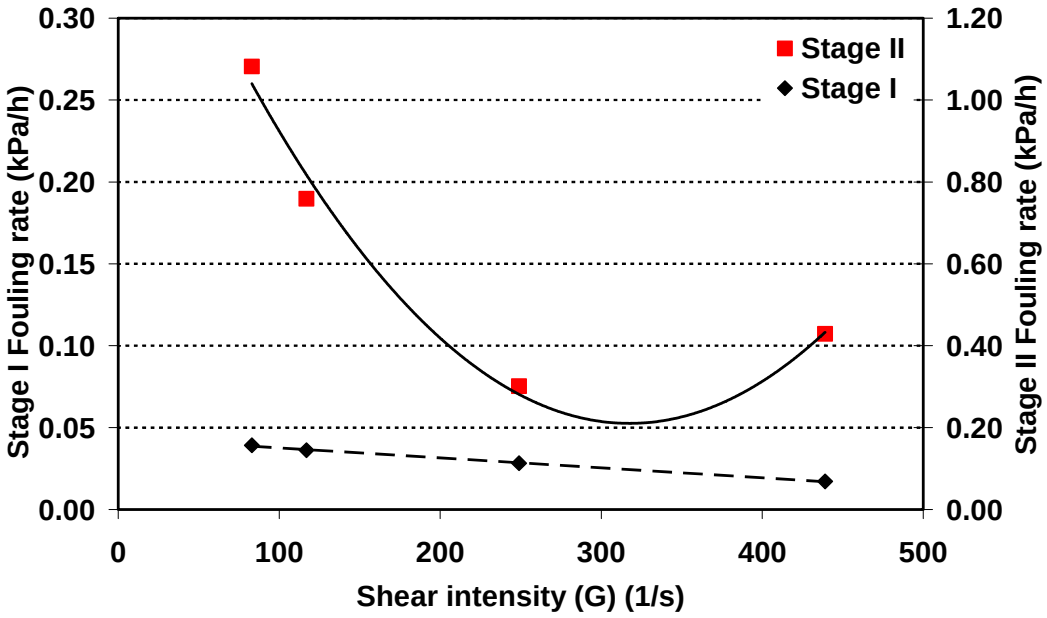

Figure 4.2: Fouling rates corresponding to shear intensities in the MBRs
Shear intensity (G): MBR_0 = 83 s^{-1}, MBR_{150} = 117 s^{-1}, MBR_{300} = 249 s^{-1}, MBR_{450} = 439 s^{-1}

The first stage fouling rates are representative of pore blocking, biopolymer deposition, biofilm attachment and growth, all contributing to steady TMP rise (Zhang et al., 2006). Figure 4.2 shows that the first stage fouling rates in the MBRs relatively decreased linearly with increase in shear intensities. Indeed, the high shear stress exerted on membrane fibers retard biofloc deposition and avoids sludge accumulation between fibers, particularly in the central region of the bundle. Wicaksana et al. (2006) found that with increased fiber movement induced by high air flow rate appears to reduce the rate of biofloc deposition on the membrane surface and slow down the rise of TMP at fixed flux. The second stage fouling rates, as expected, were found to be significantly higher than that in the first stage. However, the second stage fouling rate in MBR_{450} operation was found to be relatively higher than that in MBR_{300} which was indicative of optimum shear intensity in the MBR_{300} as shown in Figure 4.2. At this point, it can be inferred that a mixing intensity of certain extent is feasible to mitigate fouling, beyond which it becomes disadvantageous.

4.1.3 Membrane fouling resistances

The resistance-in-series model was applied to evaluate the filtration characteristics. The resistance analysis results summarized in Table 4.1 represent the averaged resistance values after replicate experimental measurements as reported in Appendix-C (Tables C-4, C-5, C-6 and C-7).

Table 4.1: Fouling resistances of membrane in the MBRs

Resistances	MBR_0	MBR_{150}	MBR_{300}	MBR_{450}
R_t ($\times 10^{12}$ m^{-1})	79.46	83.51	76.55	76.57
R_c ($\times 10^{12}$ m^{-1})	78.36	82.31	75.10	75.43
R_f ($\times 10^{12}$ m^{-1})	0.72	0.77	0.85	0.75
R_m ($\times 10^{12}$ m^{-1})	0.39	0.43	0.60	0.39
R_c/R_t (%)	98.6	98.5	98.1	98.6

Since the operational cycle in all the MBRs was terminated at TMP of 30 kPa, the total resistance (R_t) was expected to be relatively similar as presented in Table 4.1. However, the cake resistance (R_c) was the predominant resistance fraction of the total resistance (R_t) for all the MBRs contributing about 98-99%. The irreversible fouling resistance (R_f) was significantly lower as compared to the cake resistance (R_c) in the MBRs. Similar membrane resistance observations were reported in Lee et al. (2001) and Sombatsompop et al. (2006) where the cake resistance (R_c) was the main component (R_c contributing > 80%) of the total hydraulic resistance (R_t) in suspended growth MBRs. From this point onwards, the sludge characteristics and their influence on fouling propensities in the MBRs under the different shear intensities are discussed.

4.1.4 Sludge filterability characteristics

Sludge filterability was characterized by the normalized CST (CST_N) and the specific cake resistance (α). CST_N is a quantitative measure of the rate of water release from sludge per unit of SS concentration and is indicative of the filterability and dewaterability of sludge. In contrast, specific cake resistance is a more authentic and reliable parameter for measuring the fouling potential or filterability of sludge cake. Figure 4.3 shows the averaged specific cake resistance (α) and the CST_N for sludge samples from the MBRs. The filterability of sludge improved with increase in shear intensity up to 249 s^{-1} (MBR_{300}) in terms of both the specific cake resistance (α) and the CST_N. However, the filterability slightly deteriorated for the MBR_{450} sludge sample indicating that floc properties of MBR_{300} exhibited lowest fouling potential. In MBR_{450}, the low fouling rate during Stage I due to higher turbulent condition was balanced out with high fouling rate during Stage II attributed to lower sludge filterability (Figure 4.3) resulting in overall filtration duration similar to that in the MBR_{300}. It can be inferred that it was the appropriate hydrodynamic condition as well as the suitable sludge filterability of MBR_{300} which influenced the observed low fouling behavior.

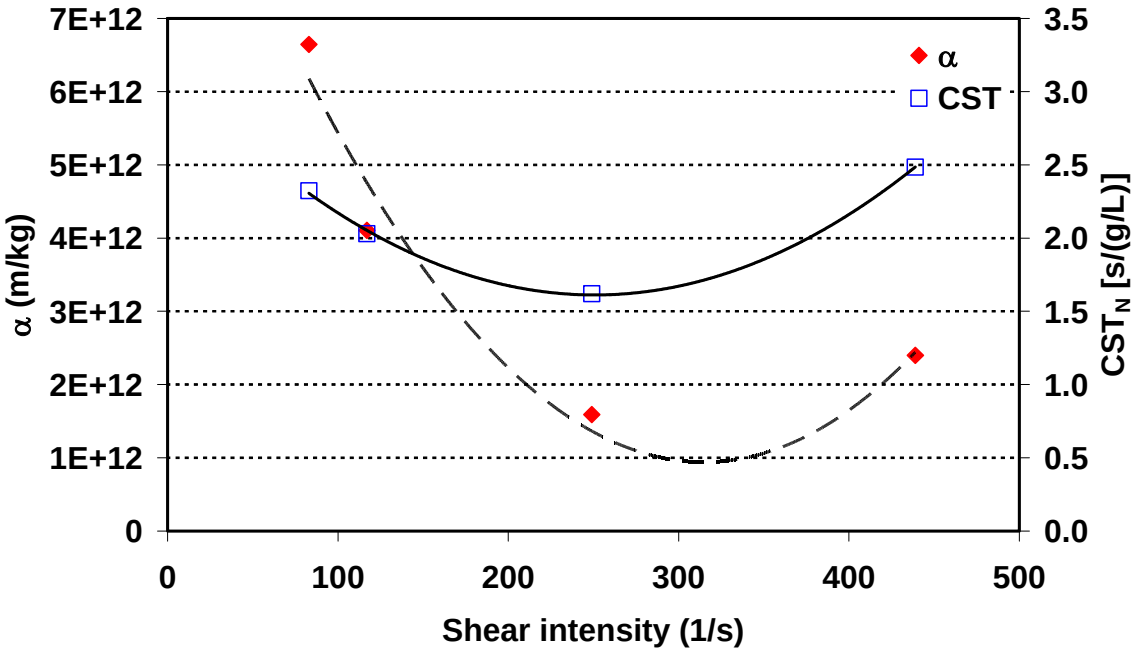

Figure 4.3: Specific cake resistance (α) and CST_N of the MBR sludge samples
Shear intensity (G): MBR_0 = 83 s^{-1}, MBR_{150} = 117 s^{-1}, MBR_{300} = 249 s^{-1}, MBR_{450} = 439 s^{-1}

4.1.5 Particle and colloidal size distribution

The particle size distribution in the MBRs was evaluated on the basis of percentage of particle diameter by volume of MBR sample at the end of the 120 days operation of Phase I. The particle size distributions within the ranges of 0.05-750 µm and 0.05-20 µm in the four MBRs are illustrated in Figures 4.4 (a) and 4.4 (b), respectively.

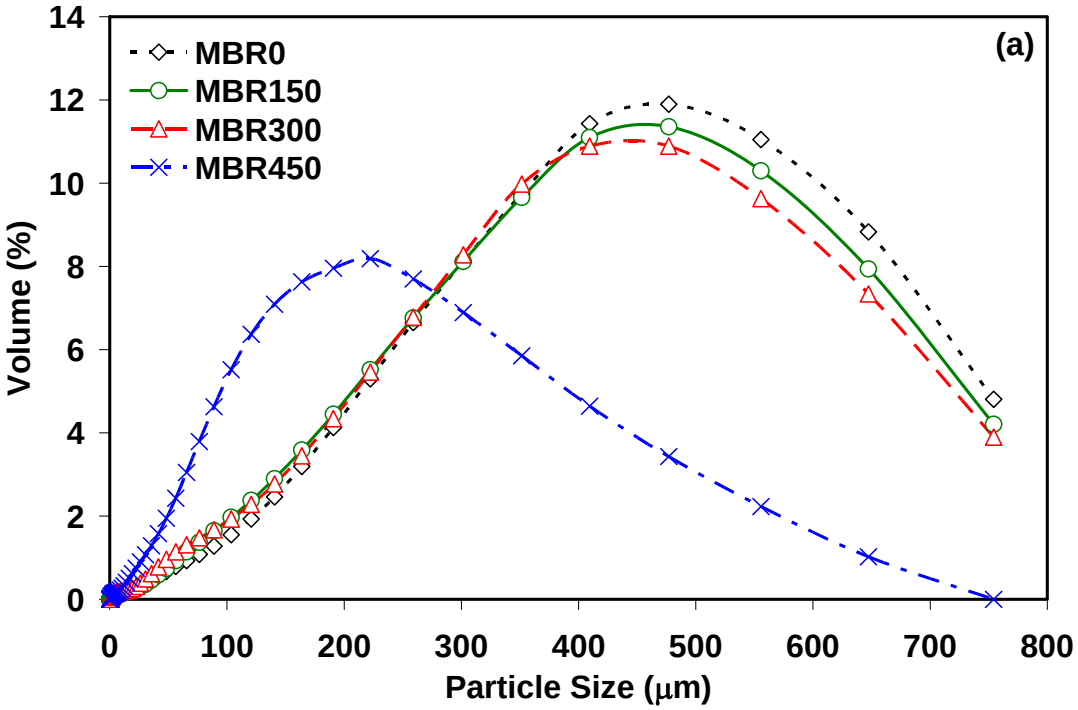

Figure 4.4 (a): Particle size distribution of sludge suspension in the MBRs (0.05-750 µm)

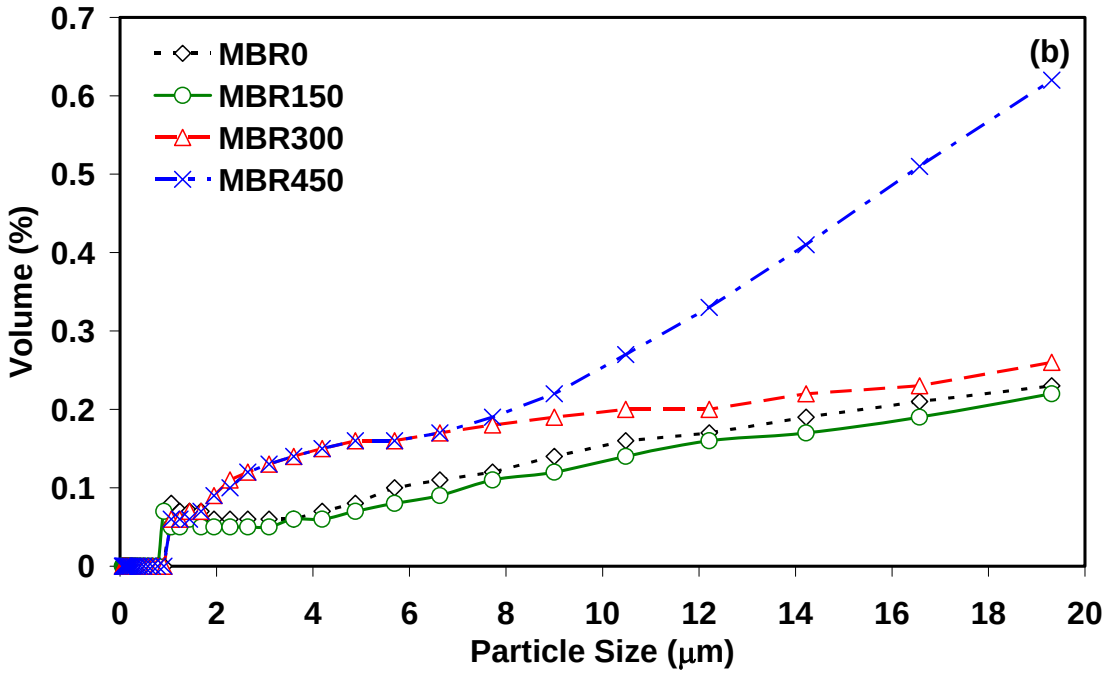

Figure 4.4 (b): Particle size distribution of sludge suspension in the MBRs (0.05-20 µm)

The median particle sizes were found to be 398, 379, 367 and 183 µm in the MBR_0, MBR_{150}, MBR_{300} and MBR_{450}, respectively. The bio-particle sizes slightly reduced with increase in G from MBR_0 to MBR_{300}. However, beyond G value of 249 s^{-1} in MBR_{300}, the median particle size was reduced to almost half of that in the MBR_{300}. It is evident from Figure 4.4 (a) that the extent of distributions from MBR_0 to MBR_{300} was slightly different but MBR_{450} not only exhibited significant reduction in particle sizes but a scattered distribution as well. This implies that the bio-flocs are able to withstand shear stress up to a certain level beyond which the flocs significantly disintegrate resulting in smaller bio-particles. The notion of significant bio-floc breakage in MBR_{450} ($G = 439\ s^{-1}$) as compared to that in the other MBRs ($G < 250\ s^{-1}$) is also established in Figure C-3 (Appendix C) showing accumulative volume (%) versus particle size (µm).

Moreover, Figure 4.4 (b) shows that the bio-particle distributions from MBR_0 to MBR_{300} revealed similar trends within the range of 0.05-20 µm with exception of MBR_{450} where higher percentage of floc sizes greater than 10 µm suggested breakage of floc structure. The floc breakage into smaller particles under severe turbulent condition of MBR_{450} could have induced the relative deterioration of the sludge filterability as depicted in Figure 4.3. However, the significantly improved fouling potential of MBR_{300} sludge could not be clearly explained with the particle distribution results.

Bai and Leow (2002) studied the effect of mechanical mixing intensity on membrane fouling in a cross-flow microfiltration (CFMF) system and observed that finer particles (<50 µm) caused severe membrane fouling. However, Sombatsompop et al. (2006) found that membrane fouling in an attached growth submerged MBR system improved in the presence of small particles (17-33 µm). Moreover, Lee et al. (2003) found that in submerged MBR operation, the increase in mean colloidal sizes with increase in SRT could not affect the overall fouling resistance. Since activated sludge is a complex broth, it is not possible to explain the membrane fouling phenomenon explicitly on the basis of particle size.

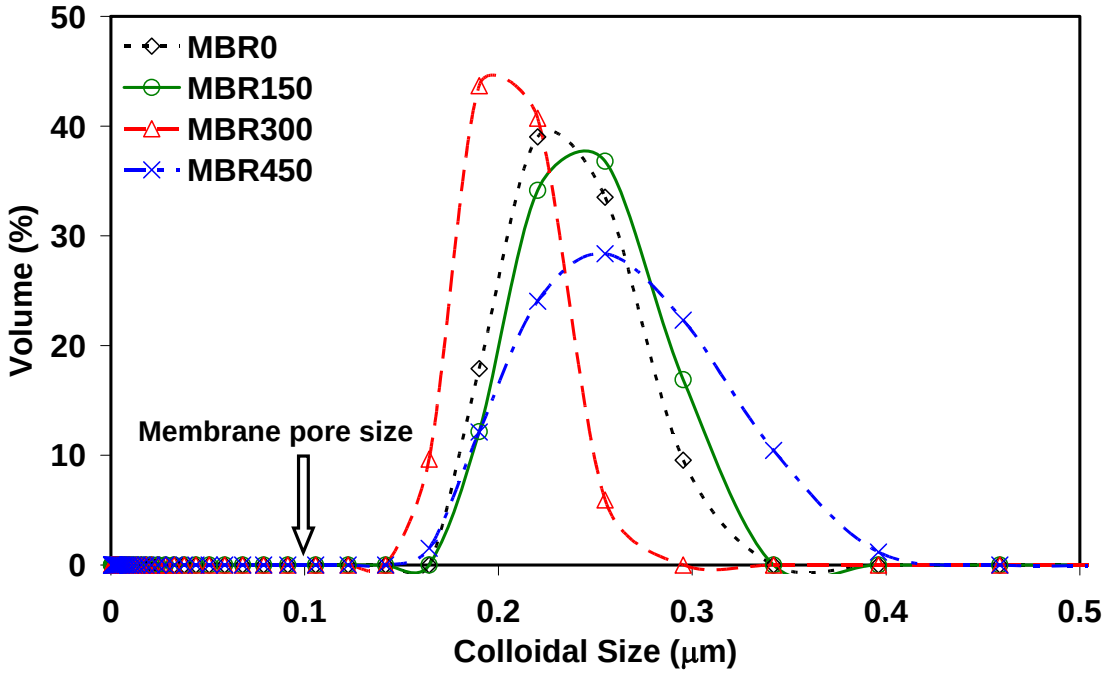

Figure 4.5: Colloidal distribution in the supernatant of sludge suspension in the MBRs

The influence of shear intensity on the colloidal distribution in the supernatant of sludge suspension was evaluated also as shown in Figure 4.5. The colloidal distribution was presented in terms of colloidal percentage by volume. The median colloidal diameters were found to be 0.236, 0.245, 0.205 and 0.263 μm in the MBR_0, MBR_{150}, MBR_{300} and MBR_{450}, respectively reflecting almost similar colloidal sizes in the four MBRs.

The colloidal particle range in wastewater has been defined from 0.01 to 1.00 μm (Metcalf and Eddy, 2003). Based on this definition, the colloids in the supernatant of the sludge in the MBRs were larger than the pore-size of the membrane (0.1 μm) discarding the possibility of colloidal fouling during the first fouling stage. This argument is supported by the low irreversible fouling resistances (R_f) of membranes in the MBRs (Table 4.1).

4.1.6 Concentration of soluble and colloidal matter

The amount of soluble and colloidal matter which is basically SMP was represented by the soluble COD and colloidal COD concentrations respectively. The soluble, effluent and colloidal COD concentrations are shown in Figure 4.6.

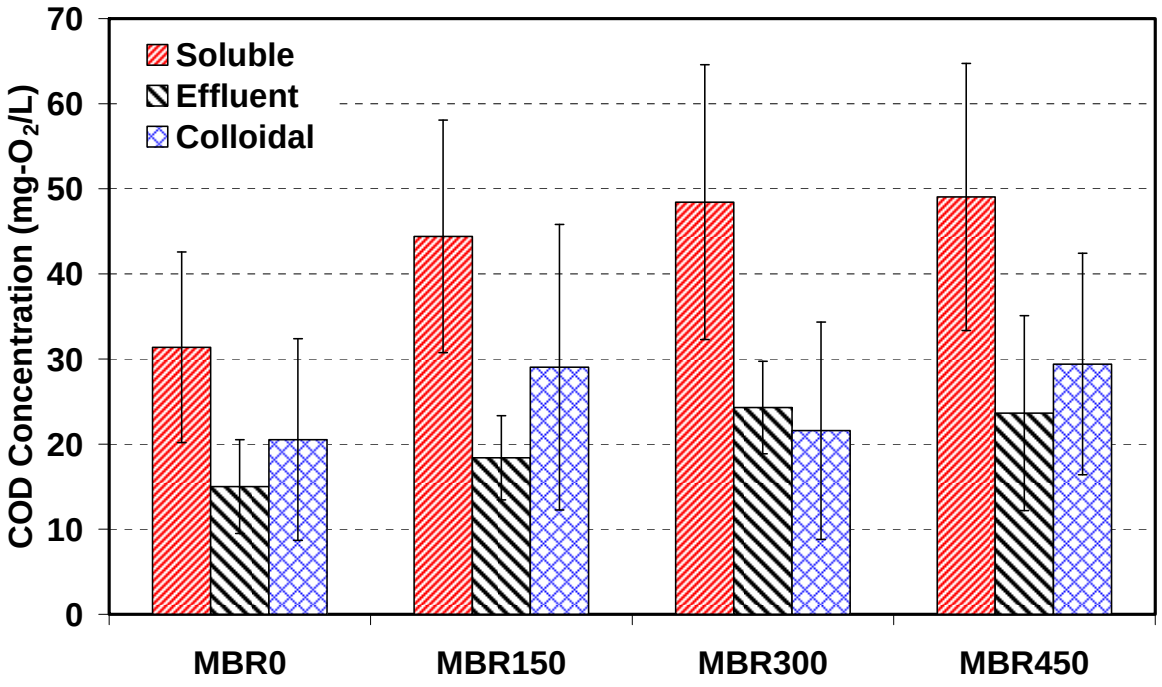

Figure 4.6: Soluble, effluent and colloidal COD concentrations in the MBRs

The soluble concentration relatively increased with increase in the shear intensity among the MBRs as shown in Figure 4.6. The average concentrations of soluble COD in the MBRs were found to be 31, 44, 48 and 49 mg/L in the MBR_0, MBR_{150}, MBR_{300} and MBR_{450}, respectively. However, this relative loss of biodegradation efficiency with increase in mixing intensity was always compensated by the physical separation by filtration mechanism in the MBRs with overall COD removal efficiency above 95%. Based on the resistance analysis results (Table 4.1), the contribution of cake resistance (R_c) and fouling resistance (R_f) remained almost unchanged in all the MBRs implying that the particle and colloidal size distributions as well as amount of soluble matter in the mixed liquor suspension had no apparent influence on the observed membrane fouling characteristics.

4.1.7 Concentration of soluble and bound EPS

Table 4.2 presents the soluble and bound EPS concentrations, characterized by the summation of protein and carbohydrate concentrations in the supernatant and re-suspended biofloc samples of the four MBRs, respectively.

Table 4.2: Soluble and bound EPS concentrations in the MBRs

Components	Soluble EPS (mg/L)				Bound EPS (mg/g-VSS)			
	MBR_0	MBR_{150}	MBR_{300}	MBR_{450}	MBR_0	MBR_{150}	MBR_{300}	MBR_{450}
Protein	2.1±1.3	3.1±1.4	2.7±1.8	2.3±0.7	22.1±4.1	26.6±5.4	29.4±4.5	36.4±8.9
Carbohydrate	9.5±1.6	8.4±1.2	9.2±4.8	9.0±1.8	6.5±1.2	6.2±2.1	7.5±1.5	6.8±1.1
Total	11.6±2.9	11.5±2.6	11.9±6.4	11.3±1.7	28.6±4.4	32.8±7.2	36.9±5.8	43.2±9.4
Protein/ carbohydrate	0.2±0.1	0.4±0.1	0.3±0.1	0.3±0.1	3.5±0.8	4.6±1.0	4.0±0.4	5.4±1.2

According to Table 4.2, the soluble EPS concentrations were relatively similar among the four MBRs. The low protein/carbohydrate (P/C) ratios of the soluble EPS exhibited that the carbohydrate was the major soluble constituent of EPS in all the MBRs. On average, carbohydrate made up 70% of the soluble EPS in the MBRs. On the contrary, there was a relative increase in the bound EPS concentration from MBR_0 to MBR_{450} corresponding to the increase in the mixing intensity. In particular, the protein content of the bound EPS increased from MBR_0 to MBR_{450} while carbohydrate content remained almost similar. The P/C ratio of the bound EPS suggests higher fraction of protein as compared to carbohydrate. The higher bound protein concentration with increase in mixing intensity could be due to the shear stress exerted on the microbial flocs causing floc disruption. The bio-floc breakage releases protein found at or outside the cell surface and in the intercellular space of microbial aggregate (Le-Clech et al., 2006).

4.1.8 Simulation of excreted biopolymers in biofilm

The temporal variation of biofilm structure on membrane surface can be considered being in close association with the changes in membrane fouling rates (Lee et al., 2007a). In order to comprehend the biofilms temporal variation, a simulation test was recently proposed by Zhang et al. (2006). Based on this test, the biopolymers released in biofilm structure on the membrane surface under low DO concentration and substrate in the four MBRs were simulated by keeping 1 L of the mixed liquor from each of the four MBRs in a cylinder without supplying air or substrate. The visual inspection of the mixed liquor samples and the amount of biopolymers released during 5 day period was carried out. The visual observations of the MBR sludge samples are shown in Figure 4.7.

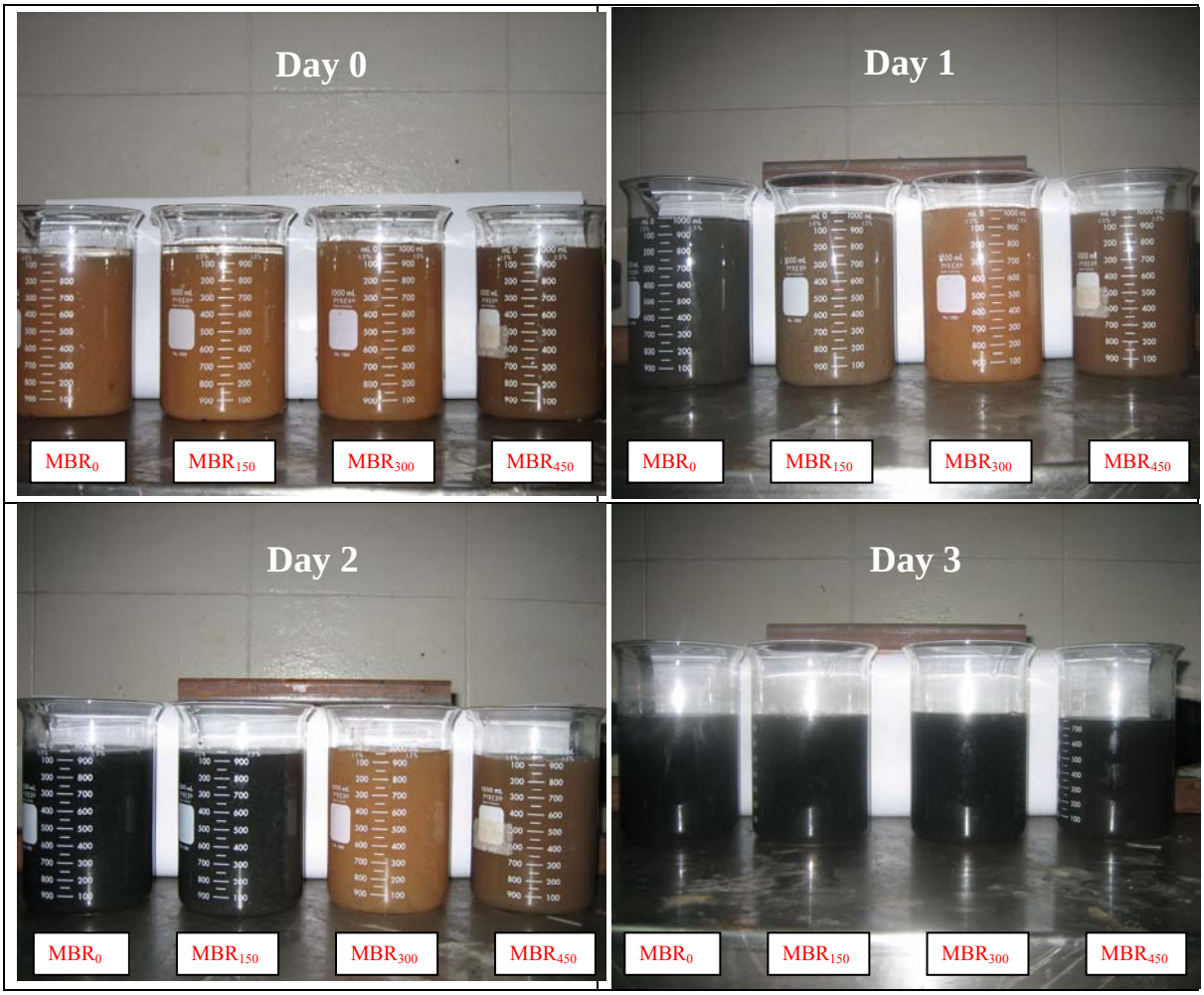

Figure 4.7: Visual observations of MBR sludge samples simulating biofilm conditions

It shows that the simulated biofilms changed color from golden-brown (yellow) to brown, then to gray and ultimately black with time under limited transfer of oxygen and substrate availability. The change of sludge color with passage of time (days) was indicative of different stages of bacterial condition from alive (yellow color) to dead (black color) according to the trends presented in Table 4.3.

Table 4.3: Bacterial condition in the simulated biofilms

Biomass color*	Day 0	Day 1	Day 2	Day 3	Day 4
MBR_0	Yellow	Grey	Black	Black	Black
MBR_{150}	Yellow	Brown	Black	Black	Black
MBR_{300}	Yellow	Yellow	Yellow	Black	Black
MBR_{450}	Yellow	Yellow	Grey	Black	Black

*yellow color = alive bacteria and black color = dead bacteria

According to Figure 4.7 and supplemented with Table 4.3, the bacterial death rate was faster in MBR_0 and MBR_{150} as compared to that in MBR_{300} and MBR_{450}. The microbial activity could be responsible for the rapid consumption of available substrate and subsequent high death rate of microbes in MBR_0 and MBR_{150} simulated biofilms as compared to the one in MBR_{300} and MBR_{450}.

The uneven distribution of shear intensity on membrane fibers, with low shear stress experienced by the central fibers as compared to that by the outer fibers, could have resulted in heterogeneous cake formation and biofilm. Thick biofilm formed in the central region of the bundle could have experienced low oxygen transfer and depleted DO in the biofilm sub-layers and consequently responsible for bacterial death. Such bacterial growth condition, with live bacteria at the surface layer and dead bacteria in the sub-layers of biofilm, could be responsible for local and temporal variations in the EPS. In this context, the amount of biopolymers released in each of the biofilms was characterized by measuring the soluble EPS and soluble COD concentrations for a period of 5 days as shown in Figures 4.8 and 4.9, respectively.

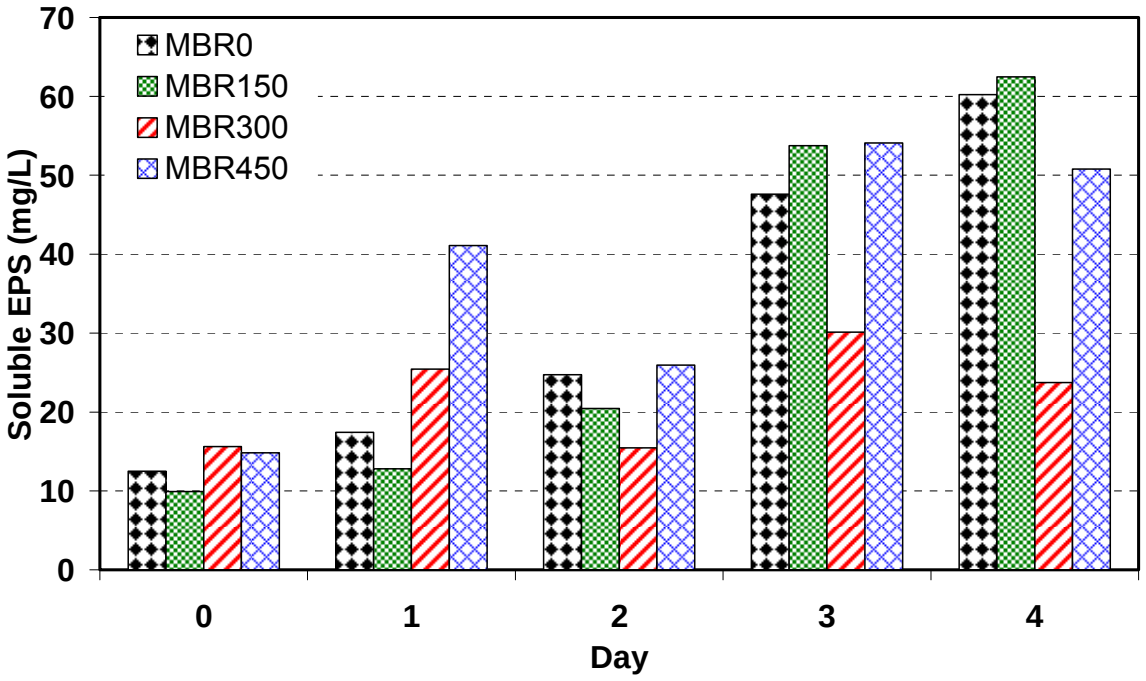

Figure 4.8: Soluble EPS released from biomass under low DO concentration and substrate

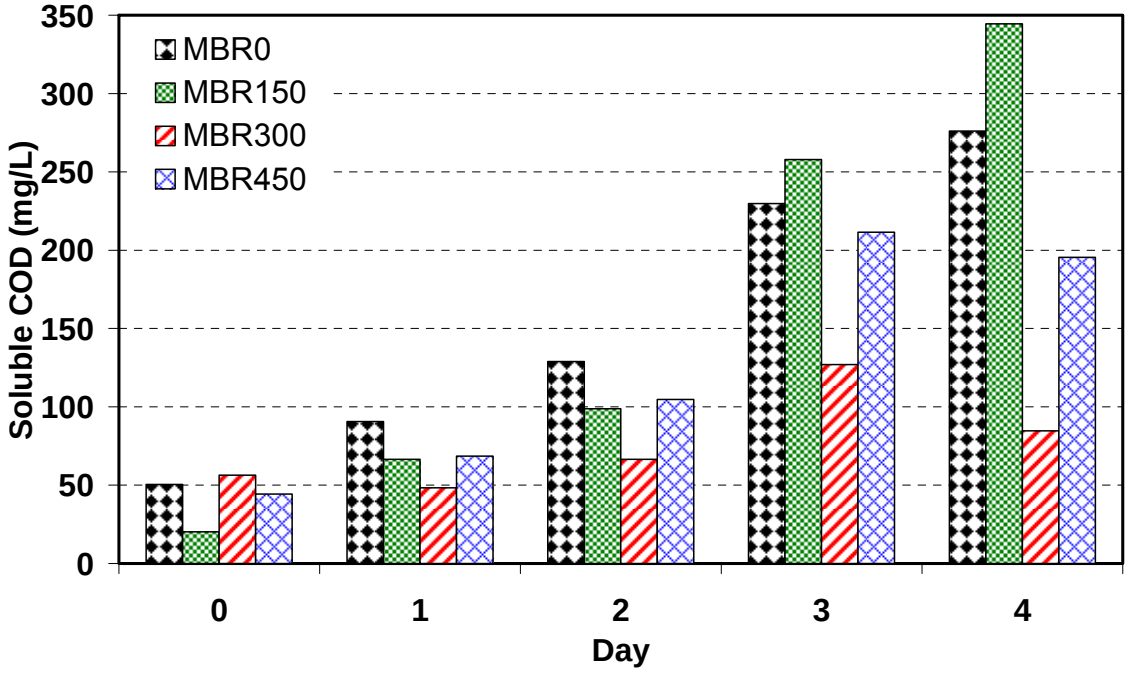

Figure 4.9: Soluble COD released from biomass under low DO concentration and substrate

Figures 4.8 and 4.9 show that the biomass released high concentration of biopolymers after 2 days in the simulated biofilm test of MBRs under low DO and substrate conditions. However, the amount of soluble EPS and soluble COD released from MBR_{300} biomass was found to be the lowest followed by the one from MBR_{450}. The amount of protein fraction in the released EPS after 5 days (as reported in Appendix-C; Table C-25) was significantly higher as compared to carbohydrate fraction indicating cell lysis due to bacterial death. The change in biopolymers concentration from low to high (Figures 4.8 and 4.9) corresponded to the change of biomass color from yellow to black (Figure 4.7) in the simulated biofilm. It can be deduced from these results that the higher amount of biopolymers released in the sub-layers of the MBR_0 and MBR_{150} biofilms as compared to that in MBR_{300} and MBR_{450} biofilms due to rapid dying of the bacteria can be the major cause of biofilm impermeability and consequent rapid fouling in MBR_0 and MBR_{150}. Pertinent to these results, Lee et al. (2007a) found that live/dead cell ratio became smaller, especially at lower sub-layers of biocake with filtration period. Moreover, the EPS concentration increased in the lower-sub layers of biocake due to the endogenous decay or cell-lysis. The EPS concentration jump in the lower sub-layers due to low live/dead cell ratio coincided with the TMP jump in the fouling profile. Thus, the influence of temporal changes in bacterial condition and the corresponding EPS in the biofilm can be significant on the membrane fouling rates and MBR filtration cycles.

4.1.9 Microbial activity in the MBRs

The bacterial condition in the thickened biofilms can be influenced by the microbial activity. In this context, the SOUR of sludge suspensions reflecting the microbial activity in the four MBRs was determined as shown in Figure 4.10.

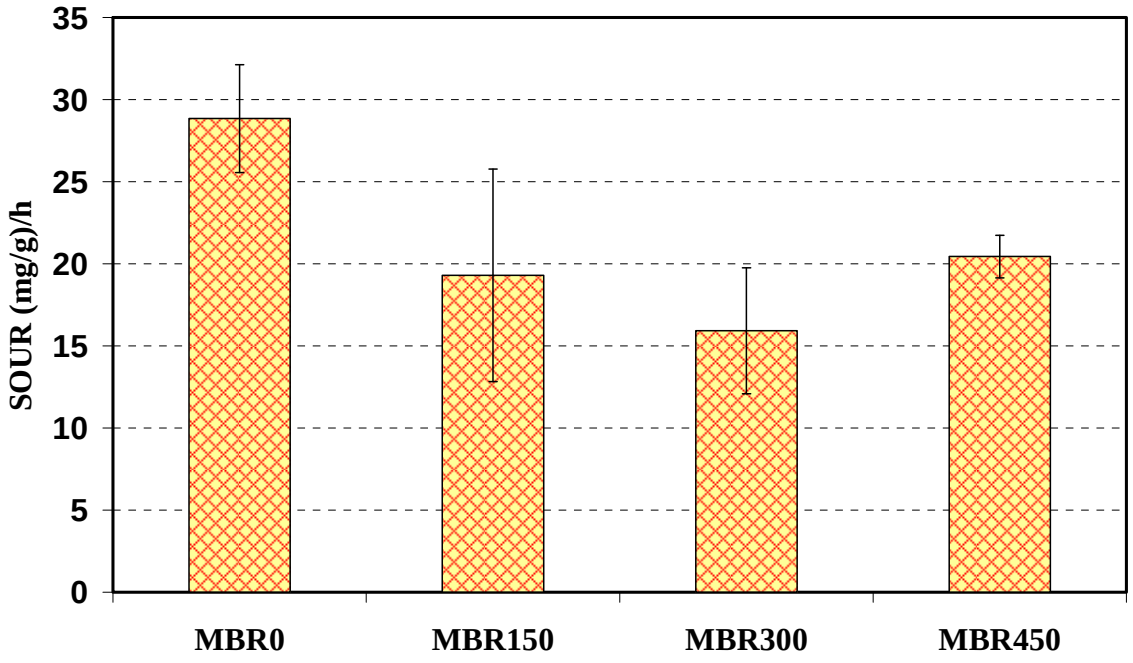

Figure 4.10: Microbial activity of sludge suspensions in the MBRs

According to Figure 4.10, microbial community from MBR_{300} demonstrated lowest SOUR which can be linked to the slow microbial death rate with passage of time in simulated biofilm and consequently responsible for low release of biopolymers. Thus, it can be postulated that optimized shear intensity condition can not only retard biomass

accumulation within the membrane bundle but also reduces the biomass activity and consequently release of EPS in the sub-layers of the biofilm. The low excretion of EPS in the biofilm structure of MBR_{300} could have been the key factor contributing to high biofilm permeability resulting in improved filtration performance.

4.1.10 Empirical relationship based on cake filtration theory

The optimum shear intensity of 249 s^{-1} in MBR_{300} achieved low fouling rates in both stages of filtration as shown in Figure 4.2. The first stage fouling was believed to be mitigated by the high shear intensity of mixed liquor turbulence inducing high fiber movement and retarded accumulation of biomass on the membrane fibers and between the fibers within the bundle. After cake formation initiates in the second fouling stage of MBR_{300} operation, the fouling rate was improved by the high porosity and connectivity of deposited sludge cake depicted by the low specific cake resistance. As the second stage fouling rates were observed to be significantly higher than that of the first stage, Stage II fouling rate retardation is of much importance. The relationship between the specific cake resistances and the second stage fouling rates of the MBRs is shown in Figure 4.11.

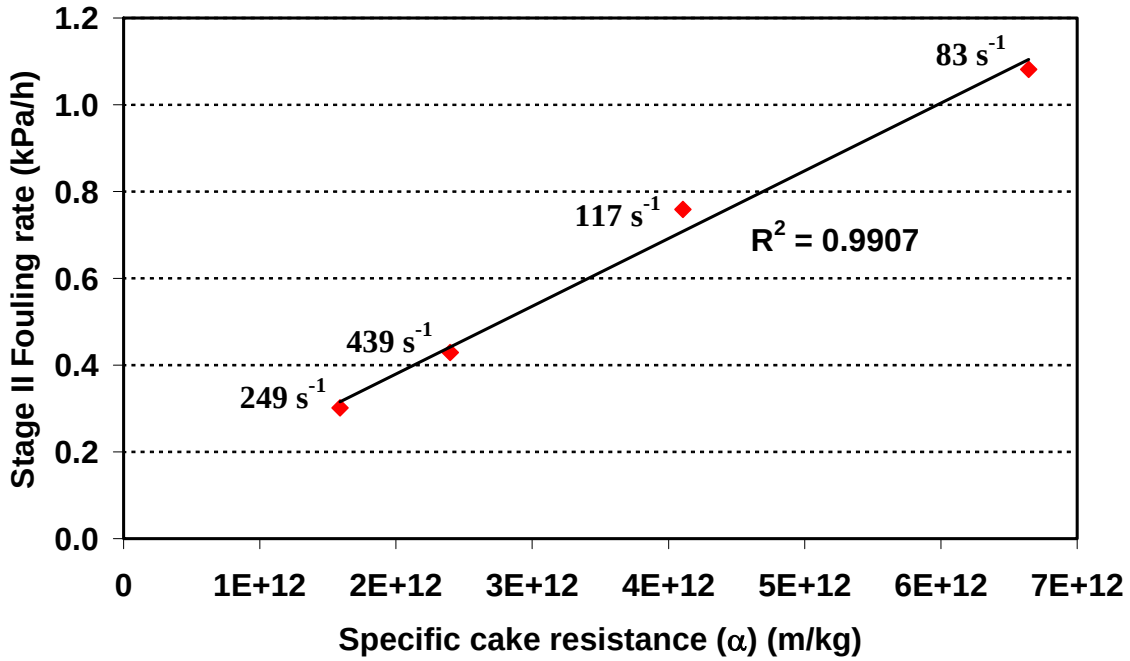

Figure 4.11: Relationship between Stage II fouling rate and specific cake resistance (α)
Shear intensity (G): MBR_0 = 83 s^{-1}, MBR_{150} = 117 s^{-1}, MBR_{300} = 249 s^{-1}, MBR_{450} = 439 s^{-1}

The linear curve shows a strong correlation between the specific cake resistance and the second stage fouling rate with an r-squared value of 0.99. Figure 4.11 shows that the lowest specific cake resistance of MBR_{300} sludge corresponded to the minimum fouling rate during the second stage while both these parameters deteriorated for MBR_{450} condition. Thus, the specific cake resistance (α) can be considered as a reliable parameter to predict the extent of second stage membrane fouling rate (dTMP/dt) in MBR filtration process.

Theoretically, the specific cake resistance (α) is related to the membrane cake resistance (R_c) according to the cake filtration theory:

$$R_c = \frac{\alpha.V.C_b}{A_m}$$ Equation 4.1

where V is the total volume filtered, C_b is the biomass concentration and A_m is the membrane filtration area.

The experimental membrane resistance analysis (Table 4.1) revealed that the cake resistance (R_c) is the major component of the total hydraulic resistance (R_t) and one can assume $R_t \approx R_c$. Incorporating this assumption in Equation 4.1 and differentiating with respect to time implies that:

$$\frac{dR_t}{dt} = \left(\frac{\alpha.C_b}{A_m}\right)\frac{dV}{dt}$$ Equation 4.2

where α, C_b and A_m are constants and R_t and V are variables.

According to Darcy law at constant flux, Equation 4.2 becomes:

$$\left(\frac{1}{\mu.J}\right)\frac{dTMP_t}{dt} = \left(\frac{\alpha.C_b}{A_m}\right)\frac{dV}{dt}$$ Equation 4.3

where μ is the permeate viscosity and J is the permeate flux and both are constant for the given condition. TMP_t rises with increase in total volume (V) of influent filtered with respect to time (t).

In context of the present MBR experiments, A_m was fixed and C_b was maintained between 6-8 g/L in the MBRs and this variation can be considered not to significantly influence the fouling rates. Thus, the only parameter that can be considered as crucial in influencing the fouling rate ($dTMP_t/dt$) in the second stage is specific cake resistance (α). The increase in shear intensity (G) was able to reduce the specific cake resistance up to a level of 249 s^{-1} beyond which value the Stage II fouling rate deteriorated as shown in Figure 4.11. Thus, a relationship was established between G and α within an effective G range between 83 and 249 s^{-1} as shown in Figure 4.12.

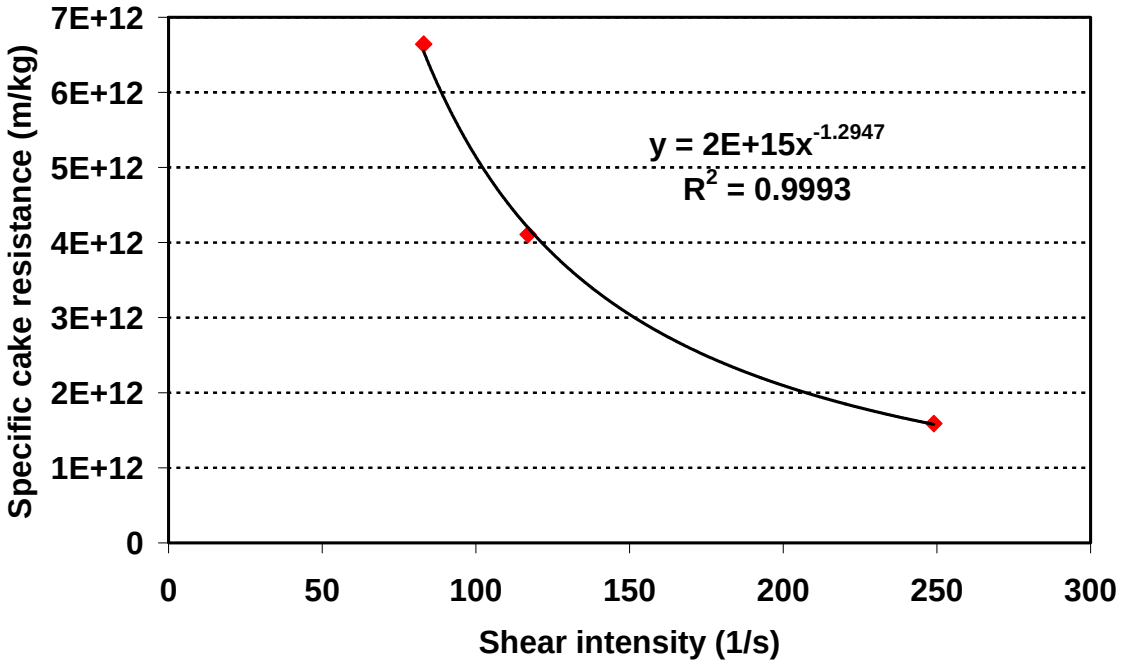

Figure 4.12: Relationship between specific cake resistance (α) and shear intensity (G)
Shear intensity (G): MBR_0 = 83 s^{-1}, MBR_{150} = 117 s^{-1}, MBR_{300} = 249 s^{-1}

It shows that the specific cake resistance (α) and shear intensity (G) can be empirically correlated by a power trend where:

$$\alpha = 2 \times 10^{15} \cdot G^{-1.2947} \qquad \text{Equation 4.4}$$

Incorporating this empirical relationship in Equation 4.3 gives:

$$\left(\frac{1}{\mu.J}\right)\frac{dTMP_t}{dt} = \left(\frac{2 \times 10^{15} \cdot G^{-1.2947}.C_b}{A_m}\right)\frac{dV}{dt} \qquad \text{Equation 4.5}$$

Equation 4.4 can be used to approximately predict the second stage fouling rate ($dTMP_t/dt$) for a given shear intensity (G) within certain limits of G (80 and 250 s^{-1}) in a MBR system.

Additional quantitative relationships from Phase I study are reported in Appendix-F.

4.2 Phase II: Hybrid MBRs

Hybrid MBRs are developed by the addition of suitable flocculent/adsorbent agents to MBRs for modification of sludge properties to enhance membrane filtration performance. The changes in sludge properties in the hybrid MBRs as compared to that in the conventional MBR mainly include bio-floc morphology (shape, size and density), microbial activity (SOUR) and soluble matter (SMP and eEPS). The modified sludge properties can improve the porosity of sludge cake formed over the membrane surface during membrane filtration.

In Phase II, the filtration performances and biomass characteristics of the three hybrid MBRs namely: MBR_{Clay}, $MBR_{Polymer}$ and MBR_{PAC} were compared to that of the conventional MBR ($MBR_{Control}$). In this section of the results and discussion, the $MBR_{Control}$ of Phase II refers to the MBR_0 of Phase I.

4.2.1 Optimum dosage of flocculent/adsorbent to the hybrid MBRs

The optimum initial dosages of clay, polymer and PAC in MBR_{clay}, $MBR_{polymer}$ and MBR_{PAC}, respectively were determined using jar test. The optimum concentration of each flocculent/adsorbent agent was determined based on visual inspection of sludge settling, settled sludge volume after 30 min and soluble COD concentrations in the centrifuged samples.

a) Jar test for Kaolin clay dosage

The Kaolin clay dosage range for the Jar test was varied between 0-2000 mg/L with an increment of 500 mg/L. The clay concentrations and the corresponding settled sludge volumes of 8 g/L biomass concentration are reported in Table 4.4.

Table 4.4: Settleability of sludge added with Kaolin clay

Concentration (mg/L)	Settled sludge volume (mL)	Settling efficiency (%)
0	340	0
500	330	3
1000	300	12
1500	300	12
2000	280	18

According to Table 4.4, the sludge settleability improvement of 12% was observed for clay concentration of 1000 mg/L. This enhanced settleability could not be further increased for 1500 mg/L and it increased only by 6% for 2000 mg/L as compared to that for 1000 mg/L. Thus, an optimum initial dosage of 1000 mg/L of clay was selected.

b) Jar test for NALCO® cationic polymer (MPE50) dosage

The MLSS concentration of the sludge used in the jar test for NALCO® cationic polymer (MPE50) dosage was approximately 6000 mg/L. Two jar tests were performed as per following concentrations:

Jar test A: MPE50 concentrations used were 0, 100, 200, 300 and 400 mg/L.
Jar test B: MPE50 concentrations used were 0, 25, 50, 75 and 100 mg/L.

Jar test A

The jar test A revealed that the settling property of the sludge significantly improved as well as the physical appearance changed in the polymer added sludge samples after 30 min settling time as shown in Figures 4.13.

Figure 4.13: Settled sludge volumes after 30 min with various MPE50 concentrations (0-400 mg/L)

It shows that the settled sludge volumes for different MPE50 concentrations were almost similar after 30 min settling period. The improvement in settling ability of sludge with the polymer infers effective flocculation even at the lowest concentration of 100 mg/L. The SCOD concentrations of the centrifuged samples from the Jar test A are presented in the Figure 4.14.

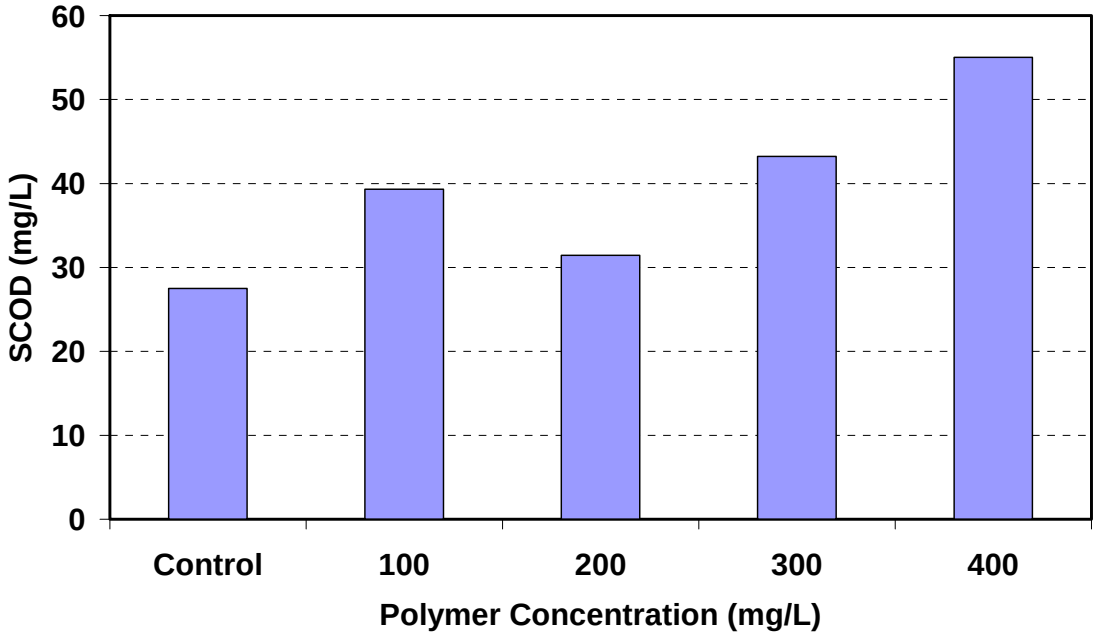

Figure 4.14: SCOD of sludge samples with concentration range 0-400 mg/L (Jar test A)

The SCOD results revealed that the SCOD concentrations in the polymer (MPE50) added sludges were above that in the control sludge as shown in Figure 4.14. In this context, the influence of the MPE50 on SCOD reduction at a lower concentration range was performed in a second jar test.

Jar test B

The second jar test demonstrated similar flocculation and settling characteristics as were observed for Jar test A. The SCOD concentrations for the jar test B are presented in Figure 4.15.

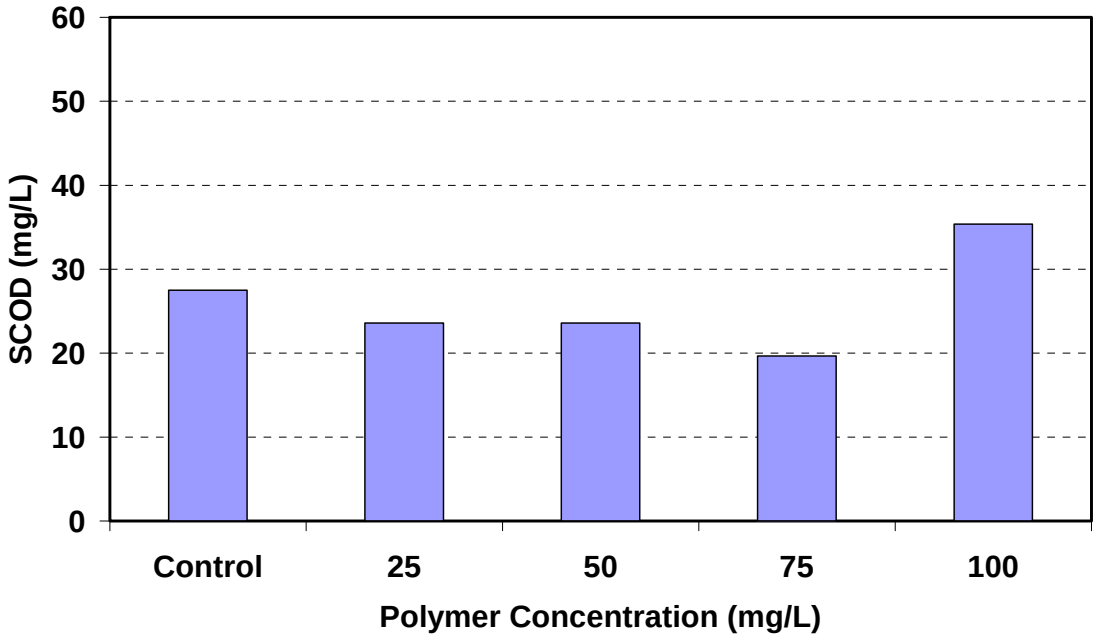

Figure 4.15: SCOD of sludge samples with concentration range 0-100 mg/L (Jar test B)

It shows that the SCOD was reduced with the low MPE50 dosage range except at 100 mg/L concentration. In this range, the dosage that resulted in highest reduction of SCOD was achieved at 75 mg/L. According to Lee et al. (2007b), the phenomenon of particle size increase with the addition of MPE50 can be explained on the flocculation and deflocculation mechanisms depending on the dosage of MPE50. In this context, the decrease in SCOD in Figure 4.15 can be attributed to its entrapment during the flocculation and a minimum concentration was reached at optimum dosage of 75 mg/L. However, an increase in SCOD after 75 mg/L can be attributed to its release during the deflocculation procedure.

Since the settling characteristics were similar, therefore the optimum dosage could be selected on the basis of SCOD concentration reduction which depicts 75 mg/L as the optimum initial dosage. According to the MPE50 supplier (NALCO®), the optimum dosage determined with jar test should be multiplied by a factor of 1.5 because a good portion of biopolymers are kinetically confined inside the floc without reacting with MPE50 and eventually come out during the aeration due to floc breakage. Thus, the initial dosage of the polymer selected was (1.5 x 75 = 112.5) 100 mg/L.

c) Jar test for powdered activated carbon (PAC) dosage

The PAC concentrations of 0, 600, 800, 1000 and 1200 mg/L were used for the Jar test to determine the optimum initial dosage for the PAC added hybrid MBR (MBR_{PAC}). The PAC concentrations and the corresponding settled sludge volumes of 8 g/L biomass concentration are reported in Table 4.5.

Table 4.5: Settleability of sludge added with PAC

Concentration (mg/L)	Settled sludge volume (mL)	Settling efficiency (%)
0	400	0
600	370	8
800	360	10
1000	350	13
1200	340	15

According to Table 4.5, the sludge settleability kept on improving with increase in PAC concentration and an optimum concentration could not be precisely determined. Moreover, the soluble COD concentrations corresponding to the PAC dosages are shown in Figure 4.16.

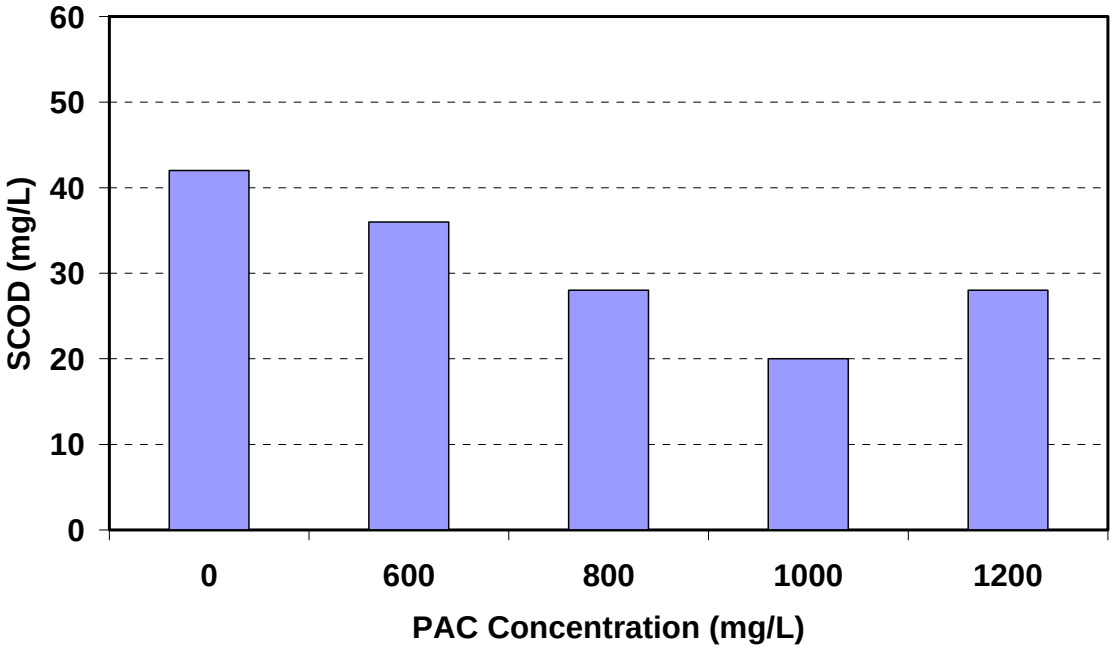

Figure 4.16: SCOD of sludge samples with PAC concentration range 0-1200 mg/L

PAC serves as an adsorbent agent adsorbing organic substances having low molecular weight (Ying and Ping, 2006). In this context, the SCOD decreased with increase in the PAC concentration up to an optimum dosage of 1,000 mg/L beyond which there was no reduction in the SCOD as shown in Figure 4.16. The PAC dosage of 1000 mg/L resulted in highest reduction of 52% in SCOD concentration as compared to that in the control sludge sample. Thus, it was recommended to use 1000 mg/L of PAC as the initial dosage to the MBR. The initial dosages selected for the flocculent/adsorbent agents addition to the MBRs and the selection criteria are reported in Table 4.6.

Table 4.6: Flocculent/adsorbent initial dosage to the hybrid MBRs

MBR	Solution/suspensions	Concentration (mg/L)	Remarks
MBR_{Clay}	Kaolin clay	1000	Based on settleability
$MBR_{Polymer}$	Cationic polymer (MPE50)	100	Based on SCOD
MBR_{PAC}	PAC	1000	Based on SCOD

The stock solutions preparation and calculation for initial and daily dosage of solution/suspensions is reported in Appendix-D.

After achieving steady state condition in the three MBRs namely MBR_{Clay}, $MBR_{Polymer}$ and MBR_{PAC}, the MLSS varied between 7 and 9 g/L and the COD removal efficiency was above 95% over a period of 80 days. The values of all the experimental parameters were averaged along with standard deviation as reported in Appendix-E.

4.2.2 Filtration behaviors in the hybrid MBRs

Typical TMP profiles depicting fouling trends among the four MBRs are shown in Figure 4.17.

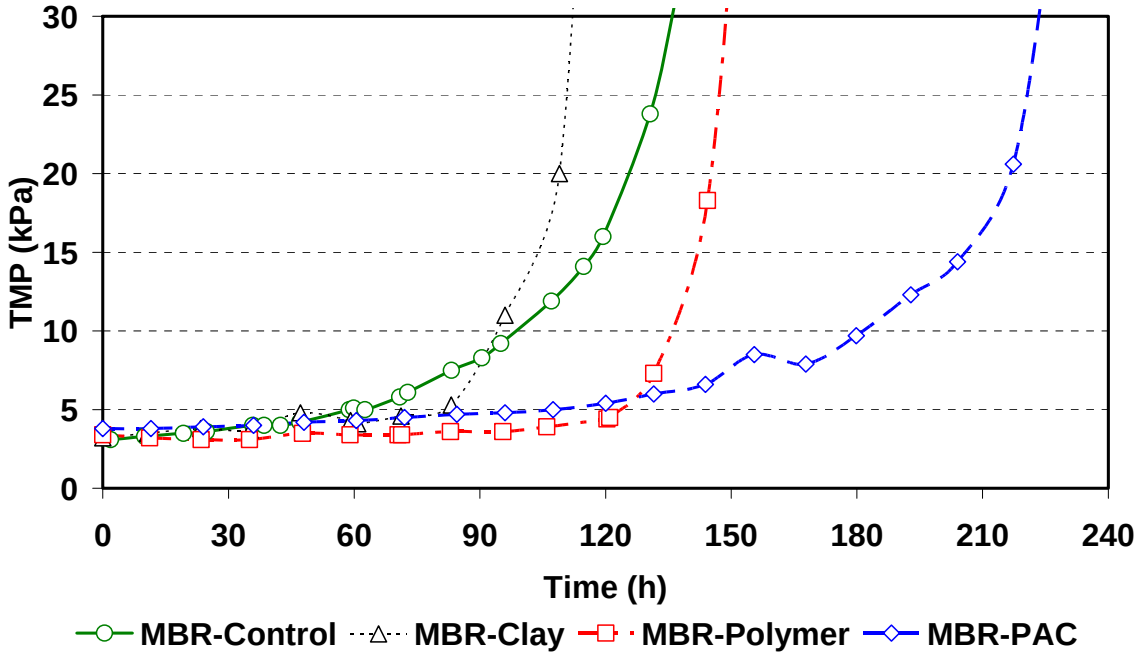

Figure 4.17: TMP profile at constant flux during the conventional and hybrid MBRs operation

It shows that the $MBR_{Control}$, MBR_{Clay} and $MBR_{Polymer}$ fouled after 140, 120 and 140 h and lastly by MBR_{PAC} after 230 h of filtration period. The addition of kaolin clay resulting in the rapid fouling of MBR_{clay} may be due to its inorganic nature and small size (100-325 mesh). On the contrary, addition of PAC achieved slow fouling of MBR_{PAC} by modifying the sludge structure with improved filterability characteristics. The fouling mitigation achieved with PAC addition (physico-chemical approach) is of the same order (230-240 h) of filtration period as achieved with mechanical mixing rate of 300 rpm (hydrodynamic approach) in Phase I. The TMP profiles of hybrid MBRs exhibit two stages of fouling, the

slow gradual TMP rise followed by rapid increase in fouling rate, as observed in Phase I, with MBR_{PAC} demonstrating retarded fouling in both the stages. Ying and Ping (2006) also observed prolong filtration period in terms of low increase in TMP versus time under 0.75 g/L PAC addition to MBR as compared to that in the conventional MBR. However, addition of MPE50 in present study could not exhibit significant fouling control as was recently observed in the study by Lee et al. (2007b) where addition of 50 mg/L MPE50 to submerged MBR was able to prolong filtration duration by 7.4 times than that of the control reactor.

Accurate reproducibility of fouling trends as shown in Figure 4.18 was effectively achieved in Phase II as the membrane module in the $MBR_{Control}$ as well as the hybrid MBRs were not covered with the plastic net as was the case with the modules in mechanically mixed MBRs of Phase I eliminating the possibility of net clogging and allowing free fiber movement.

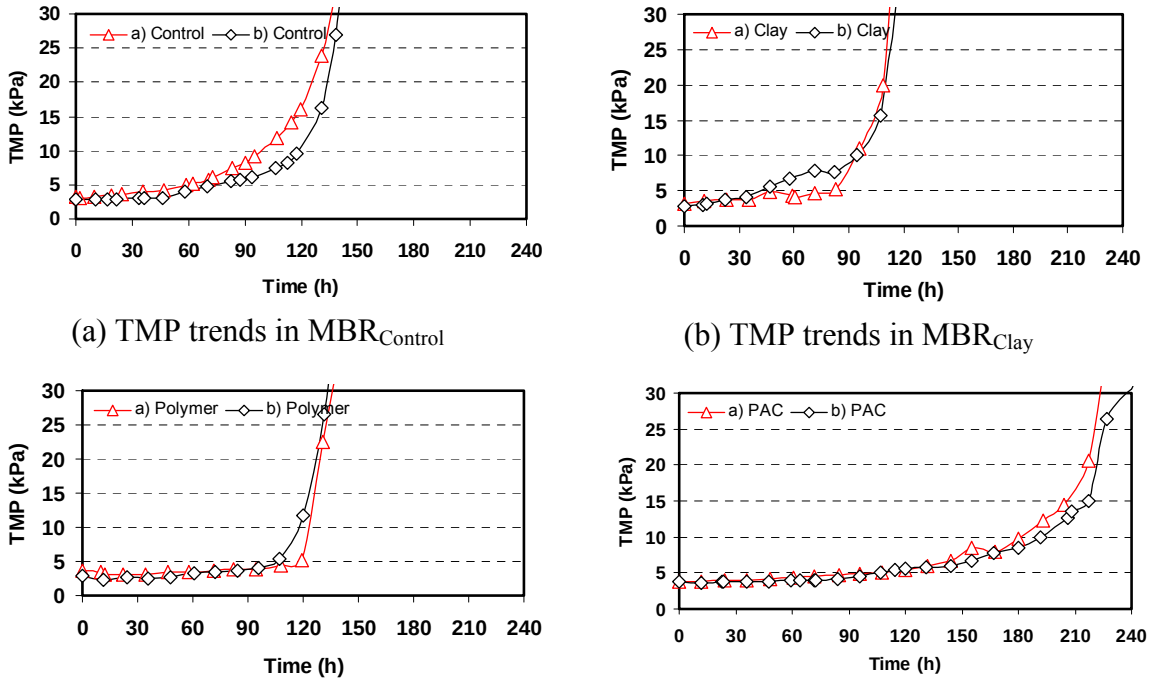

(a) TMP trends in $MBR_{Control}$

(b) TMP trends in MBR_{Clay}

(c) TMP trends in $MBR_{Polymer}$

(d) TMP trends in MBR_{PAC}

Figure 4.18: TMP trends reproducibility in the conventional and hybrid MBRs

4.2.3 Membrane fouling rates in the hybrid MBRs

The fouling rates during the two stages in the TMP profiles of the MBRs based on Figure 4.17 are shown in Figure 4.19 and the corresponding data is reported in Appendix-E (Figures E-1 and E-2).

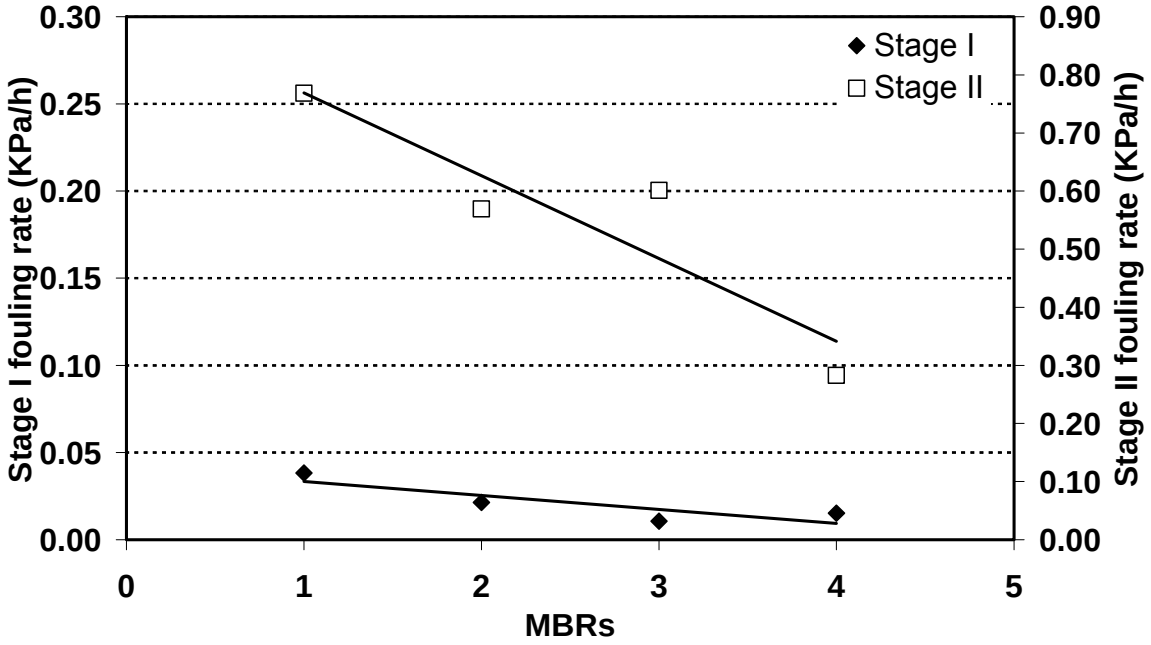

Figure 4.19: Fouling rates in the conventional and hybrid MBRs
MBRs: 1 = $MBR_{Control}$; 2 = MBR_{Clay}; 3 = $MBR_{Polymer}$; 4 = MBR_{PAC}

Figure 4.19 shows that the first stage fouling rates were observed to be much lower as compared to the second stage fouling rates in the MBRs. The first stage fouling rates being relatively similar in the MBRs could be attributed to similar hydrodynamic conditions experienced by the HF membranes. However, a reduction of 60% was observed in the second stage fouling rate in the MBR_{PAC} as compared to that in the $MBR_{Control}$. Moreover, the slight decrease in fouling rate observed in MBR_{clay} and $MBR_{Polymer}$ could not influence the respective filtration cycles. Ying and Ping (2006) found that the fouling rates of the first and the second phases were controlled with the addition of optimum dosage of PAC to hybrid MBR.

4.2.4 Membrane fouling resistances in the hybrid MBRs

The resistance-in-series model was applied to evaluate the filtration characteristics. The resistance analysis results summarized in Table 4.7 represent the averaged resistance values after replicate experimental measurements as reported in Appendix-E (Tables E-4, E-5 and E-6).

Table 4.7: Fouling resistances of membrane in the conventional and hybrid MBRs

Resistances	$MBR_{Control}$	MBR_{Clay}	$MBR_{Polymer}$	MBR_{PAC}
R_t ($\times 10^{12}$ m^{-1})	79.46	67.30	72.63	66.71
R_c ($\times 10^{12}$ m^{-1})	78.36	65.34	70.97	63.94
R_f ($\times 10^{12}$ m^{-1})	0.72	1.47	1.33	2.40
R_m ($\times 10^{12}$ m^{-1})	0.39	0.49	0.33	0.37
R_c/R_t (%)	98.6	97.1	97.7	95.8

According to Table 4.7, the cake resistance (R_c) was the main component of the total hydraulic resistance (R_t) at the end of operation cycles in the MBRs while membranes were subjected to low levels of irreversible fouling (R_f) as observed in the Phase I of study. However, the low percentage of R_c/R_t in the MBR_{PAC} suggests that the R_c was relatively lower than that in the other MBRs. The application of PAC could be responsible for reduction in R_c as it forms incompressible particulate layer of high fluid permeability. In contrast, the R_f was slightly higher in the MBR_{PAC} as compared to that in the other MBRs. Ying and Ping (2006) investigated resistance analysis with different dosages of PAC to MBR and found that the application of PAC was responsible for reduction of R_c.

The biomass characteristics of hybrid MBRs were compared to that of conventional MBR ($MBR_{Control}$) in order to determine the influence of modified MBR sludges on the observed fouling behaviors.

4.2.5 Sludge filterability characteristics of the hybrid MBRs

The sludge filterability was characterized by the normalized-capillary suction time (CST_N) and the specific cake resistance (α). The results for both these parameters are reported in the Figures 4.20 and 4.21.

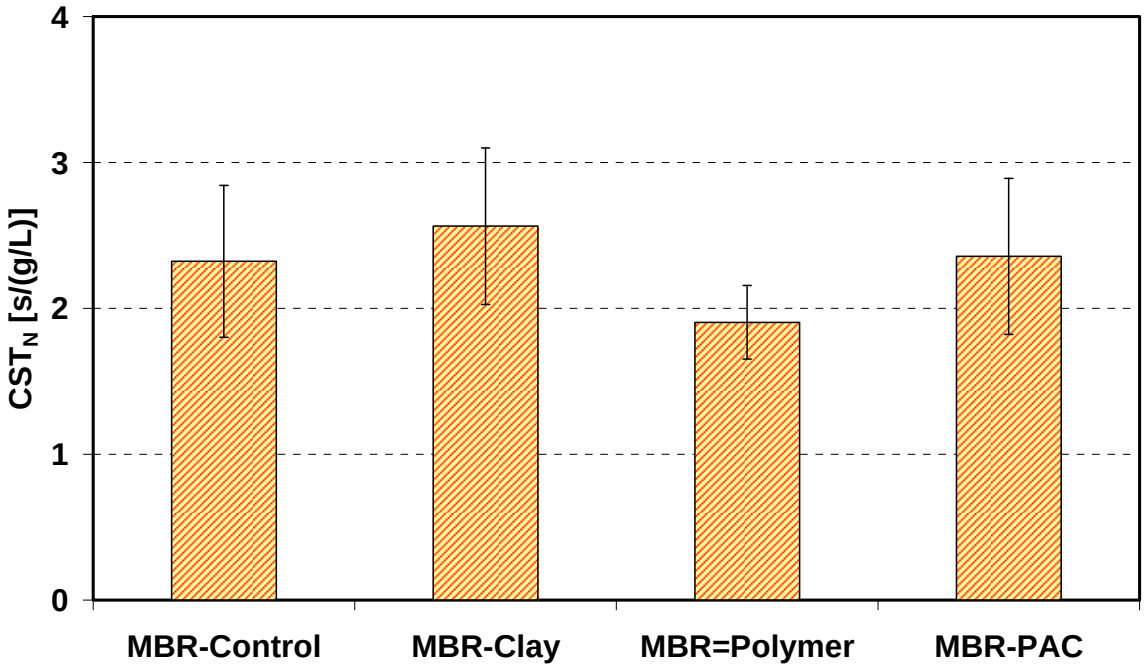

Figure 4.20: CST_N of sludge samples from the conventional and hybrid MBRs

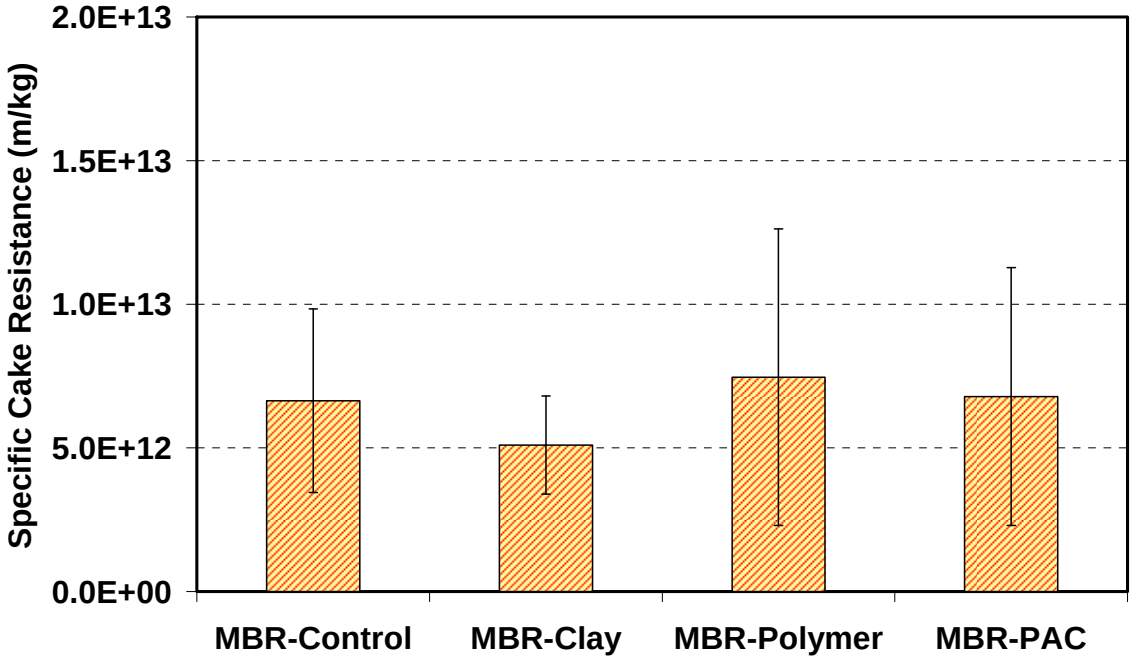

Figure 4.21: Specific cake resistance (α) of sludge samples from the conventional and hybrid MBRs

Figure 4.20 revealed insignificant difference of sludge filterability in terms of CST_N among the MBR sludge samples. Similarly, the specific cake resistance of the modified sludge samples also did not exhibit significant change as compared to that of the conventional MBR sludge as shown in Figure 4.21. Thus, a relationship between the observed fouling rates and the sludge filterability characteristics could not be established in Phase II.

4.2.6 Particle size distribution (PSD) in the hybrid MBRs

The PSD in the conventional and hybrid MBRs at the end of the 80 days operation of Phase II is shown in Figure 4.22.

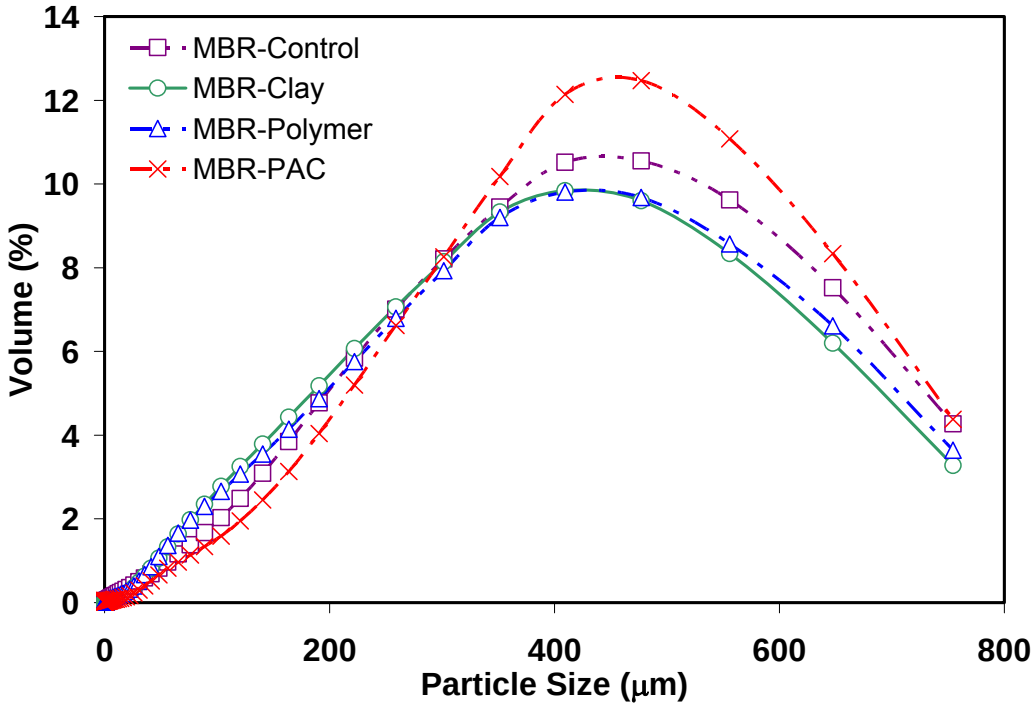

Figure 4.22: Particle size distribution of sludge suspensions in the conventional and hybrid MBRs

Table 4.8: Median particle size and uniformity of sludge suspensions in the conventional and hybrid MBRs

MBR	$MBR_{Control}$	MBR_{Clay}	$MBR_{Polymer}$	MBR_{PAC}
Median particle size (μm)	363	331	336	401
Uniformity coefficient	0.48	0.52	0.52	0.42

The median particle sizes and the uniformity coefficients in the MBRs are reported in Table 4.8. Figure 4.22 shows that the percentage of large bio-particles (300-700 μm) by volume was higher in MBR_{PAC} as compared to that in the other MBRs. According to Table 4.8, the median particle size was also larger in the MBR_{PAC} sludge suspension as compared to the other median particle sizes. Moreover, the extent of distribution in MBR_{PAC} was comparatively tapered represented by the low uniformity coefficient (Table 4.8). These results suggest that the MBR_{PAC} with high percentage of large bio-particles and uniformity could have provided high cake layer porosity on the membrane surface resulting in the observed low fouling tendency.

4.2.7 Microscopic investigation of sludge morphology

The microscopic observations of the different MBR sludges are shown in Figure 4.23.

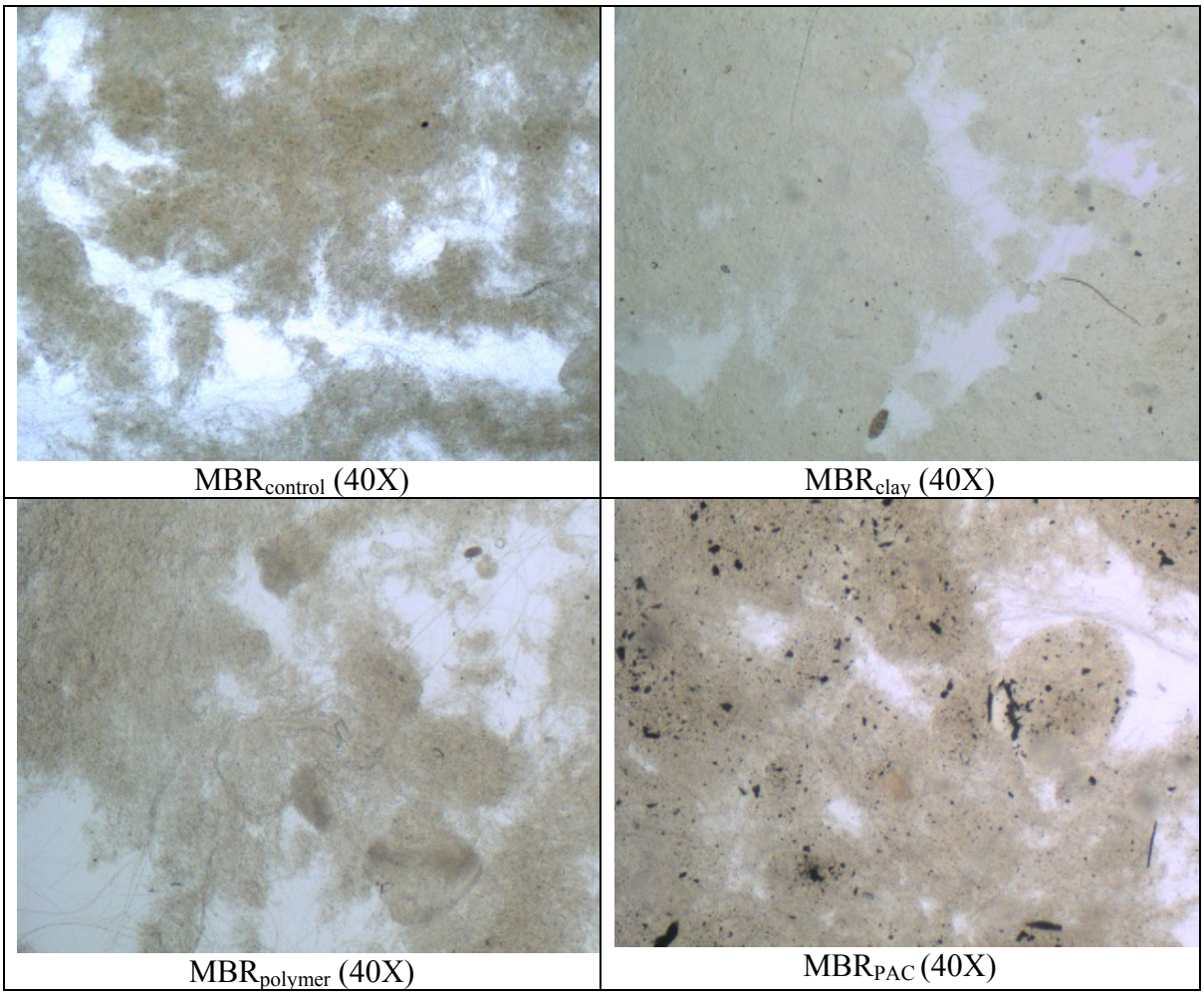

Figure 4.23: Microscopic observations of sludge from the conventional and hybrid MBRs

The microscopic observations in Figure 4.23 were used to analyze the morphological characteristics of the MBR flocs. The bio-flocs in MBR_{PAC} were observed to be more or less rounded and firm with the surrounding liquid distinctly separated from the floc itself. In constrast, the bio-flocs in the other MBRs were observed to be irregular and the interface between the floc and the liquid phase was not sharply defined. The PAC served as a media over which the biofilm growth occurred resulting in biologically activated carbon. Such floc formation was not visible in the other MBR sludges.

The biomass activity which depends on the sludge morphology and hydrodynamic environment plays a major role in fouling retardation as was concluded in Phase I and therefore was investigated in Phase II as well.

4.2.8 Microbial Activity in the hybrid MBRs

The microbial activity of sludge suspensions in the conventional and hybrid MBRs was measured in terms of the SOUR as shown in Figure 4.24.

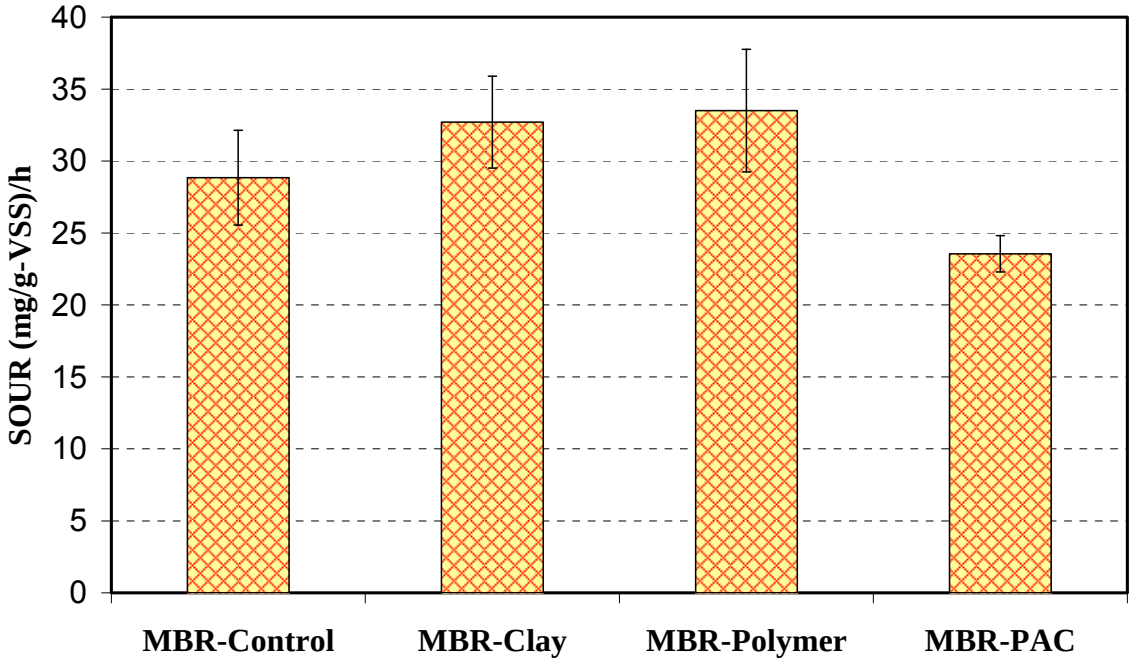

Figure 4.24: Microbial activity in the conventional and hybrid MBRs

On average, the SOUR of microorganisms in MBR_{PAC} was found to be 23.6 (mg/g-VSS)/h as compared to 28.8, 32.7 and 33.5 (mg/g-VSS)/h in $MBR_{Control}$, MBR_{Clay} and $MBR_{Polymer}$, respectively as shown in Figure 4.24. With large and closely packed bio-flocs in MBR_{PAC} (Figure 4.23) having less surface area for given volume, the microorganisms could experience limited oxygen transfer and exposure to substrate concentration inducing reduction of the SOUR. The large bio-flocs with low SOUR could be the basis of improved filtration performance in the MBR_{PAC}.

4.2.9 Concentration of soluble and bound EPS in the hybrid MBRs

The soluble EPS was measured in the supernatant of centrifuged mixed liquor samples as shown in Figure 4.25.

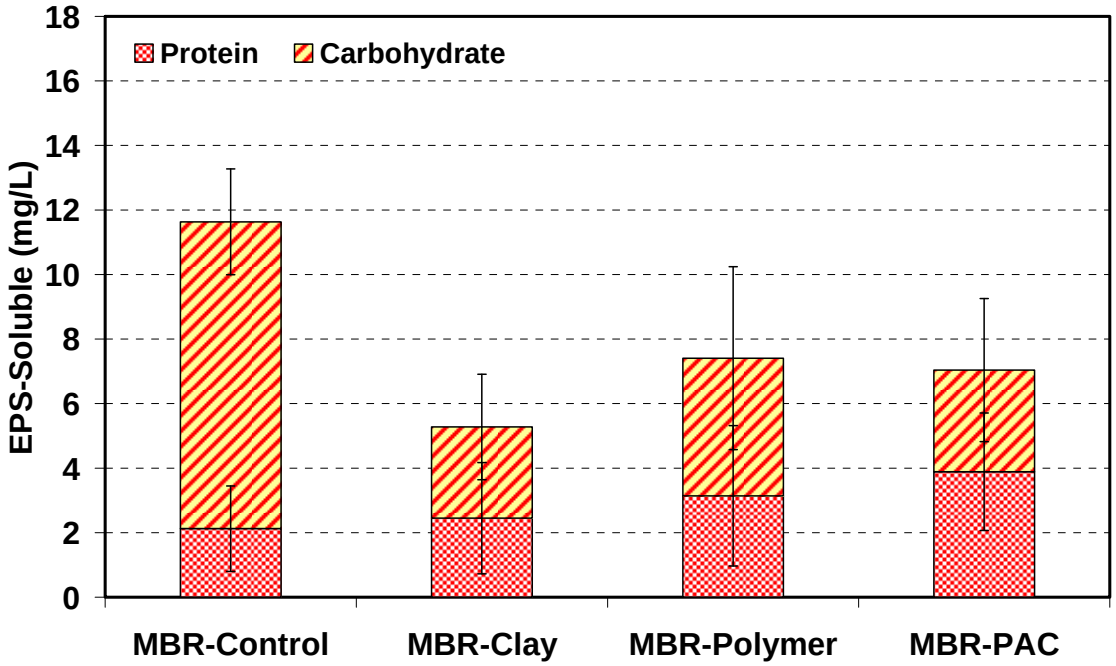

Figure 4.25: Soluble EPS in mixed liquor of the conventional and hybrid MBRs

Figure 4.25 shows that the soluble EPS, considered as a major foulant, was reduced by almost 50% in the hybrid MBRs as compared to that in the conventional (control) MBR. The protein content almost remained the same in all the MBRs but the carbohydrate content was reduced from approximately 10 to 4 mg/L. This infers that the soluble EPS removed was mostly composed of carbohydrate fraction. The reduction in soluble carbohydrate concentration could have been achieved by the mechanisms of flocculation and adsorption in the hybrid MBRs. A decrease in soluble foulants is supposed to diminish the irreversible fouling and enhance cake layer porosity. In this context, hybrid MBR studies using PAC have been reported to be able to decrease the soluble EPS (SMP) in the reactors partly due to the degradation by biologically activated carbon and partly due to the direct adsorption onto PAC (Munz et al., 2007; Ying and Ping, 2006). Moreover, comparison of conventional MBR to hybrid MBR using MPE50 as membrane fouling reducer (MFR) revealed about 50% reduction in the soluble EPS (from 11.1 to 5.9 mg/L) as well as soluble COD (from 28.3 to 15.2 mg/L) (Lee et al., 2007b). However, the reduction of soluble EPS concentration in the hybrid MBRs of present study could not induce low TMP tendencies and/or fouling rates with exception of MBR_{PAC}. This suggests that concentration of soluble foulants cannot be considered as the primary indicator of fouling propensity and it may only serve as a part of the complex membrane fouling mechanism in MBR where bio-particle structure and activity also plays a predominant role.

The bound EPS concentration was measured in the re-suspended bio-floc samples as shown in Figure 4.26.

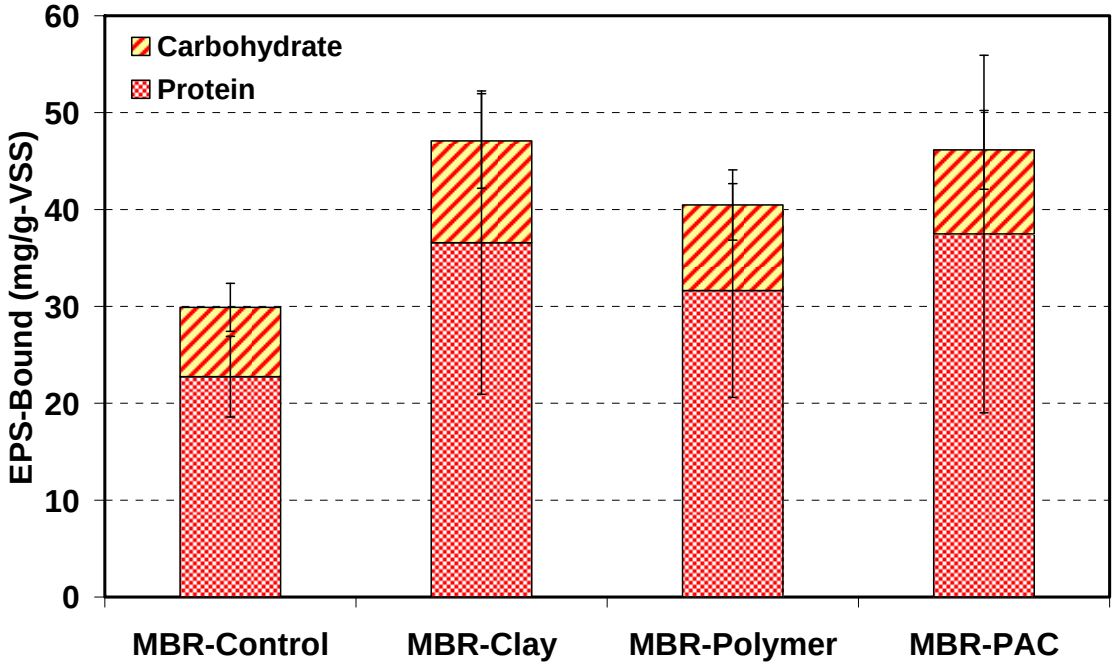

Figure 4.26: Bound EPS in mixed liquor of the conventional and hybrid MBRs

Figure 4.26 shows that the bound EPS concentration was lower in the control MBR as compared to the hybrid MBRs. Ying and Ping (2006) found that the bound EPS in terms of both the extracted carbohydrate and protein fractions decreased under optimum PAC dosage. On the contrary, it was found that the addition of MPE50 to MBR increased the bound EPS and behaved oppositely to the decrease of soluble EPS (Lee et al., 2007b). This behavior was explained by the notion of soluble EPS entrapment during flocculation leading to high concentration of the bound EPS. In the present study also, the same notion of soluble EPS enmeshment due to flocculation mechanism in hybrid MBRs can be the cause of high bound EPS levels. Overall, it is found that the soluble and bound EPS concentration in the mixed liquor of conventional and hybrid MBRs were not able to significantly influence the membrane fouling tendencies.

Chapter 5

Conclusions and Recommendations

The aim of this study was to investigate the influence of hydrodynamic and physico-chemical approaches on fouling mitigation in submerged-MBR systems using hollow-fiber membrane modules. The hydrodynamic approach was investigated by varying the shear intensity (G) induced by different mechanical mixing speeds at constant airflow rate in MBRs referred to as mechanically mixed MBRs. In contrast, the physico-chemical approach included the modification of sludge properties with the addition of specified flocculent/adsorbent agents to MBRs referred to as hybrid MBRs. In the context of the two approaches, the study was divided into two phases namely: a) mechanically mixed MBR phase and b) hybrid MBR phase.

The mechanically mixed MBR phase comprised of four MBRs operated with aeration only in a control reactor (MBR_0) supplemented by mechanical stirring at 150, 300 and 450 rpm in MBR_{150}, MBR_{300} and MBR_{450}, respectively. The first phase focused on the membrane fouling behaviors and the biomass characteristics under the influence of variable shear intensities and understanding of the membrane fouling mechanism in submerged hollow fiber membranes.

The hybrid MBR phase comprised of three MBRs where Kaolin clay, NALCO® cationic polymer (MPE50) and powdered activated carbon (PAC) were added to MBR_{Clay}, $MBR_{Polymer}$ and MBR_{PAC}, respectively. The second phase focused on the membrane filtration performances and the modified biomass characteristics under the influence of different flocculent/adsorbent agents added MBRs. The fouling propensities and the modified biomass properties in hybrid MBRs were compared to that in the conventional MBR ($MBR_{Control}$).

The conclusions drawn from the two phases of the study are mentioned in the following section.

5.1 Conclusions

5.1.1 Mechanically mixed MBR phase

The following specific conclusions were drawn from the mechanically mixed MBR phase:

1. Prolong filtration cycle with low fouling tendency was observed during MBR_{300} operation with G of 249 s^{-1} as compared to that in the other MBRs.

2. Two distinct fouling stages were observed in the TMP profiles, the slow gradual TMP rise followed by rapid rise in TMP. During the first stage, the fouling rate decreased and the critical time (t_{crit}) increased with increase in shear intensity due to slow accumulation of biomass on fiber surface and within adjacent fibers. The second stage fouling rate, being predominant than the first stage one, was found to be the lowest in MBR_{300} as compared to the other MBRs. The fouling rate deteriorated in MBR_{450} which was indicative of the fact that shear intensity of certain extent is feasible to mitigate fouling beyond which it becomes disadvantageous.

3. Specific cake resistance (α) and normalized-CST (CST_N) were found to be lower for MBR_{300} sludge suggesting higher filterability as compared to that in the other MBRs. Based on improved filtration performance, low fouling rates and high sludge filterability, MBR_{300} was considered having the optimum shear intensity condition to control fouling hydrodynamically using mechanical stirring.

4. Bio-particles were found to be relatively stable in terms of floc size in MBR_0, MBR_{150} and MBR_{300} corresponding to G values of 83, 117 and 249 s^{-1}, respectively. However, bio-particles were found to disintegrate in MBR_{450} (G of 439 s^{-1}) resulting in small particles and scattered distribution implying that the bio-flocs were able to withstand shear stress up to a certain level beyond which the flocs were broken. The population of small flocs with low porosity in MBR_{450} could have resulted in relatively poor sludge filterability and consequently higher second stage fouling rate than that in the MBR_{300}.

5. Cake resistance (R_c) was found to be the predominant resistance fraction of the total hydraulic resistance (R_t) as compared to the irreversible fouling resistance (R_f) for all the MBRs. Soluble EPS concentration and colloids ranging from 0.1-1 μm, known as irreversible foulants, were relatively similar among the MBRs with minimal variation under the different shear intensities.

6. SOUR was found to be lower in the MBR_{300} sludge as compared to that in the other MBRs which was associated with the slow microbial death rate in the simulated biofilm and consequently responsible for low biopolymers concentration. These results suggest that the excretion of EPS in the biofilm sub-layers due to low oxygen and substrate transfer can be of significance in temporal variation of biofilm structure. The low excretion of EPS in the biofilm structure of MBR_{300} could have been the key factor contributing to high biofilm permeability resulting in improved filtration performance.

7. Strong linear relationship was observed between the specific cake resistances (α) and the second stage fouling rates (dTMP/dt) of the MBRs. The lowest specific cake resistance in MBR_{300} corresponded to the minimum fouling rate during the second stage. Based on this experimental data and cake filtration theory, an empirical relationship was established, provided a certain extent of shear intensity (249 s^{-1}) was not exceeded, as given below:

$$\left(\frac{1}{\mu.J}\right)\frac{dTMP_t}{dt} = \left(\frac{2\times10^{15}\cdot G^{-1.2947}.C_b}{A_m}\right)\frac{dV}{dt} \qquad \text{Equation 5.1}$$

This equation can be used to approximately predict the second stage fouling rate ($dTMP_t/dt$) for a given shear intensity (G) within certain limits of G (80 and 250 s^{-1}) in a MBR system.

5.1.2 Hybrid MBR phase

The following specific conclusions were drawn from the hybrid MBR phase:

1. Prolong filtration cycle with low fouling tendency was observed in the MBR_{PAC} as compared to that in the other MBRs.

2. Two-stage fouling was observed in the TMP profiles of the hybrid MBRs. The first stage fouling rates being relatively similar in the conventional as well as hybrid MBRs was attributed to similar hydrodynamic conditions experienced by the HF membranes. However, there was a reduction of 60% in the second stage fouling rate of the MBR_{PAC} as compared to that of the $MBR_{Control}$.

3. Cake resistance (R_c) was found to be the predominant resistance fraction of the total hydraulic resistance (R_t) for the hybrid MBRs as was the case in phase I. The modified biomass characteristics in the hybrid MBRs were not able to significantly influence the membrane resistance fractionation.

4. Improved filtration performance and low fouling rate in MBR_{PAC} was attributed to the flocculation and adsorption phenomena. The effective flocculation of biomass by PAC was verified by the particle size distribution (PSD) analysis and the microscopic investigation of sludge morphology. The PSD in MBR_{PAC} revealed higher proportion of large bio-particles by volume in the range of 300-700 µm and relatively narrow particle distribution as compared to that in the other MBRs. Moreover, the microscopic observations revealed that bio-flocs in MBR_{PAC} were more or less rounded and firm as compared to irregular and weak flocs in the other MBRs as the PAC served as a media for the biofilm growth.

5. Soluble EPS was reduced by almost 50% in the hybrid MBRs as compared to that in the $MBR_{Control}$. However, the decrease in soluble EPS concentration could not be correlated with the TMP tendencies and/or fouling rates observed in the MBRs. This suggests that observed reduction of soluble EPS by adsorption and/or flocculation was not able to significantly contribute to the membrane fouling behaviors.

6. SOUR of microorganisms in the MBR_{PAC} was found to be lower than that in the other MBRs. The large PAC assisted bio-flocs having less surface area for given volume and consequently low microorganism exposure to substrate concentration could have resulted in reduction of the SOUR. The large bio-flocs with low SOUR could have been the basis of improved filtration performance in the MBR_{PAC}.

5.2 Recommendations

The following recommendations for further study are noteworthy:

1. Present study revealed that high shear intensity (G) can hydrodynamically mitigate fouling by increasing the power (P) input in terms of optimum mechanical stirring speed in addition to aeration. However, G can also be increased by reducing the reactor volume (V). In this context, an airlift mechanism by providing risers inside a MBR provides less effective cross-sectional area relative to aeration which induces higher superficial aeration velocity (U_G) and corresponding higher G value at a given aeration rate. Such investigation can of great interest to MBR fouling control as G can be enhanced without additional power requirements.

2. The investigation of fouling tendency in MBRs from the present study revealed two stages of fouling i.e., the slow gradual TMP rise followed by the rapid rise in TMP. As the second fouling stage of rapid TMP rise causes severe membrane fouling leading to membrane chemical cleaning requirement, this stage can be retarded or avoided by implementing membrane regeneration techniques such as back washing at the end of the first fouling stage. The investigation based on backwashing intensity, duration and cycle at the end of the first fouling stage during MBR operation can be tremendous importance to achieve prolong membrane filtration cycles as well as maintaining high net permeate flux.

3. The empirical model developed in this research work was limited to the second fouling stage based on cake filtration theory. However, the modeling work can also be extended to the first fouling stage as well which eventually dictates the second fouling stage. Formulating a unified model which takes into account the first as well as the second fouling stages can be of great interest as it can be capable of precisely predicting fouling tendencies in MBR operations.

4. For given aeration intensity, a) fiber density, b) bundle diameter and c) location of aerators are the three important aspects which are not in the limelight of submerged hollow-fiber membrane researches and their investigation may be of interest to propose novel fouling control strategies in MBR operation.

5. Thorough microbial culture investigation under different shear intensity conditions in MBRs and hybrid MBRs can be of interest for further understanding of the bio-kinetics and bio-mechanisms of microbes in the these MBR systems.

6. Up-scaling of the laboratory-scale mechanically mixed MBR with optimum shear intensity and hybrid MBR with PAC addition to pilot-scale MBRs and usage of real wastewater for further understanding of fouling behavior under actual MBR design and operational conditions is recommended.

References

AWWARF, LdE and WRC (1996). *Water Treatment Membrane Processes*. McGraw-Hill, USA, ISBN: 0-07-001559-7.

APHA, AWWA and WEF (2005). *Standard Methods for the Examination of Water and Wastewater*. 21st Edition, USA, ISBN: 0875530478.

Bacchin, P. (2004). A possible link between critical and limiting flux for colloidal systems: consideration of critical deposit formation along a membrane. *Journal of Membrane Science*, 228, 237-241.

Bacchin, P., Aimar, P. and Field, R.W. (2006). Critical and sustainable fluxes: Theory, experiments and applications. *Journal of Membrane Science*, 281, 42-69.

Bae, T.H. and Tak, T.M. (2005). Interpretation of fouling characteristics of ultrafiltration membranes during the filtration of membrane bioreactor mixed liquor. *Journal of Membrane Science,* 264, 151-160.

Bai, R. and Leow, H.F. (2002). Microfiltration of activated sludge wastewater-the effect of system operation parameters. *Separation and Purification Technology*, 29, 189-198.

Bouhabila, E.H., Aim, R.B., and Buisson, H. (2001). Fouling characterisation in membrane bioreactors. *Separation and Purification Technology*, 22-23, 123–132.

Bowen, W.R. and Jenner, F. (1995). Theoretical descriptions of membrane filtration of colloids and fine particles: an assessment and review. *Advances in Colloid and Interface Science*, 56, 141-200.

Chang, I.-S., Le-Clech, P., Jefferson, B. and Judd, S. (2002). Membrane fouling in membrane bioreactors for wastewater treatment. *Journal of Environmental Engineering, ASCE*, 128, 1018-1029.

Cho, B. D. and Fane, A. G. (2002). Fouling transient in nominally sub-critical flux operation of a membrane bioreactor. *Journal of Membrane Science*, 209, 391-403.

Churchouse, S. and Wildgoose, D. (1999). Membrane bioreactors progress from the laboratory to full-scale use. *Membrane Technology*, 111, 4-8.

Defrance, L., Jaffrin, M.Y., Gupta, B., Paullier, P. and Gaeugey, V. (2000). Contribution of various constituents of activated sludge to membrane bioreactor fouling. *Bioresource Technology,* 73, 105-112.

Defrance, L. and Jaffrin, M.Y. (1999). Comparison between filtrations at fixed transmembrane pressure and fixed permeate flux: application to a membrane bioreactor used for wastewater treatment. *Journal of Membrane Science*, 152, 203-210.

Dubois, M., Gilles, K. A., Hamilton, J. K., Rebers, P. A. and Smith, F. (1956). Colorimetric method for determination for sugars and related substances. *Analytical Chemistry*, 28, 350-356.

Field, R.W., Wu, D., Howell, J.A. and Gupta, B.B. (1995). Critical flux concept for microfiltration fouling. *Journal of Membrane Science*, 100, 259-272.

Foley, G. (2006). A review of factors affecting filter cake properties in dead-end microfiltration of microbial suspensions. *Journal of Membrane Science,* 274, 38–46

Frølund, B., Palmgren, R., Keiding, K. and Nielsen, P.H. (1996). Extraction of extracellular polymer from activated sludge using a cation exchange resin. *Water Research*, 30, 1749-1758.

Gander, M., Jefferson, B. and Judd, S. (2000). Aerobic MBRs for domestic wastewater treatment: a review with cost considerations. *Separation and Purification Technology*, 18, 119-130.

Germain, E., Stephenson, T. and Pearce, P. (2005). Biomass characteristics and membrane aeration: Toward a better understanding of membrane fouling in submerged membrane bioreactors (MBRs). *Biotechnology and Bioengineering*, 90, 316-322

Ji, L. and Zhou, J. (2006). Influence of aeration on microbial polymers and membrane fouling in submerged membrane bioreactors. *Journal of Membrane Science*, 276, 168-177.

Jin, Y.-L., Lee, W.-N., Lee, C.-H., Chang, I.-S., Huang, X. and Swaminathan, T. (2006). Effect of DO concentration on biofilm structure and membrane filterability in submerged membrane bioreactor. *Water Research*, 40, 2829-2836.

Judd, S. (2004). A review of fouling of membrane bioreactors in sewage treatment. *Water Science and Technology*, 49, 229-235.

Lebegue, J., Heran, M. and Grasmick, A. (2007). Membrane bioreactor: Distribution of critical flux throughout immersed HF bundle. *Proceedings of International Workshop on Membranes and Separation Processes, INSA-Toulouse, France, 11 July 2007.*

Le-Clech, P., Jefferson, B. and Judd, S. (2003a). Impact of aeration, solids concentration and membrane characteristics on the hydraulic performance of a membrane bioreactor. *Journal of Membrane Science*, 218, 117-129.

Le-Clech, P., Jefferson, B., Chang, I.S. and Judd, S. (2003b). Critical flux determination by the flux-step method in a submerged membrane bioreactor. *Journal of Membrane Science*, 227, 81-93.

Le-Clech, P., Chen, V. and Fane, A.G. (2006). Fouling in membrane bioreactors used in wastewater treatment. *Journal of Membrane Science*, 284, 17-53.

Lee, J.M., Ahn, W.Y. and Lee, C.H. (2001). Comparison of the filtration characteristics between attached and suspended growth microorganisms in submerged membrane bioreactor. *Water Research*, 35, 2435-2445.

Lee, W., Kang, S., and Shin, H. (2003). Sludge characteristics and their contribution to microfiltration in submerged membrane bioreactors. *Journal of Membrane Science*, 216, 217–227.

Lee, W.-N., Kang, I.-J. and Lee, C.H. (2006). Factors affecting filtration characteristics in membrane-coupled moving bed biofilm reactor. *Water Research*, 40, 1827-1835.

Lee, C.H., Park, P.K., Lee, W.N., Hwang, B.K., Hong, S.H., Yeon, K.M., Oh, H.S. and Chang, I.S. (2007a). Correlation of biofouling with biocake architecture in MBR. *Proceedings of IWA International Conference on Membranes for Water and Wastewater Treatment, Harrogate International Conference Centre, UK, 15 - 17 May 2007.*

Lee, W.-N., Chang, I.-S., Hwang, B.-K., Park, P.-K., Lee, C.-H. and Huang, X. (2007b). Changes in biofilm architecture with addition of membrane fouling reducer in a membrane bioreactor. *Process Biochemistry*, 42, 655-661.

Li, X., Gao, F., Hua, Z., Du, G. and Chen, J. (2005). Treatment of synthetic wastewater by a novel MBR with granular sludge developed for controlling membrane fouling. *Separation and Purification Technology*, 46, 19-25.

Liang, S., Liu, C. and Song, L. (2007). Soluble microbial products in membrane bioreactor operation: Behaviors, characteristics and fouling potential. *Water Research*, 41, 95-101.

Lowry, O.H., Rosebrough, N.R., Farr, A.L. and Randall, R.J. (1951). Protein measurement with the folin phenol reagent. *Journal of Biological Chemistry*, 193, 265-275.

Mathieu, S. and Etienne, P. (2000). Estimation of wastewater biodegradable COD fractions by combining respirometric experiments in various So/Xo ratios. *Water Research*, 34, 1233-1246.

Metcalf and Eddy (2003). *Wastewater Engineering: Treatment and Reuse*. Fourth Edition, McGraw-Hill, USA, ISBN: 0-07-041878-0.

Mitsubishi Rayon (2004). *Standard Use Conditions for SteraporeSUR Series Hollow-Fiber Membrane Units*. Mitsubishi Rayon Engineering Co. Ltd., Japan.

Mulder, M. (1996). *Basic Principle of Membrane Technology.* Kluwer Academic Publishers, USA, ISBN: 0-7923-4248-8.

Munz, G., Gori, R., Mori, G. and Lubello, C. (2007). Powdered activated carbon and membrane bioreactors (MBR-PAC) for tannery wastewater treatment: Long term effect on biological and filtration process performances. *Desalination*, 207, 349-360.

Ng, H.Y. and Hermanowicz, S.W. (2005). Membrane bioreactor operation at short solids retention times: performance and biomass characteristics. *Water Research*, 39, 981-992.

Ognier, S., Wisniewski, C. and Grasmick, A. (2002). Influence of macromolecule adsorption during filtration of a membrane bioreactor mixed liquor suspensions. *Journal of Membrane Science*, 209, 27-37.

Ognier, S., Wisniewski, C. and Grasmick, A. (2004). Membrane bioreactor fouling in sub-critical filtration conditions: a local critical flux concept. *Journal of Membrane Science*, 229, 171-177.

Pollice, A., Brookes, A., Jefferson, B. and Judd, S. (2005). Sub-critical flux fouling in membrane bioreactors - a review of recent literature. *Desalination*, 174, 221-230.

Roest, H.F., Lawrence, D.P. and Bentem, A.G.N. (2002). *Membrane Bioreactors for Municipal Wastewater Treatment*. Stowa Report, IWA publishing, UK, ISBN: 90-5773-169-X.

Rogenberger, S., Laabs, C., Lesjean, B., Gnirss, R., Jekel, M. and Schrotter, J.-C. (2006). Impact of colloidal and soluble organic material on membrane performance in membrane bioreactors for municipal wastewater treatment. *Water Research*, 40, 710-720.

Sombatsompop, K., Visvanathan, C. and Aim, R.B. (2006). Evaluation of biofouling phenomenon is suspended and attached growth membrane bioreactor systems. *Desalination*, 201, 138-149.

Stephenson, T., Judd, S., Jefferson, B. and Brindle, K. (2000). *Membrane Bioreactors for Wastewater Treatment.* IWA publishing, UK, ISBN: 1-900222-07-8

Trussell, R.S., Merlo, R.P., Hermanowicz, S.W., and Jenkins, D. (2007). Influence of mixed liquor properties and aeration intensity on membrane fouling in a submerged membrane bioreactor at high mixed liquor suspended solids concentrations. *Water Research*, 41, 947-958.

Ueda, T., Hata, K., Kikuoka, Y. and Seino, O. (1997). Effects of aeration on suction pressure in a submerged membrane bioreactor. *Water Research*, 31, 489-494.

Visvanathan, C., Aim, R.B. and Parameshwaran, K. (2000). Membrane separation bioreactors for wastewater treatment. *Critical Reviews in Environmental Science and Technology*, 30, 1-48.

Wang, X.-M., Li, X.-Y. and Huang, X. (2007). Membrane fouling in a submerged membrane bioreactor (SMBR): Characterisation of the sludge cake and its high filtration resistance. *Separation and Purification Technology,* 52, 439-445

Wicaksana, F., Fane, A.G. and Chen, V. (2006). Fiber movement induced by bubbling using submerged hollow fiber membranes. *Journal of Membrane Science*, 271, 186-195.

Wisniewski, C. and Grasmick, A. (1998). Floc size distribution in a membrane bioreactor and consequences for membrane fouling. *Colloids and Surfaces A: Physicochemical and Engineering Aspects,* 138, 403-411

Wu, D., Howell, J.A. and Field, R.W. (1999). Critical flux measurement for model colloids. *Journal of Membrane Science*, 152, 89-98.

Xing, C.-H., Qian, Y., Wen, X.-H., Wu, W.-Z. and Sun, D. (2001). Physical and biological characteristics of tangential-flow MBR for municipal wastewater treatment. *Journal of Membrane Science*, 191, 31-42.

Yamamoto, K., Hiasa, M., Mahmood, T. and Matsuo T. (1989). Direct solid-liquid separation using hollow fiber membrane in an activated sludge aeration tank. *Water Science and Technology*, 21, 43-54.

Yang, W., Cicek, N. and Ilg, J. (2006). State-of-the-art of membrane bioreactors: Worldwide research and commercial applications in North America. *Journal of Membrane Science*, 270, 201-211.

Yeo, A.P.S., Law, A.W.K. and Fane, A.G. (2006). Factors affecting the performance of a submerged hollow fiber bundle. *Journal of Membrane Science*, 280, 969-982.

Ying, Z. and Ping G. (2006). Effect of powdered activated carbon dosage on retarding membrane fouling in MBR. *Separation and Purification Technology*, 52, 154-160.

Yoon, S.-H., Collins, J.H., Musale, D., Sundararajan, S., Tsai, S.-P., Hallsby, G.A., Kong, J.F., Koppes, J. and Cachia, P. (2005). Effects of flux enhancing polymer on the characteristics of sludge in membrane bioreactor process. *Water Science and Technology*, 51, 151-157.

Yoon, S.-H. and Collins, J.H. (2006). A novel flux enhancing method for membrane bioreactor (MBR) process using polymer. *Desalination*, 191, 52-61.

Zhang, B., Yamamoto, K., Ohgaki, S. and Kamibo, N. (1997). Floc size distribution and bacterial activities in membrane separation activated sludge processes for small-scale wastewater treatment/reclamation. *Water Science & Technology*, 35, 37-44.

Zhang, J., Chua, H.C., Zhou, J. and Fane, A.G. (2006). Factors affecting the membrane performance in submerged membrane bioreactors. *Journal of Membrane Science,* 284, 54-66.

APPENDIX-A

Shear intensity (G) induced by mechanical and pneumatic mixing

Turbulence can be induced mechanically and/or pneumatically. Mechanical mixing through rotating impeller is quantified in terms of mean velocity gradient or shear intensity (G) with units of s^{-1}. Similarly, pneumatic mixing induced by volume of air released under compressed conditions can be quantified in terms of G.

The laminar and turbulent flow conditions are quantified in terms of Reynolds number (N_R) where a value less than 10 is considered as laminar, between 10 and 10,000 as transitional phase and greater than 10,000 as turbulent. The Reynolds number (N_R) is determined using the following equation:

$$N_R = \frac{D^2 n \rho}{\mu} \qquad \text{Equation A.1}$$

where D is the diameter of the propeller n is the mixing speed (rev/s), ρ is the density of water and μ is the dynamic viscosity.

The power requirement (P) is calculated for each mixer using the following equation:

$$P = N_p.\rho.n^3.D^5 \ (N_R > 10{,}000) \qquad \text{Equation A.2}$$

where N_p is power number for impeller

Power dissipated by air release is determined using the following expression:

$$P = p_a.V_a \ln \frac{p_c}{p_a} \qquad \text{Equation A.3}$$

where P is power dissipated (kW), p_a is atmospheric pressure (kPa), p_c is air pressure at the point of discharge (kPa) and V_a is volume of air released at atmospheric pressure (m^3/s)

Shear intensity (G) in the fluid is determined as:

$$G = \sqrt{\frac{P}{\mu.V}} \qquad \text{Equation A.4}$$

where P is the power input or dissipated (W) and V is the reactor volume (m^3).

Calculation

The following shear intensities (G) are calculated for MBR_0, MBR_{150}, MBR_{300} and MBR_{450} with mechanical mixing speeds of 0, 150, 300 and 450 rpm, respectively.

Reynolds number (N_R):

$$N_R = \frac{D^2 n \rho}{\mu}$$

Diameter of impeller (D) = 0.1 m

Density of mixed liquor (ρ) = 1000 kg/m^3 (approximately)

Vicosity of mixed liquor (μ) = 2.5 x 10^{-3} N-s/m^2 (Assumed)

Note: Sludge viscosity assumption based on literature review: Wang et al. (2006) found that for MLSS concentration between 4.6-11.6 g/L, the viscosity varied between 1-3 x 10^{-3} N-s/m^2 in submerged MBR.

Table A.1: Mechanical mixing speeds and corresponding Reynolds number in the MBRs

MBR	Mechanical mixing rpm (rps)	Reynolds number (N_R)
MBR_0	0	0
MBR_{150}	150 (2.5)	10,000
MBR_{300}	300 (5.0)	20,000
MBR_{450}	450 (7.5)	30,000

Pneumatic power (P_p):

$$P_p = p_a V_a \ln \frac{p_c}{p_a}$$

Atmospheric pressure (P_a) = 101.35 kPa (14.7 psi)

Compressed pressure (P_c) = 103.42 kPa (15 psi) (Assumed)

Note: Since the compressed pressure value after the airflow meter was not available, it was assumed to be slightly higher than the atmospheric pressure.

Airflow rate (V_a) = 8.33 x 10^{-5} m^3/s (5 L/min)

Pneumatic power dissipated in all the MBRs:

P_p = 1.71 x 10^{-4} kW = 0.17 W (in all the MBRs)

Mechanical power (P_m):

$$P_m = N_p \rho \, n^3 D^5$$

N_p = 1.1 for pitched-blade turbine (32^o PBT) (Medcalf and Eddy, 2003, p-354)

Table A.2: Mechanical mixing speeds and corresponding power requirements in the MBRs

MBR	Mechanical mixing rpm (rps)	P_m (W)
MBR_0	0	0
MBR_{150}	150 (2.5)	0.17
MBR_{300}	300 (5.0)	1.38
MBR_{450}	450 (7.5)	4.64

Total power requirement (P_T) and shear intensity (G):

$P_T = P_p + P_m$

$$G = \sqrt{\frac{P_T}{\mu V}}$$

Reactor volume (V) = 10 L (0.01 m^3)

Table A.3: Total power requirements (P_T) and corresponding shear intensities (G) in the MBRs

MBR	P_T (W)	G (1/s)
MBR_0	0.17	83
MBR_{150}	0.34	117
MBR_{300}	1.55	249
MBR_{450}	4.81	439

Appendix-B

EPS measurement

The EPS was measured in the form of soluble EPS and bound EPS. The two forms of EPS were extracted by the procedure outlined in the following figure.

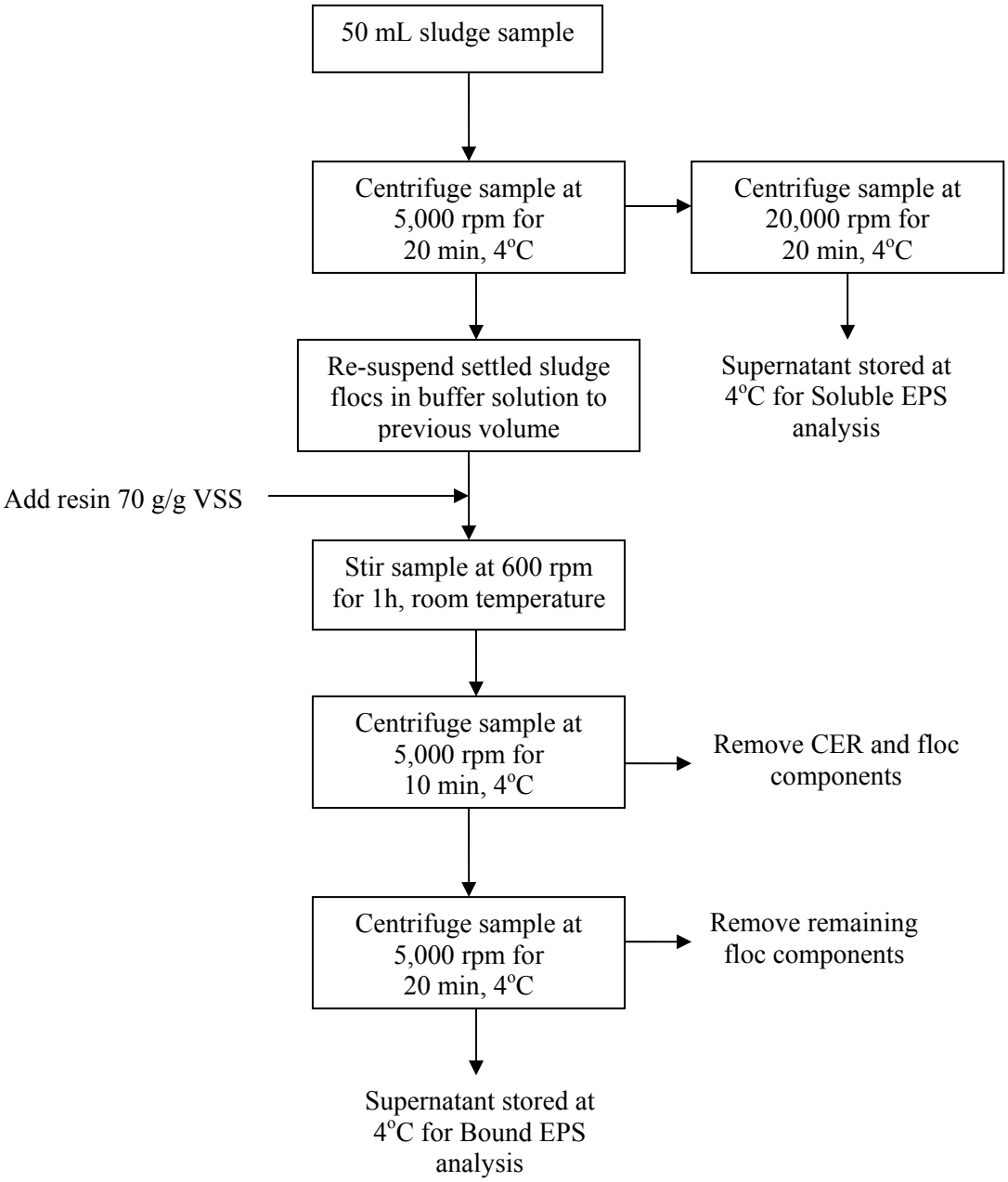

Figure B-1: EPS extraction procedure

The commercial grade CER resin from Dow Chemical Company was used for the EPS extraction. The specifications of the resin are as follows:

Table B-1: CER resin specifications

Product	DOWEX HCR-S/S
Type	Strong acid cation (Na^+ form)
Matrix	Styrene-DVB gel
Functional group	Sulphonic acid
Bead size distribution range0	0.3-1.2 mm (50-16 mesh)
Water content	48-52 %
Maximum operating temperature	120^oC
pH range	0-14

The CER was required to be soaked for 1 h in the extraction buffer solution and dried in room temperature for 1 h before usage. The CER buffer solution consists of the following constituents and respective concentrations.

Table B-2: CER buffer solution constituents

Chemical name	Concentration	Amount in 1 L DI water
$Na_3PO_4.12H_2O$	2 mM	380*2/1000 = 0.76 g
$NaH_2PO_4.2H_2O$	4 mM	156*4/1000 = 0.624 g
NaCl	9 mM	58.5*9/1000 = 0.5265 g
KCl	1 mM	74.6*1/1000 = 0.0746 g

Carbohydrate and protein fractions of the soluble and bound EPS were measured by the colorimetric methods of Dubois et al. (1956) and Lowry et al. (1951), respectively using spectrophotometer (U-2001, Hitachi, Japan). The two colorimetric methods are explained in detail in the following sections.

Measurement of carbohydrate: Phenol-sulfuric acid method (Dubois method)

Principle

Simple sugars, oligosaccharides. polysaccharides and their derivatives give a stable orange-yellow color when treated with phenol and concentrated sulfuric acid. Under proper conditions, the accuracy of the method is within 2%.

Chemical Reagents

- 5 w% Phenol solution
- Sulfuric acid (H_2SO_4)
- D-Glucose for standard solution

Procedure

Standardization:

1. Make all measurements in duplicate
2. Pipette 2 mL of sugar solution (D-Glucose) containing 0, 5, 10, 15, 20, 25, 30, 35, 40 and 50 mg/L of glucose into test tubes

3. Add 1 mL of the 5% phenol solution and 5 mL of the concentrated sulfuric acid to the test tubes. The addition should be rapid. In addition, direct the stream of acid against the liquid surface, rather than against the side of the test tube for good mixing.
4. Allow the tubes to stand 10 min.
5. Thoroughly mix the solutions using vertex machine.
6. Place in water bath for 15 min to cool the solutions
7. Measure absorbance at 490 nm.
8. Prepare a calibration curve of concentration of sugar (Glucose-D) versus absorbance.

A standard curve of carbohydrate concentrations using Glucose-D as standard solution versus absorbances at 490 nm is shown in Figure B-2.

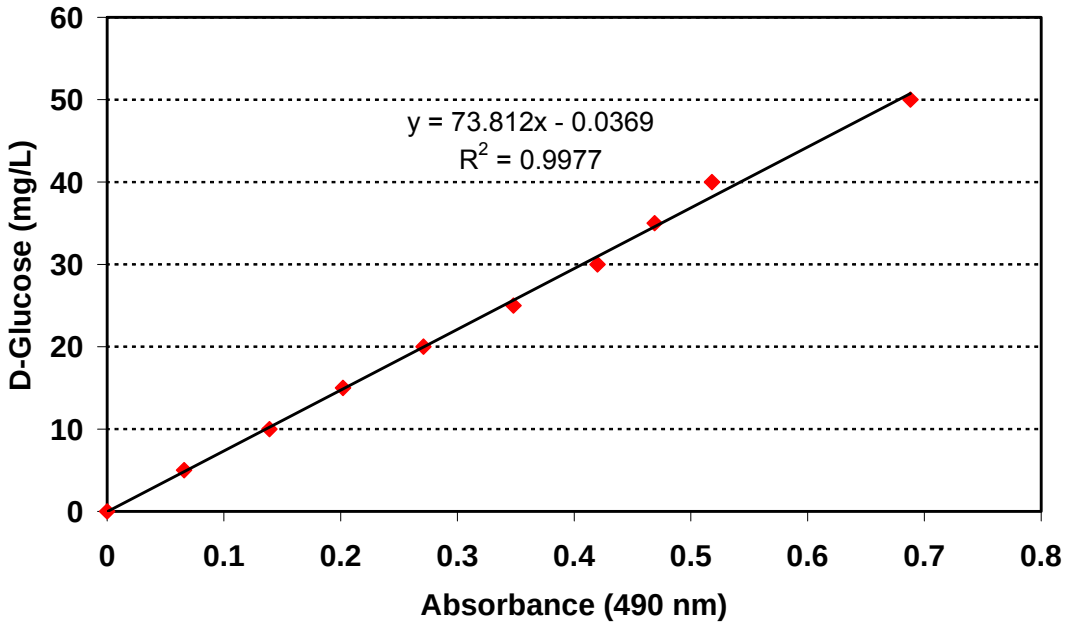

Figure B-2: Carbohydrate Standard Curve

Analysis: (Sample for soluble and bound EPS)

1. Soluble and bound EPS were determined with dilution factor 2 i.e. 1 mL sample and 1 mL deionized (DI) water were pipetted into the test tubes.
2. Remaining procedure was identical to the one followed for carbohydrate standardization mentioned above.
3. Measured absorbance of sample solution at 490 nm was correlated to the carbohydrate concentration in the sample using the carbohydrate standard curve (Figure B-2).
4. Carbohydrate concentration was reported in mg/L for soluble EPS and mg/gVSS for bound EPS.

Calculation

Soluble EPS

According to the carbohydrate standard curve and with the dilution factor (2):

$$Carbohydrate\ (mg/L) = 2 \times (73.812 \times ABS - 0.0369)(mg/L) \qquad \text{Equation B-1}$$

Bound EPS

According to the carbohydrate standard curve and with the dilution factor (2):

$$Carbohydrate\ (mg/gVSS) = \frac{2 \times (73.812 \times ABS - 0.0369)(mg/L) \times Final\ \text{volume}\ (mL)}{VSS(mg/L) \times \text{Original volume}\ (mL)} \times 1000(mg/g)$$

Equation B-2

Measurement of Protein: Lowry method

Principle

This is a standard and quantitative method for determining protein content in a solution. Lowry method is a reliable method for protein quantification and little variation among different proteins has been observed.

Chemical Reagents

- CuSO4.5H2O
- Sodium Citrate
- Na2CO3
- NaOH
- Folin-Ciocalteu phenol reagent
- Bovine Serum Albumin (BSA) for standard solution

Solution A, 100 mL;

0.5 g $CuSO_4.5H_2O$
1 g $Na_3C_6H_5O_7.2H_2O$ (Sodium citrate)

Solution B, 1L;

20g Na_2CO_3
4 g NaOH

Solution C, 51 mL;

1 mL solution A
50 mL solution B

Solution D, 20mL;

10 mL Folin-Ciocalteu phenol reagent + 10 mL DI water

Procedure

Standardization:

1. Make all measurements in duplicate
2. Pipette 0.5 mL of BSA solution containing 0, 20, 30, 40, 50, 60, 80 and 100 mg/L of BSA into test tubes
3. Add 2.5 mL solution C
4. Thoroughly mix the solutions using vertex machine and let them stand at room temperature for 10 min
5. Add 0.25 mL Solution D and thoroughly mix again.
6. After 20 min, measure absorbance at 750 nm.
7. Prepare a calibration curve of protein (BSA) concentration (mg/L) versus absorbance.

A standard curve of protein concentrations using BSA as standard solution versus absorbances at 490 nm is shown in Figure B-3.

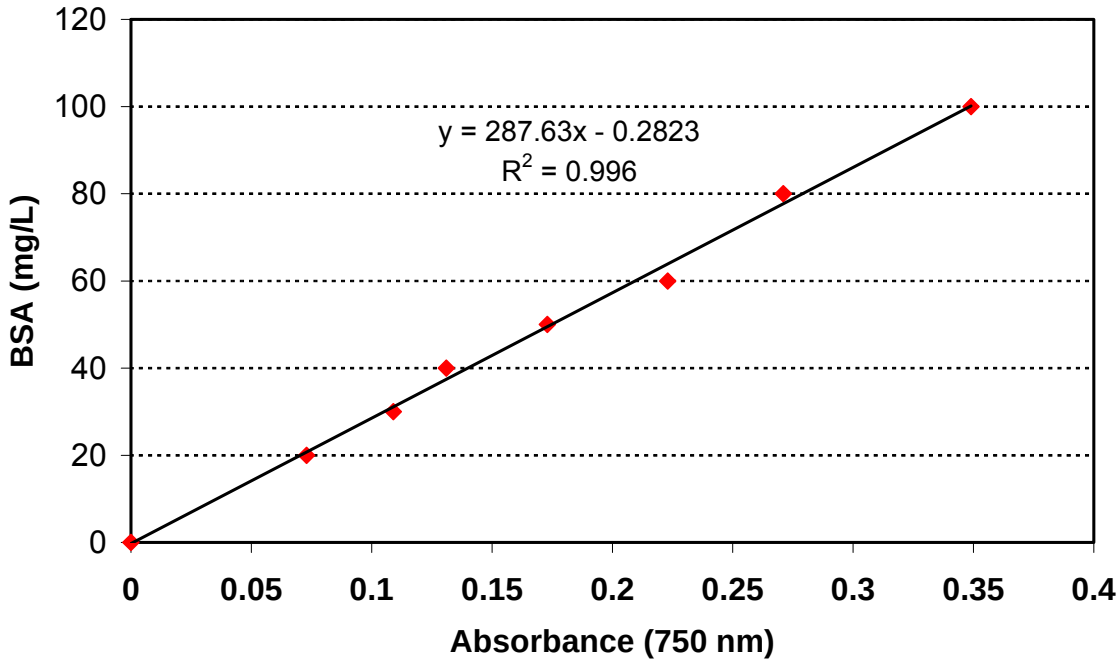

Figure B-3: Protein standard curve

Analysis: (Sample for soluble and bound EPS)

1. Soluble EPS was determined with no dilution while bound EPS was determined with dilution factor 2 i.e. 1 mL sample and 1 mL deionized (DI) water were pipetted into the test tubes.
2. Remaining procedure was identical to the one followed for protein standardization mentioned above.
3. Measured absorbance of sample solution at 750 nm was correlated to the protein concentration in the sample using the protein standard curve (Figure B-3).
4. Protein concentration was reported in mg/L for soluble EPS and mg/gVSS for bound EPS.

Calculation:

Soluble EPS

According to the protein standard curve:

$$\text{Protein } (mg/L) = 287.63 \times ABS - 0.2823(mg/L) \qquad \text{Equation B-3}$$

Bound EPS

According to the protein standard curve and with the dilution factor (2):

$$PS\ (mg/gVSS) = \frac{2 \times (287.63 \times ABS - 0.2823)(mg/L) \times Final\ volume(mL)}{VSS(mg/L) \times Original\ volume(mL)} \times 1000(mg/g)$$

Equation B-4

Appendix-C

Phase I experimental results: Mechanically mixed MBRs

Table C-1: Trans-membrane pressure (TMP), permeate flux versus filtration duration in the mechanically mixed MBRs

Time (h)	MBR_0		Time (h)	MBR_{150}		Time (h)	MBR_{300}		Time (h)	MBR_{450}	
	TMP (kPa)	Flux ($L/m^2.h$)		TMP (kPa)	Flux ($L/m^2.h$)		TMP (kPa)	Flux ($L/m^2.h$)		TMP (kPa)	Flux ($L/m^2.h$)
0	3.2	3.7	0	3.1	4.0	0	2.6	4.1	0	3.3	3.8
2	3.3		2	3.2		2	2.6		2	3.3	
6	3.3	3.8	6	3.4	4.2	6	2.6	4.2	6	3.7	3.8
7	3.4		7	3.4		7	2.6		7	3.7	
18	3.6	3.9	18	3.6	4.2	18	2.6	4.2	18	4.0	4.0
25	3.8		25	3.5		25	2.7		25	3.9	
30	4.2	4.0	30	3.6	4.2	30	2.9	4.2	30	4.0	3.9
33	4.8		33	3.8		33	2.9		33	4.1	
43	14.2	3.9	43	4.0	4.2	43	3.0	4.1	43	4.1	3.9
44	16.8		44	4.0		44	3.1		44	4.1	
46	30.5		46	3.9		46	3.1		46	4.1	
			48	3.8		48	3.1		48	4.0	
			53	4.2		53	3.1		53	3.8	
			55	4.3	4.2	55	3.2	4.2	55	3.9	3.9
			57	4.5		57	3.3		57	4.2	
			67	5.2		67	3.5		67	4.5	
			71	5.3		71	3.6		71	4.4	
			75	5.8		75	3.7		75	4.4	
			79	6.4	4.1	79	3.8	4.1	79	4.5	4.0
			80	6.6		80	3.8		80	4.5	
			82	7.1		82	3.8		82	4.5	
			90	9.3	4.2	90	4.2	4.1	90	4.7	4.0
			99	11.4		99	4.5		99	4.8	

Time (h)	MBR_0		Time (h)	MBR_{150}		Time (h)	MBR_{300}		Time (h)	MBR_{450}	
	TMP (kPa)	Flux ($L/m^2.h$)		TMP (kPa)	Flux ($L/m^2.h$)		TMP (kPa)	Flux ($L/m^2.h$)		TMP (kPa)	Flux ($L/m^2.h$)
			103	13.7	4.1	103	4.5	4.1	103	4.8	4.0
			104	14.4		104	4.8		104	4.8	
			115	22.4	4.1	115	5.9	4.2	115	5.4	4.0
			118	24.5		118	5.9		118	5.4	
			122	27.8		122	6.2		122	5.4	
			127	32.8	3.9	127	6.6	4.1	127	5.6	4.0
						138	8.5	4.1	138	6.8	4.0
						140	8.6		140	6.8	
						142	9.0		142	7.0	
						151	10.9		151	7.8	
						152	11.1		152	8.0	
						163	12.8	4.0	163	9.3	4.1
						170	12.9		170	10.7	
						175	13.7		175	12.1	
						187	16.6	4.1	187	14.9	4.1
						194	17.9		194	17.5	
						199	19.7		199	19.1	
						210	22.0	4.1	210	26.0	4.1
						217	25.7		217	29.8	
						218	25.9		218	30.5	
						219	26.9		219	31.0	3.4
						223	29.0				
						226	29.6	3.5			

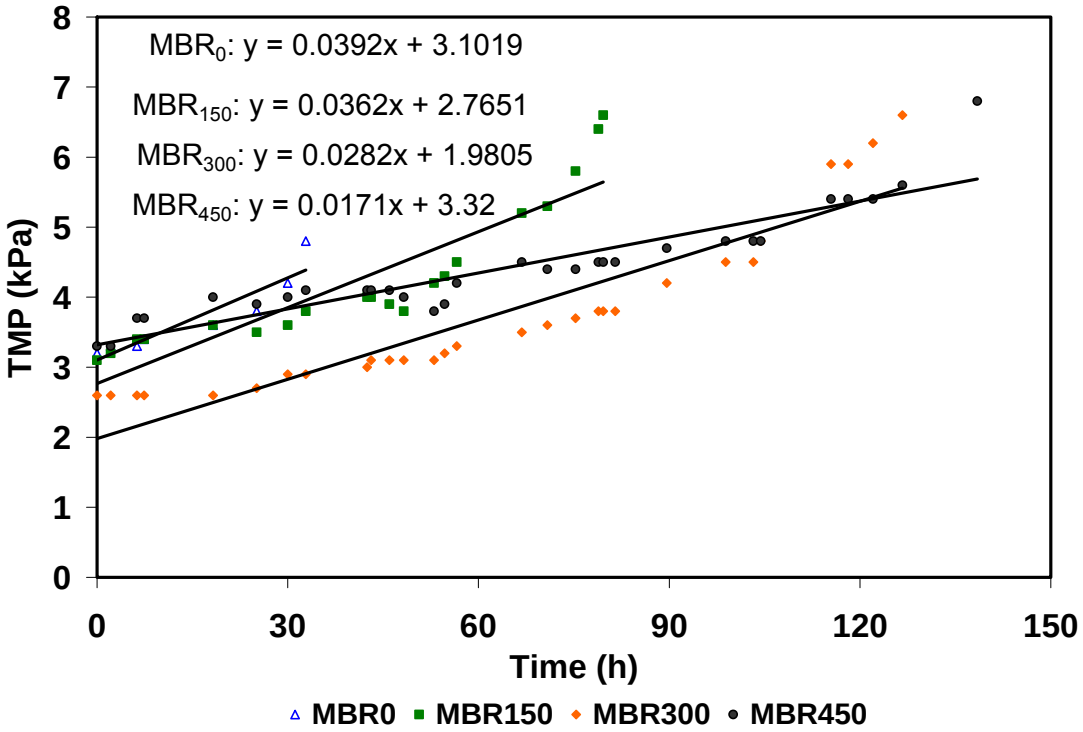

Figure C-1: First stage fouling rates in the mechanically mixed MBRs

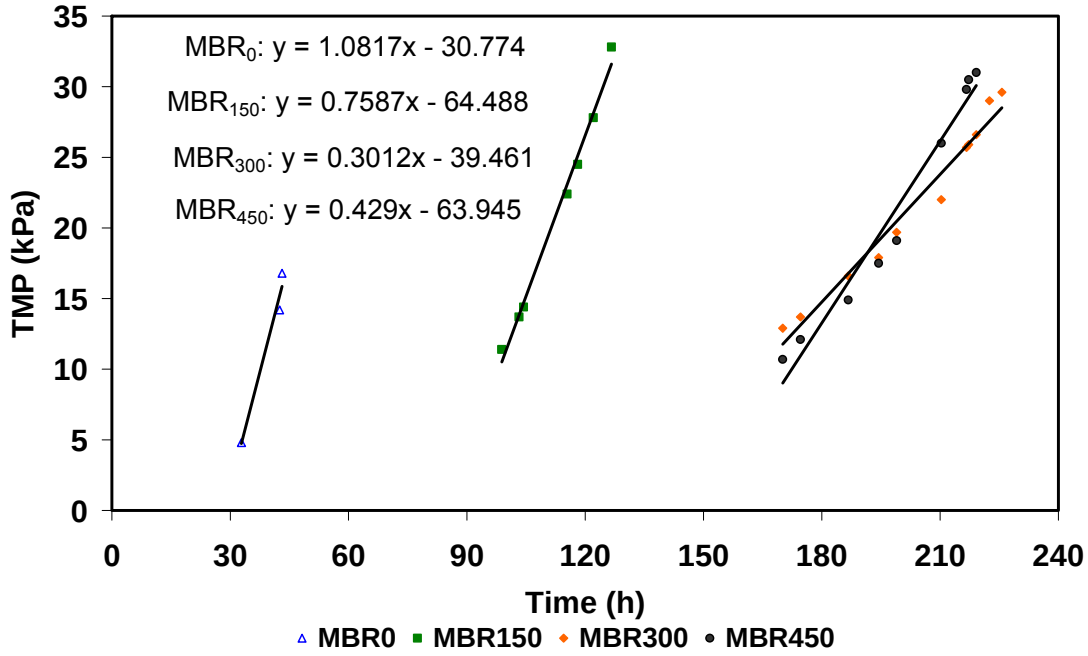

Figure C-2: Second stage fouling rates in the mechanically mixed MBRs

Table C-2: Fouling rates in the mechanically mixed MBRs

Fouling rate (kPa/h)	MBR_0	MBR_{150}	MBR_{300}	MBR_{450}
First stage	0.039	0.036	0.028	0.017
Second stage	1.082	0.759	0.301	0.429

Table C-3: MLSS, MLVSS concentrations and MLVSS/MLSS ratio in the mechanically mixed MBRs

Operation	MBR_0			MBR_{150}			MBR_{300}			MBR_{450}		
(Day)	MLSS (mg/L)	MLVSS (mg/L)	MLVSS/ MLSS	MLSS (mg/L)	MLVSS (mg/L)	MLVSS/ MLSS	MLSS (mg/L)	MLVSS (mg/L)	MLVSS/ MLSS	MLSS (mg/L)	MLVSS (mg/L)	MLVSS/ MLSS
0	7650	6740	88	5890	5110	87	7900	7060	89	6220	5600	90
5	6260	5580	89	6880	6180	90	8620	7800	90	6660	5980	90
8	7420	6700	90	7380	6660	90	9000	8280	92	7800	7100	91
13	8300	7600	92	9140	8400	92	8400	7720	92	7620	6860	90
20	7060	6440	91	5540	5160	93	6560	5920	90	6860	6240	91
25	7633	6967	91	7500	6920	92	6920	6320	91	6880	6280	91
28	7680	6900	90	8560	7780	91	6160	5600	91	6120	5560	91
32	7800	7086	91	7480	6820	91	6720	6400	95	6220	5700	92
36	8240	7520	91	7130	6540	92	7280	6680	92	6660	6120	92
40	6460	5760	89	6200	5660	91	7380	6720	91	6560	6040	92
43	6340	5780	91	6880	6240	91	6660	6100	92	6600	6000	91
47	5640	5020	89	6760	6040	89	6800	6200	91	6380	5700	89
51	6180	5440	88	5960	5320	89	5460	4740	87	6480	5720	88
54	6560	5960	91	6720	6080	90	5120	4720	92	6060	5520	91
56	6900	6220	90	8260	7540	91	6680	6060	91	7500	6760	90
58	8260	7220	87	8960	8160	91	5400	4800	89	6600	5920	90
60	8580	7660	89	8260	7380	89	5580	4960	89	6460	5820	90
62	8960	8140	91	9220	8440	92	6160	5640	92	6060	5500	91
66	8260	7480	91	8220	7500	91	6500	5940	91	5860	5300	90
68	8420	7580	90	7520	6780	90	6360	5760	91	6340	5660	89
72	7400	6620	89	7120	6240	88	6400	6120	96	6020	5400	90
76	9200	8400	91	7240	6640	92	8520	7760	91	6320	5660	90
94	9740	8720	90	8480	7600	90	8400	7540	90	5000	4400	88
104	9420	8220	87	6860	6500	95	8100	7400	91	4100	3740	91
108	8140	7460	92	5920	5420	92	6380	5820	91	4400	4080	93

Operation (Day)	MBR_0			MBR_{150}			MBR_{300}			MBR_{450}		
	MLSS (mg/L)	MLVSS (mg/L)	MLVSS/ MLSS	MLSS (mg/L)	MLVSS (mg/L)	MLVSS/ MLSS	MLSS (mg/L)	MLVSS (mg/L)	MLVSS/ MLSS	MLSS (mg/L)	MLVSS (mg/L)	MLVSS/ MLSS
112	8660	7740	89	6220	5620	90	7180	6420	89	4320	4140	96
118	8220	7440	91	6360	5700	90	7740	7020	91	5520	4980	90
125	7400	6760	91	6120	5620	92	6540	5940	91	4800	4340	90
Average	**7798**	**7031**	**90**	**7219**	**6548**	**91**	**7022**	**6392**	**91**	**6029**	**5453**	**90**
Standard deviation	**1031**	**942**	**1**	**1039**	**964**	**2**	**1055**	**976**	**2**	**1025**	**925**	**2**

Table C-4: Membrane fouling resistances in MBR_0

Experiment No.	Total resistance (R_t) ($\times 10^{12}$ m^{-1})	Cake resistance (R_c) ($\times 10^{12}$ m^{-1})	Fouling resistance (R_f) ($\times 10^{12}$ m^{-1})	Intrinsic membrane resistance (R_m) ($\times 10^{12}$ m^{-1})	R_c/R_t (%)
1	47.08	46.51	0.09	0.48	98.8
2	136.36	134.43	1.53	0.40	98.6
3	54.95	54.14	0.53	0.29	98.5
Average	**79.46**	**78.36**	**0.72**	**0.39**	**98.6**

Table C-5: Membrane fouling resistances in MBR_{150}

Experiment No.	Total resistance (R_t) ($\times 10^{12}$ m^{-1})	Cake resistance (R_c) ($\times 10^{12}$ m^{-1})	Fouling resistance (R_f) ($\times 10^{12}$ m^{-1})	Intrinsic membrane resistance (R_m) ($\times 10^{12}$ m^{-1})	R_c/R_t (%)
1	97.00	96.10	0.36	0.53	99.1
2	72.19	70.77	0.98	0.44	98.0
3	81.36	80.07	0.96	0.32	98.4
Average	**83.51**	**82.31**	**0.77**	**0.43**	**98.5**

Table C-6: Membrane fouling resistances in MBR_{300}

Experiment No.	Total resistance (R_t) ($\times 10^{12}$ m^{-1})	Cake resistance (R_c) ($\times 10^{12}$ m^{-1})	Fouling resistance (R_f) ($\times 10^{12}$ m^{-1})	Intrinsic membrane resistance (R_m) ($\times 10^{12}$ m^{-1})	R_c/R_t (%)
1	74.48	73.46	0.45	0.57	98.6
2	65.64	63.95	0.98	0.72	97.4
3	89.54	87.91	1.11	0.52	98.2
Average	**76.55**	**75.10**	**0.85**	**0.60**	**98.1**

Table C-7: Membrane fouling resistances in MBR_{450}

Experiment No.	Total resistance (R_t) ($\times 10^{12}$ m^{-1})	Cake resistance (R_c) ($\times 10^{12}$ m^{-1})	Fouling resistance (R_f) ($\times 10^{12}$ m^{-1})	Intrinsic membrane resistance (R_m) ($\times 10^{12}$ m^{-1})	R_c/R_t (%)
1	67.34	66.64	0.33	0.38	99.0
2	85.81	84.22	1.18	0.40	98.2
Average	**76.57**	**75.43**	**0.75**	**0.39**	**98.6**

Table C-8: Normalized capillary suction time (CST_N) in MBR_0

Experiment No.	CST (s)	MLSS (g/L)	CST_N [s/(g/L)]
1	22.6	8.3	2.7
2	25.0	9.2	2.7
3	19.5	8.6	2.3
4	12.9	8.7	1.5
5	16.2	8.2	2.0
6	20.6	7.4	2.8
Average	**19.4**	**8.4**	**2.3**
Standard deviation	**4.4**	**0.6**	**0.5**

Table C-9: Normalized capillary suction time (CST_N) in MBR_{150}

Experiment No.	CST (s)	MLSS (g/L)	CST_N [s/(g/L)]
1	11.5	8.2	1.4
2	14.0	7.2	1.9
3	15.9	7.5	2.1
4	13.5	6.2	2.2
5	13.2	6.4	2.1
6	15.3	6.1	2.5
Average	**13.9**	**7.0**	**2.0**
Standard deviation	**1.6**	**0.9**	**0.4**

Table C-10: Normalized capillary suction time (CST_N) in MBR_{300}

Experiment No.	CST (s)	MLSS (g/L)	CST_N [s/(g/L)]
1	11.0	6.5	1.7
2	13.9	8.5	1.6
3	10.2	8.6	1.2
4	10.7	7.2	1.5
5	13.6	7.0	1.9
6	11.8	6.5	1.8
Average	**11.8**	**7.4**	**1.6**
Standard deviation	**1.5**	**0.9**	**0.3**

Table C-11: Normalized capillary suction time (CST_N) in MBR_{450}

Experiment No.	CST (s)	MLSS (g/L)	CST_N [s/(g/L)]
1	10.2	5.9	1.7
2	17.4	6.3	2.8
3	10.4	4.3	2.4
4	11.3	4.3	2.6
5	13.3	5.5	2.4
6	14.4	4.8	3.0
Average	**12.8**	**5.2**	**2.5**
Standard deviation	**2.8**	**0.8**	**0.4**

Table C-12: Specific cake resistance (α) in MBR_0

Experiment No.	(t/V)/V ($\times 10^{10}$ s/m^6)	MLSS (kg/m^3)	α ($\times 10^{12}$ m/kg)
1	4.40	8.26	5.57
2	8.63	8.26	10.93
3	5.82	9.74	6.25
4	3.52	8.60	4.28
5	2.22	8.22	2.83
6	7.07	7.40	10.00
Average	**5.28**	**8.41**	**6.64**
Standard deviation	**2.36**	**0.76**	**3.20**

Table C-13: Specific cake resistance (α) in MBR_{150}

Experiment No.	(t/V)/V ($\times 10^{10}$ s/m^6)	MLSS (kg/m^3)	α ($\times 10^{12}$ m/kg)
1	1.71	8.96	2.00
2	4.83	8.22	6.15
3	4.10	8.48	5.06
4	2.59	7.54	3.59
5	2.51	6.36	4.13
6	2.17	6.12	3.71
Average	**2.99**	**7.61**	**4.11**
Standard deviation	**1.21**	**1.16**	**1.41**

Table C-14: Specific cake resistance (α) in MBR_{300}

Experiment No.	(t/V)/V ($\times 10^{10}$ s/m^6)	MLSS (kg/m^3)	α ($\times 10^{12}$ m/kg)
1	1.37	5.58	2.57
2	0.86	6.50	1.38
3	0.65	8.40	0.81
4	0.70	8.60	0.85
5	1.74	7.74	2.35
6	0.98	6.54	1.57
Average	**1.05**	**7.23**	**1.59**
Standard deviation	**0.43**	**1.20**	**0.74**

Table C-15: Specific cake resistance (α) in MBR_{450}

Experiment No.	(t/V)/V ($\times 10^{10}$ s/m^6)	MLSS (kg/m^3)	α ($\times 10^{12}$ m/kg)
1	2.08	6.60	3.30
2	0.90	5.86	1.61
3	0.94	5.00	1.97
4	0.88	4.34	2.12
5	1.26	5.52	2.39
6	1.38	4.80	3.01
Average	**1.24**	**5.35**	**2.40**
Standard deviation	**0.46**	**0.81**	**0.64**

Table C-16: Soluble COD, effluent COD and colloidal COD in the mechanically-mixed MBRs

Experiment No.	Soluble COD (mg/L)				Effluent COD (mg/L)				Colloidal COD (COD_{sol} - COD_{eff}) (mg/L)			
	MBR_0	MBR_{150}	MBR_{300}	MBR_{450}	MBR_0	MBR_{150}	MBR_{300}	MBR_{450}	MBR_0	MBR_{150}	MBR_{300}	MBR_{450}
1	41.3	41.3	43.2	59.0	19.7	23.6	23.6	19.7	21.6	17.7	19.7	39.3
2	20.5	36.9	38.9	75.8	8.2	24.6	32.8	32.8	12.3	12.3	6.1	43.0
3	21.6	47.2	70.7	41.3								
4	24.0	71.9	57.9	44.0	16.0	16.0	24.0	16.0	8.0	55.9	34.0	28.0
5	27.7	34.0	63.9	61.9								
6	19.7	34.0	26.0	20.0								
7	36.2	57.1	64.7	47.6	22.8	19.0	26.6	41.9	13.4	38.1	38.1	5.7
8	51.0	49.1	32.1	41.5	11.3	15.1	22.7	11.3	39.6	34.0	9.4	30.2
9	40.3	28.2	38.3	50.4	12.1	12.1	16.1	20.1	28.2	16.1	22.2	30.2
Average	**31.4**	**44.4**	**48.4**	**49.0**	**15.0**	**18.4**	**24.3**	**23.6**	**20.5**	**29.0**	**21.6**	**29.4**
Standard deviation	**11.2**	**13.7**	**16.1**	**15.7**	**5.5**	**4.9**	**5.4**	**11.4**	**11.8**	**16.8**	**12.8**	**13.0**

Table C-17: Soluble EPS in MBR_0

Experiment No.	Protein (P) (mg/L)	Carbohydrate (C) (mg/L)	EPS (P + C) (mg/L)	P/C
1	0.3	7.1	7.4	0.0
2	3.2	10.6	13.7	0.3
3	3.0	10.5	13.5	0.3
4	2.0	9.9	11.9	0.2
Average	**2.1**	**9.5**	**11.6**	**0.2**
Standard deviation	**1.3**	**1.6**	**2.9**	**0.1**

Table C-18: Soluble EPS in MBR_{150}

Experiment No.	Protein (P) (mg/L)	Carbohydrate (C) (mg/L)	EPS (P + C) (mg/L)	P/C
1	3.2	8.6	11.7	0.4
2	4.9	9.9	14.8	0.5
3	1.4	7.1	8.5	0.2
4	3.0	7.9	10.9	0.4
Average	**3.1**	**8.4**	**11.5**	**0.4**
Standard deviation	**1.4**	**1.2**	**2.6**	**0.1**

Table C-19: Soluble EPS in MBR_{300}

Experiment No.	Protein (P) (mg/L)	Carbohydrate (C) (mg/L)	EPS (P + C) (mg/L)	P/C
1	0.7	2.2	2.9	0.3
2	5.0	12.6	17.7	0.4
3	1.9	9.9	11.8	0.2
4	3.0	12.2	15.2	0.2
Average	**2.7**	**9.2**	**11.9**	**0.3**
Standard deviation	**1.8**	**4.8**	**6.4**	**0.1**

Table C-20: Soluble EPS in MBR_{450}

Experiment No.	Protein (P) (mg/L)	Carbohydrate (C) (mg/L)	EPS (P + C) (mg/L)	P/C
1	2.2	8.4	10.6	0.3
2	3.3	8.8	12.1	0.4
3	1.9	7.4	9.3	0.3
4	1.7	11.5	13.2	0.2
Average	**2.3**	**9.0**	**11.3**	**0.3**
Standard deviation	**0.7**	**1.8**	**1.7**	**0.1**

Table C-21: Bound EPS in MBR_0

Experiment No.	Protein (P) (mg/L)	Carbohydrate (C) (mg/L)	EPS (P + C) (mg/L)	P/C
1	24.2	5.8	30.0	4.2
2	22.2	6.1	28.4	3.6
3	26.7	6.1	32.9	4.4
4	28.7	7.4	36.1	3.9
5	18.9	5.2	24.1	3.6
6	17.6	5.2	22.9	3.4
7	19.6	8.7	28.3	2.2
8	18.5	7.4	25.9	2.5
Average	**22.1**	**6.5**	**28.6**	**3.5**
Standard deviation	**4.1**	**1.2**	**4.4**	**0.8**

Table C-22: Bound EPS in MBR_{150}

Experiment No.	Protein (P) (mg/L)	Carbohydrate (C) (mg/L)	EPS (P + C) (mg/L)	P/C
1	21.1	4.1	25.2	5.2
2	22.9	5.3	28.2	4.3
3	29.8	5.7	35.5	5.2
4	28.2	8.7	36.9	3.3
5	33.9	7.9	41.8	4.3
6	33.4	8.9	42.3	3.8
7	21.3	3.4	24.7	6.3
8	22.5	5.5	28.0	4.1
Average	**26.6**	**6.2**	**32.8**	**4.6**
Standard deviation	**5.4**	**2.1**	**7.2**	**1.0**

Table C-23: Bound EPS in MBR_{300}

Experiment No.	Protein (P) (mg/L)	Carbohydrate (C) (mg/L)	EPS (P + C) (mg/L)	P/C
1	26.8	5.8	32.6	4.6
2	27.4	6.4	33.8	4.3
3	22.7	6.0	28.7	3.8
4	31.6	10.0	41.6	3.2
5	25.7	6.7	32.3	3.9
6	32.9	8.4	41.3	3.9
7	36.4	8.6	45.0	4.2
8	31.6	8.2	39.8	3.9
Average	**29.4**	**7.5**	**36.9**	**4.0**
Standard deviation	**4.5**	**1.5**	**5.8**	**0.4**

Table C-24: Bound EPS in MBR_{450}

Experiment No.	Protein (P) (mg/L)	Carbohydrate (C) (mg/L)	EPS (P + C) (mg/L)	P/C
1	26.2	6.7	32.8	3.9
2	32.5	6.3	38.9	5.1
3	45.4	8.2	53.6	5.6
4	49.6	8.1	57.7	6.1
5	35.3	5.5	40.8	6.4
6	28.2	5.7	33.9	5.0
7	44.2	6.3	50.4	7.0
8	29.5	7.9	37.4	3.7
Average	**36.4**	**6.8**	**43.2**	**5.4**
Standard deviation	**8.9**	**1.1**	**9.4**	**1.2**

Table C-25: Soluble EPS released from biomass under low DO concentration and substrate

Simulation	MBR_0			MBR_{150}			MBR_{300}			MBR_{450}		
(Day)	P (mg/L)	C (mg/L)	EPS (mg/L)	P (mg/L)	C (mg/L)	EPS (mg/L)	P (mg/L)	C (mg/L)	EPS (mg/L)	P (mg/L)	C (mg/L)	EPS (mg/L)
0	2.6	9.9	12.5	2.0	7.9	9.9	3.5	12.2	15.6	3.3	11.5	14.8
1	13.5	3.9	17.4	9.9	2.9	12.8	4.3	21.1	25.4	6.3	34.8	41.1
2	19.7	5.0	24.7	14.4	6.1	20.4	10.6	4.8	15.4	18.4	7.5	25.9
3	36.4	11.2	47.6	41.3	12.5	53.8	22.0	8.1	30.1	42.4	11.7	54.1
4	45.6	14.6	60.2	49.2	13.3	62.5	15.4	8.3	23.7	36.0	14.8	50.8

Table C-26: Soluble COD released from biomass under low DO concentration and substrate

Simulation	MBR_0	MBR_{150}	MBR_{300}	MBR_{450}
(Day)	COD (mg/L)	COD (mg/L)	COD (mg/L)	COD (mg/L)
0	50.4	20.1	56.4	44.3
1	90.7	66.5	48.4	68.5
2	128.9	98.7	66.5	104.8
3	229.7	257.9	126.9	211.6
4	276.0	344.5	84.6	195.4

Table C-27: Specific oxygen uptake rate (SOUR) in MBR_0

Experiment No.	OUR (mg/L/h)	MLVSS (g/L)	SOUR (mg/g/h)
1	305.48	8.72	35.03
2	230.40	8.22	28.03
3	212.07	7.74	27.40
4	186.55	6.28	29.70
5	132.22	5.12	25.82
6	167.89	6.20	27.08
Average	**205.77**	**7.05**	**28.84**
Standard deviation	**59.67**	**1.39**	**3.29**

Table C-28: Specific oxygen uptake rate (SOUR) in MBR_{150}

Experiment No.	OUR (mg/L/h)	MLVSS (g/L)	SOUR (mg/g/h)
1	186.86	7.60	24.59
2	172.20	6.50	26.49
3	134.11	5.58	24.03
4	88.06	7.12	12.37
5	94.47	7.68	12.30
6	87.82	5.48	16.03
Average	**127.25**	**6.66**	**19.30**
Standard deviation	**44.24**	**0.97**	**6.48**

Table C-29: Specific oxygen uptake rate (SOUR) in MBR_{300}

Experiment No.	OUR (mg/L/h)	MLVSS (g/L)	SOUR (mg/g/h)
1	111.01	7.54	14.72
2	87.86	7.40	11.87
3	84.10	6.48	12.98
4	119.71	5.28	22.67
5	98.34	5.74	17.13
6	82.49	5.10	16.18
Average	**97.25**	**6.26**	**15.93**
Standard deviation	**15.32**	**1.05**	**3.84**

Table C-30: Specific oxygen uptake rate (SOUR) in MBR_{450}

Experiment No.	OUR (mg/L/h)	MLVSS (g/L)	SOUR (mg/g/h)
1	82.01	4.40	18.64
2	76.87	3.74	20.55
3	70.73	3.66	19.33
4	95.66	4.32	22.14
5	59.62	2.90	20.56
6	86.97	4.06	21.42
Average	**78.64**	**3.85**	**20.44**
Standard deviation	**12.63**	**0.55**	**1.29**

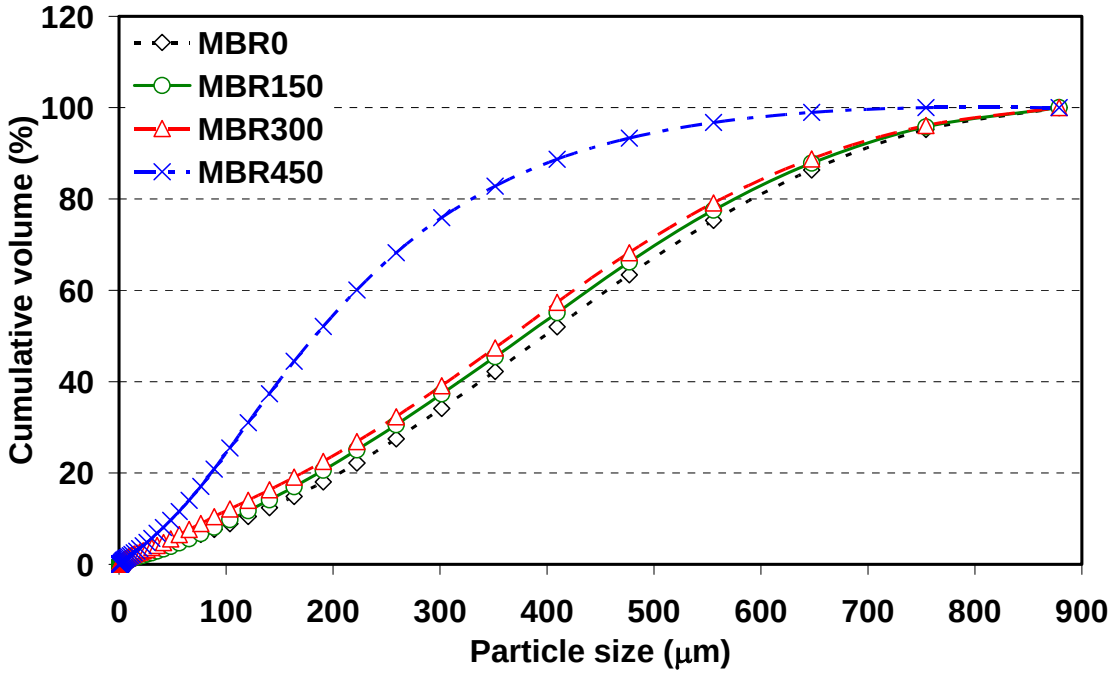

Figure C-3: Cumulative volume of bio-particle sizes in sludge suspension of the MBRs

APPENDIX-D

Hybrid MBRs daily dosage of flocculent/adsorbent

The following table illustrates the initial and daily dosage condition for the three hybrid MBRs:

Table D-1: Initial and daily dosage of flocculent/adsorbent agents to hybrid MBRs

Reactors	$MBR_{Control}$	MBR_{Clay}	$MBR_{Polymer}$	MBR_{PAC}
Condition	Conventional MBR	Clay (1 g/L)	Polymer (0.1 g/L)	PAC (1 g/L)
Dosage*	None	25 mg/L	3 mg/L	25 mg/L

* MBRs were dosed daily based on 40 d SRT

$MBR_{Control}$ serves as conventional MBR which is operated without flocculent/adsorbent addition and compared to the hybrid MBRs.

Calculation:

Clay and PAC dosage:

Initial Clay/PAC concentration = 1 g/L

Total Clay/PAC dosage for 10 L working volume = 10 g

Daily dosage = Initial dosage/SRT = 10,000 mg/40 d = 250 mg

Daily dosage = 25 mg/L

Stock solution:

12.5 g of Clay/PAC was diluted in 500 mL DI water
$\Rightarrow$ 1 mL = 25 mg
$\Rightarrow$ 10 mL = 250 mg

Daily addition of Clay/PAC = 25 mg/L (10 mL of stock solution)

MPE50 dosage

Recommended daily dosage from MPE50 supplier:

1. Initial dosage was recommended to be 100 mg/L for 3000 mg/L of MLSS
2. Daily dosage was recommended to be 6% of initial dosage for 20 d SRT
3. Daily dosage = Initial dosage x (1/SRT + 0.01)

Initial dosage based on Jar test results = 100 mg/L for approximately 6000 mg/L of MLSS

1. Daily dosage (without considering polymer degradation) = Initial dosage/SRT $\Rightarrow$ 100 (mg/L)/40 d = 2.5 mg/L

2. Daily dosage (considering polymer degradation) = 100 mg/L (1/40 d + 0.01) = 3.5 mg/L

3. 6% of initial dosage for 20 d SRT $\Rightarrow$ 3% of initial dosage for 40 d SRT $\Rightarrow$ 3/100 x 100 mg/L = 3 mg/L

Based on the above three calculations for daily dosage, 3 mg/L was chosen based on considering SRT and 0.5% daily degradation of the initial concentration

Daily polymer dosage for 10 L working volume = 30 mg

Stock solution:

5 g (4.8 mL) of polymer (MPE50) was dissolved in 500 mL of DI water
$\Rightarrow$ 1 mL = 10 mg
$\Rightarrow$ 3 mL = 30 mg

Daily addition of polymer (MPE50) = 30 mg (3 mL of stock solution)

Appendix-E

Phase II experimental results: Hybrid MBRs

Table E-1: Trans-membrane pressure (TMP), permeate flux versus filtration duration in the hybrid MBRs

Time (h)	$MBR_{Control}$		Time (h)	MBR_{Clay}		Time (h)	$MBR_{Polymer}$		Time (h)	MBR_{PAC}	
	TMP (kPa)	Flux ($L/m^2.h$)		TMP (kPa)	Flux ($L/m^2.h$)		TMP (kPa)	Flux ($L/m^2.h$)		TMP (kPa)	Flux ($L/m^2.h$)
0	3.2	4.0	0	3.2		0	3.4	4.0	0	3.8	3.6
2	3.1		11	3.5	3.8	11	3.2		11	3.8	3.6
10	3.3	4.1	23	3.8		24	3.1	4.0	24	3.9	3.6
19	3.5		35	3.7	3.8	35	3.1		36	4.0	3.6
25	3.6	4.1	47	4.8		48	3.5	4.0	48	4.2	3.6
36	4.0	4.1	59	4.3	3.7	59	3.4		61	4.3	3.6
47	4.2	4.1	61	4.1		70	3.4	3.9	72	4.5	3.6
59	5.0	4.1	71	4.6		71	3.4		85	4.7	3.6
63	5.1		83	5.3	3.7	83	3.6	3.9	96	4.8	3.6
71	5.8	4.1	96	11.0		96	3.6		107	5.0	3.6
73	6.1		109	20.0		106	3.9	3.9	120	5.4	3.6
83	7.5	4.0	119	63.0	2.3	120	4.4		131	6.0	3.6
90	8.3					121	4.5	3.9	144	6.6	3.6
95	9.2					132	7.3		155	8.5	3.6
107	11.9	4.0				144	18.3		168	7.9	3.6
115	14.1					155	51.3	2.8	180	9.7	3.4
119	16.0								193	12.3	3.4
131	23.8	3.9							204	14.4	3.4
137	31.5	3.4							217	20.6	
									228	38.6	3.0

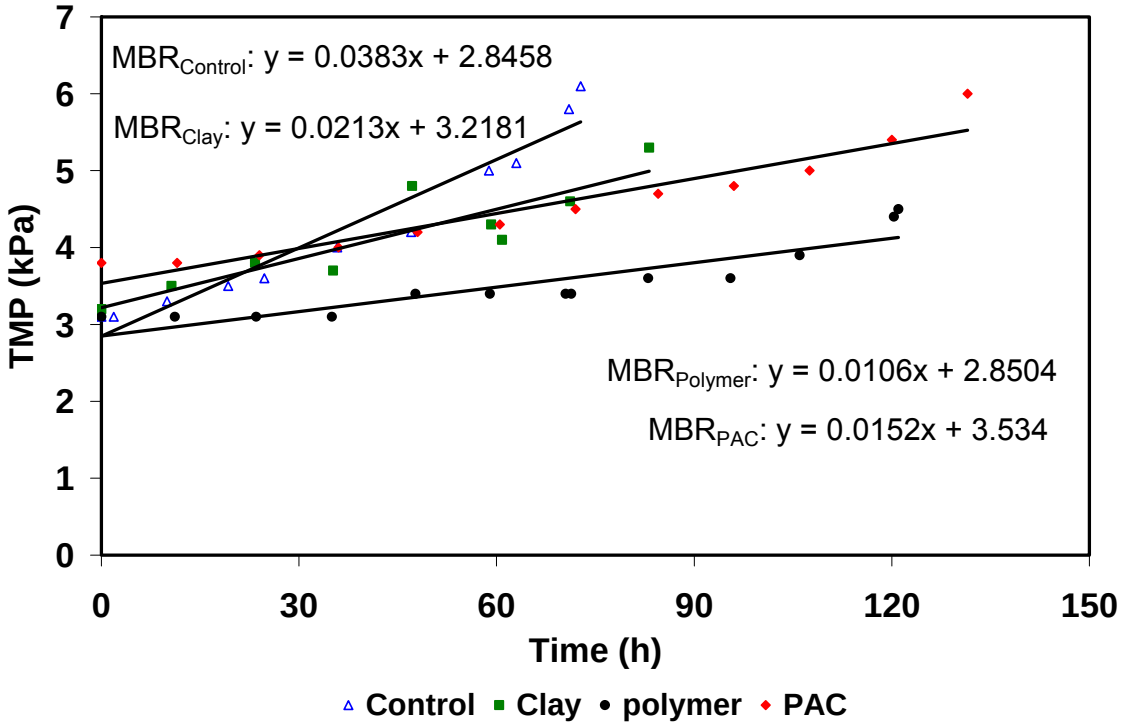

Figure E-1: First stage fouling rates in the hybrid MBRs

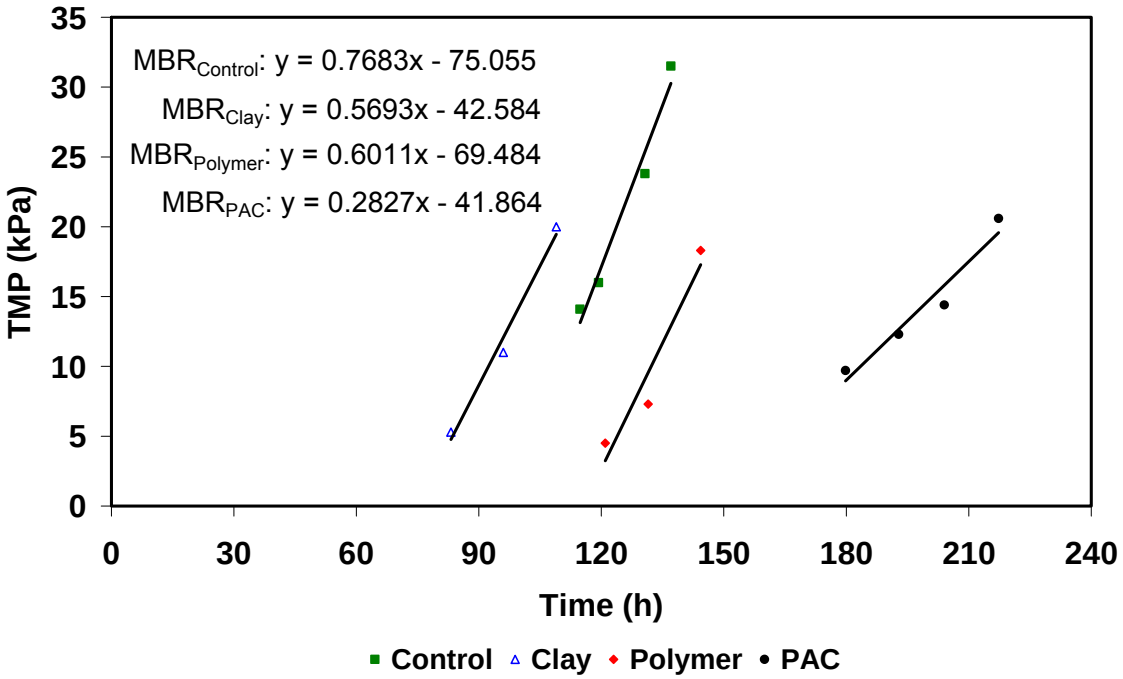

Figure E-2: Second stage fouling rates in the hybrid MBRs

Table E-2: Fouling rates in the hybrid MBRs

Fouling rate (kPa/h)	$MBR_{Control}$	MBR_{Clay}	$MBR_{Polymer}$	MBR_{PAC}
First stage	0.038	0.021	0.011	0.015
Second stage	0.768	0.569	0.601	0.283

Table E-3: MLSS, MLVSS concentrations and MLVSS/MLSS ratio in the hybrid MBRs

Operation	MBR_{Clay}			$MBR_{Polymer}$			MBR_{PAC}		
(Day)	MLSS (mg/L)	MLVSS (mg/L)	MLVSS/ MLSS	MLSS (mg/L)	MLVSS (mg/L)	MLVSS/ MLSS	MLSS (mg/L)	MLVSS (mg/L)	MLVSS/ MLSS
0	6380	5460	86	5920	5310	90	5170	4600	89
1	6740	5770	86	6310	5680	90	5310	4750	89
2	6920	5930	86	6510	5850	90	6900	6130	89
3	6830	5950	87	6720	6180	92	6240	5700	91
4	7270	6240	86	7180	6530	91	6560	5940	91
7	6730	5780	86	7840	7050	90	7140	6450	90
8	7170	6220	87	8170	7430	91	7450	6810	91
9	7200	6180	86	8210	7390	90	8210	7490	91
11	7400	6430	87	8140	7350	90	7370	6650	90
14	7760	6630	85	8440	7580	90	8450	7650	91
15	7000	6040	86	8010	7280	91	7930	7180	91
16	7300	6330	87	8590	7840	91	8830	7970	90
17	7260	6250	86	8290	7510	91	8590	7760	90
18	7420	6360	86	9130	8220	90	9210	8180	89
21	7460	6530	88	9580	8680	91	9340	8470	91
22	7220	6320	88	8680	7910	91	8660		
23	7150	6280	88	9270	8560	92	8640	7920	92
24	6920	6030	87	8780	7990	91	8690	7850	90
25	7280	6320	87	9620			8750	7920	91
28	7290	6370	87	9650	8800	91	8810	8040	91
29	6310	5610	89	8110	7470	92	8320	7710	93
30	6140	5370	87	8260	7460	90	8670	7810	90
31	6930	6040	87	8920	8070	90	8490	7660	90
32	6600	5700	86	8690	7820	90	8640	7790	90
36	7870	6870	87	9170	8330	91	9390	8560	91
37	6420	5580	87	9840	8840	90	8710	7870	90

Operation (Day)	MBR_{Clay}			$MBR_{Polymer}$			MBR_{PAC}		
	MLSS (mg/L)	MLVSS (mg/L)	MLVSS/ MLSS	MLSS (mg/L)	MLVSS (mg/L)	MLVSS/ MLSS	MLSS (mg/L)	MLVSS (mg/L)	MLVSS/ MLSS
39	7350	6430	87	9020	8110	90	8400	7540	90
42	6630	5870	89	8490	7630	90	8450	7630	90
50	7270	6430	88	8790	7910	90	8820	7980	90
53	7710	6910	90	9490	8600	91	9520	8680	91
56	8440	7510	89	9550	8600	90	9000	8190	91
63	8670	7730	89	9620	8720	91	9720	8870	91
65	8970	7980	89	8880	8000	90	9850	8950	91
70	8410	7570	90	9220	8360	91	9590	8740	91
75	8200	7350	90	9340	8540	91	9060	8370	92
77	8180	7190	88	9280	8350	90	9330	8470	91
78	8700	7720	89	9970	9030	91	9770	8890	91
79	9140	8180	89	9550	8720	91	10410	9560	92
81	9190	8180	89	9800	8910	91	9910	9040	91
Average	**7412**	**6487**	**87**	**8647**	**7809**	**91**	**8473**	**7681**	**91**
Standard deviation	**795**	**765**	**1**	**997**	**911**	**1**	**1176**	**1107**	**1**

Table E-4: Membrane fouling resistances in MBR_{Clay}

Experiment No.	Total resistance (R_t) ($\times 10^{12}$ m^{-1})	Cake resistance (R_c) ($\times 10^{12}$ m^{-1})	Fouling resistance (R_f) ($\times 10^{12}$ m^{-1})	Intrinsic membrane resistance (R_m) ($\times 10^{12}$ m^{-1})	R_c/R_t (%)
1	71.30	69.33	1.57	0.40	97.2
2	65.56	64.22	0.79	0.55	98.0
3	65.04	62.46	2.05	0.53	96.0
Average	**67.30**	**65.34**	**1.47**	**0.49**	**97.1**

Table E-5: Membrane fouling resistances in $MBR_{Polymer}$

Experiment No.	Total resistance (R_t) ($\times 10^{12}$ m^{-1})	Cake resistance (R_c) ($\times 10^{12}$ m^{-1})	Fouling resistance (R_f) ($\times 10^{12}$ m^{-1})	Intrinsic membrane resistance (R_m) ($\times 10^{12}$ m^{-1})	R_c/R_t (%)
1	62.56	61.22	1.03	0.32	97.9
2	64.17	63.11	0.66	0.40	98.4
3	91.15	88.56	2.30	0.28	97.2
Average	**72.63**	**70.97**	**1.33**	**0.33**	**97.8**

Table E-6: Membrane fouling resistances in MBR_{PAC}

Experiment No.	Total resistance (R_t) ($\times 10^{12}$ m^{-1})	Cake resistance (R_c) ($\times 10^{12}$ m^{-1})	Fouling resistance (R_f) ($\times 10^{12}$ m^{-1})	Intrinsic membrane resistance (R_m) ($\times 10^{12}$ m^{-1})	R_c/R_t (%)
1	57.95	55.31	2.37	0.28	95.4
2	68.47	65.84	2.17	0.46	96.2
3	73.72	70.68	2.65	0.39	95.8
Average	**66.71**	**63.94**	**2.40**	**0.37**	**95.8**

Table E-7: Normalized capillary suction time (CST_N) in MBR_{Clay}

Experiment No.	CST (s)	MLSS (g/L)	CST_N [s/(g/L)]
1	14.9	7.3	2.0
2	13.3	7.3	1.8
3	26.7	8.4	3.2
4	23.0	9.0	2.6
5	25.0	8.2	3.1
6	25.1	9.1	2.7
Average	**21.3**	**8.2**	**2.6**
Standard deviation	**5.7**	**0.8**	**0.5**

Table E-8: Normalized capillary suction time (CST_N) in $MBR_{Polymer}$

Experiment No.	CST (s)	MLSS (g/L)	CST_N [s/(g/L)]
1	14.8	9.6	1.5
2	15.8	8.8	1.8
3	20.9	9.6	2.2
4	15.6	8.9	1.8
5	19.5	9.3	2.1
6	19.7	9.6	2.1
Average	**17.7**	**9.3**	**1.9**
Standard deviation	**2.6**	**0.4**	**0.3**

Table E-9: Normalized capillary suction time (CST_N) in MBR_{PAC}

Experiment No.	CST (s)	MLSS (g/L)	CST_N [s/(g/L)]
1	14.4	8.8	1.6
2	16.5	8.8	1.9
3	21.0	9.0	2.3
4	26.1	9.9	2.6
5	28.8	9.3	3.1
6	26.9	10.4	2.6
Average	**22.3**	**9.4**	**2.4**
Standard deviation	**5.9**	**0.6**	**0.5**

Table E-10: Specific cake resistance (α) in MBR_{Clay}

Experiment No.	(t/V)/V ($\times 10^{10}$ s/m^6)	MLSS (kg/m^3)	α ($\times 10^{12}$ m/kg)
1	1.32	6.63	2.08
2	2.82	7.27	4.06
3	4.65	8.44	5.76
4	5.18	8.97	6.04
5	4.78	8.18	6.11
6	5.70	9.14	6.52
Average	**4.08**	**8.11**	**5.10**
Standard deviation	**1.66**	**0.98**	**1.71**

Table E-11: Specific cake resistance (α) in $MBR_{Polymer}$

Experiment No.	(t/V)/V ($\times 10^{10}$ s/m^6)	MLSS (kg/m^3)	α ($\times 10^{12}$ m/kg)
1	2.54	8.49	3.13
2	2.38	8.79	2.83
3	10.51	9.55	11.51
4	13.33	8.88	15.71
5	6.23	9.28	7.02
6	4.15	9.55	4.55
Average	**6.52**	**9.09**	**7.46**
Standard deviation	**4.49**	**0.44**	**5.16**

Table E-12: Specific cake resistance (α) in MBR_{PAC}

Experiment No.	(t/V)/V ($\times 10^{10}$ s/m^6)	MLSS (kg/m^3)	α ($\times 10^{12}$ m/kg)
1	1.59	8.45	1.97
2	2.41	8.82	2.86
3	3.12	9.00	3.63
4	8.71	9.85	9.25
5	11.06	9.33	12.40
6	11.73	10.41	10.60
Average	**6.44**	**9.31**	**6.79**
Standard deviation	**4.59**	**0.72**	**4.49**

Table E-13: Soluble EPS in MBR_{Clay}

Experiment No.	Protein (P) (mg/L)	Carbohydrate (C) (mg/L)	EPS (P + C) (mg/L)	P/C
1	1.4	4.5	5.9	0.3
2	4.5	4.3	8.8	1.0
3	2.2	3.0	5.1	0.7
4	0.3	0.9	1.2	0.3
5	3.9	1.5	5.4	2.6
Average	**2.5**	**2.8**	**5.3**	**1.0**
Standard deviation	**1.7**	**1.6**	**2.7**	**1.0**

Table E-14: Soluble EPS in $MBR_{Polymer}$

Experiment No.	Protein (P) (mg/L)	Carbohydrate (C) (mg/L)	EPS (P + C) (mg/L)	P/C
1	1.4	4.4	5.9	0.3
2	5.3	3.0	8.3	1.8
3	4.8	8.9	13.6	0.5
4	3.9	3.8	7.7	1.0
5	0.3	1.3	1.5	0.2
Average	**3.1**	**4.3**	**7.4**	**0.8**
Standard deviation	**2.2**	**2.8**	**4.4**	**0.6**

Table E-15: Soluble EPS in MBR_{PAC}

Experiment No.	Protein (P) (mg/L)	Carbohydrate (C) (mg/L)	EPS (P + C) (mg/L)	P/C
1	3.6	5.7	9.3	0.6
2	6.6	2.5	9.1	2.7
3	2.6	1.0	3.6	2.5
4	2.0	5.3	7.3	0.4
5	4.6	1.3	5.9	3.7
Average	**3.9**	**3.2**	**7.0**	**2.0**
Standard deviation	**1.8**	**2.2**	**2.4**	**1.4**

Table E-16: Bound EPS in MBR_{Clay}

Experiment No.	Protein (P) (mg/L)	Carbohydrate (C) (mg/L)	EPS (P + C) (mg/L)	P/C
1	44.2	13.9	58.1	3.2
2	58.6	16.4	75.0	3.6
3	53.9	16.3	70.2	3.3
4	27.9	8.0	35.9	3.5
5	30.4	7.9	38.4	3.8
6	20.7	5.4	26.1	3.8
7	20.3	5.5	25.9	3.7
Average	**36.6**	**10.5**	**47.1**	**3.6**
Standard deviation	**15.6**	**4.9**	**20.5**	**0.3**

Table E-17: Bound EPS in $MBR_{Polymer}$

Experiment No.	Protein (P) (mg/L)	Carbohydrate (C) (mg/L)	EPS (P + C) (mg/L)	P/C
1	34.8	15.0	49.8	2.3
2	48.4	11.7	60.1	4.1
3	44.5	10.5	55.0	4.2
4	22.5	6.9	29.4	3.2
5	23.9	5.7	29.6	4.2
6	22.1	6.0	28.1	3.7
7	25.3	5.9	31.2	4.3
Average	**31.6**	**8.8**	**40.5**	**3.7**
Standard deviation	**11.0**	**3.6**	**13.9**	**0.7**

Table E-18: Bound EPS in MBR_{PAC}

Experiment No.	Protein (P) (mg/L)	Carbohydrate (C) (mg/L)	EPS (P + C) (mg/L)	P/C
1	45.7	12.8	58.5	3.6
2	66.8	15.0	81.8	4.5
3	53.1	10.0	63.1	5.3
4	29.2	7.0	36.2	4.2
5	30.7	7.2	37.9	4.3
6	14.8	4.1	18.9	3.6
7	21.9	4.8	26.7	4.6
Average	**37.5**	**8.7**	**46.2**	**4.3**
Standard deviation	**18.5**	**4.1**	**22.3**	**0.6**

Table E-19: Specific oxygen uptake rate (SOUR) in MBR_{Clay}

Experiment No.	OUR (mg/L/h)	MLVSS (g/L)	SOUR (mg/g/h)
1	259.81	7.57	34.32
2	249.94	7.19	34.76
3	224.10	7.72	29.03
Average	**244.62**	**7.49**	**32.70**
Standard deviation	**18.44**	**0.27**	**3.19**

Table E-20: Specific oxygen uptake rate (SOUR) in $MBR_{Polymer}$

Experiment No.	OUR (mg/L/h)	MLVSS (g/L)	SOUR (mg/g/h)
1	256.39	8.36	30.67
2	262.49	8.35	31.44
3	346.79	9.03	38.40
Average	**288.56**	**8.58**	**33.50**
Standard deviation	**50.52**	**0.39**	**4.26**

Table E-21: Specific oxygen uptake rate (SOUR) in MBR_{PAC}

Experiment No.	OUR (mg/L/h)	MLVSS (g/L)	SOUR (mg/g/h)
1	232.56	8.74	23.48
2	280.80	8.47	22.33
3	260.64	8.89	24.86
Average	**258.00**	**8.70**	**23.55**
Standard deviation	**24.23**	**0.21**	**1.27**

Appendix-F

Additional quantitative relationships from Phase I study

Relationships between the sludge properties and the shear intensities (G) in the MBRs from Phase I were established as presented in Table F-1.

Table F-1: Influence of shear intensities (G) on sludge properties

MBR	Shear intensity (G) (1/s)	Median bio-particle size (μm)	Bio-activity (SOUR) (mg/g)/h	SCOD (mg/L)	Soluble EPS (mg/L)	Bound EPS (mg/g-VSS)
MBR0	83	398	29	31	12	29
MBR_{150}		379	19	44	12	33
MBR_{300}	249	367	16	48	12	37
MBR_{450}	439	183	20	49	11	43

The average soluble EPS concentrations were found to be similar in the four MBRs as reported in Table F-1. These results indicate that the variation in shear intensity (G) among the four MBRs had insignificant influence on the soluble EPS measured. However, the relationships between shear intensity and the other parameters were found to be significant as presented in Table F-1. Further understanding of the shear intensity (G) influence on the bio-particle size (μm) is shown in Figure F-1.

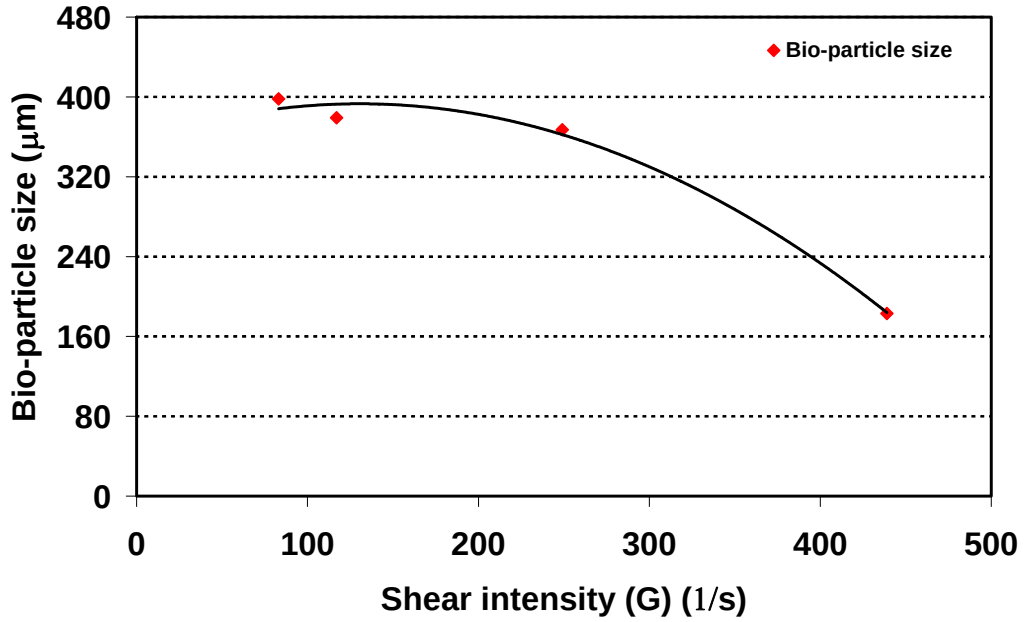

Figure F-1: Relationship between shear intensity (G) and bio-particle size

It shows that the average bio-particle size slightly decreased from MBR_0 to MBR_{300} with increase in shear intensity (G) up to the certain limit of 249 (1/s) beyond which there was significant floc breakage and the average floc size reduced to almost half in MBR_{450} (439 1/s) as compared to that in the MBR_{300}. The results suggest that the bio-flocs are able to withstand shear stress up to a certain level beyond which the flocs significantly disintegrate

resulting in smaller bio-particles as discussed in section 4.1.5 Particle and colloidal size distribution.

The influence of the bio-particle sizes induced by the shear intensities in the MBRs on the SMP (SCOD) and EPS (bound) concentrations are shown in Figure F-2.

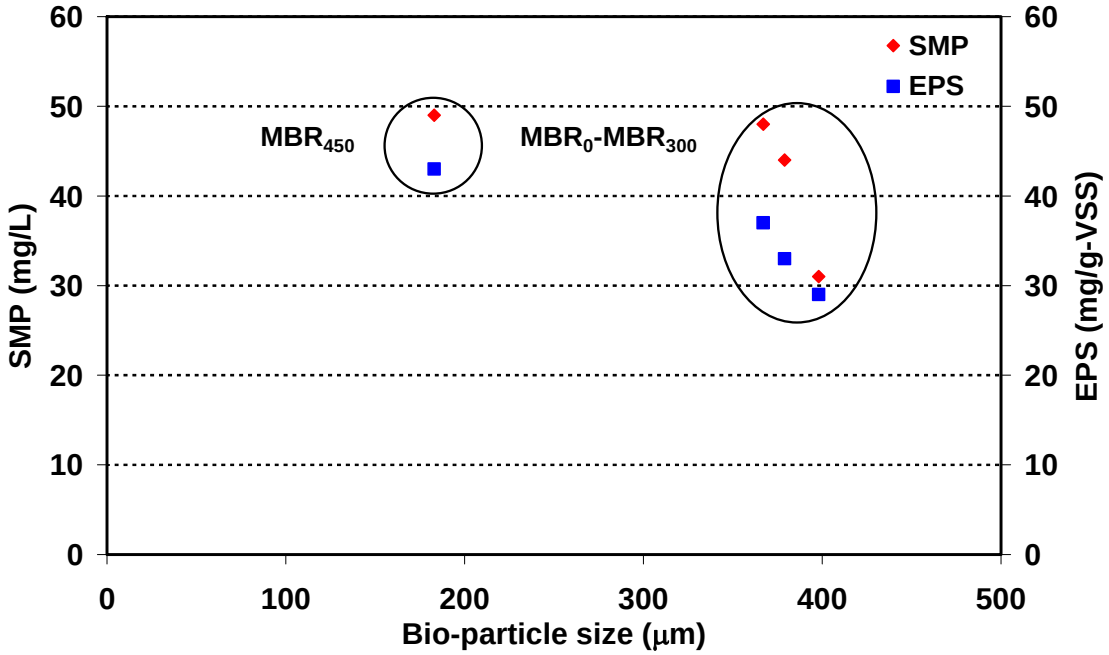

Figure F-2: Influence of bio-particle size on SMP and EPS

According to Figure F-2, the MBR_{450} demonstrated significant variation and trend in terms of SMP and EPS as compared to that in MBR_0-MBR_{300} which can be attributed to the significant reduction in particle size. In order to establish precise linkage between particle size and biopolymer generation before significant breakage of the bio-flocs, data from MBR_0-MBR_{300} was considered only in Figure F-3.

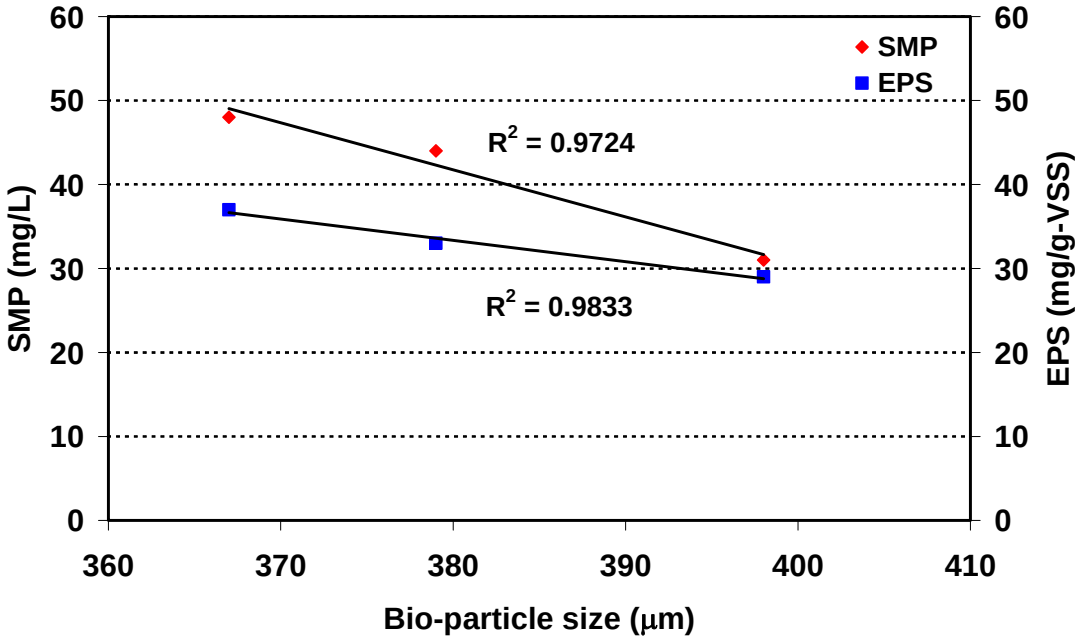

Figure F-3: Influence of bio-particle size on SMP and EPS before bloc breakage

It shows that the SMP and EPS generation increased with relative decrease in particle size which could be due to the excretion of EPS from the relative breakage of bio-flocs under higher shear stress conditions. Both the curves in Figure F-3 exhibit strong linear relationship between particle size and biopolymer concentrations inferring the dependence of bioactivity on the structure of bio-flocs. However, the EPS generation within the bottom layers of biofilm in MBR_0 and MBR_{150} were observed to be significantly higher as compared to that in the MBR_{300} and MBR_{450} which could be considered to offset the disadvantage observed in Figure F-3 and consequently resulting in improved filtration performances in MBR_{300} and MBR_{450} as compared to MBR_0 and MBR_{150}. Further details are discussed in section 4.1.8 Simulation of excreted bio-polymers from biofilm.

Furthermore, the influence of shear intensity (G) on the SOUR and the soluble COD concentrations among the four MBR was established as shown in Figure F-4.

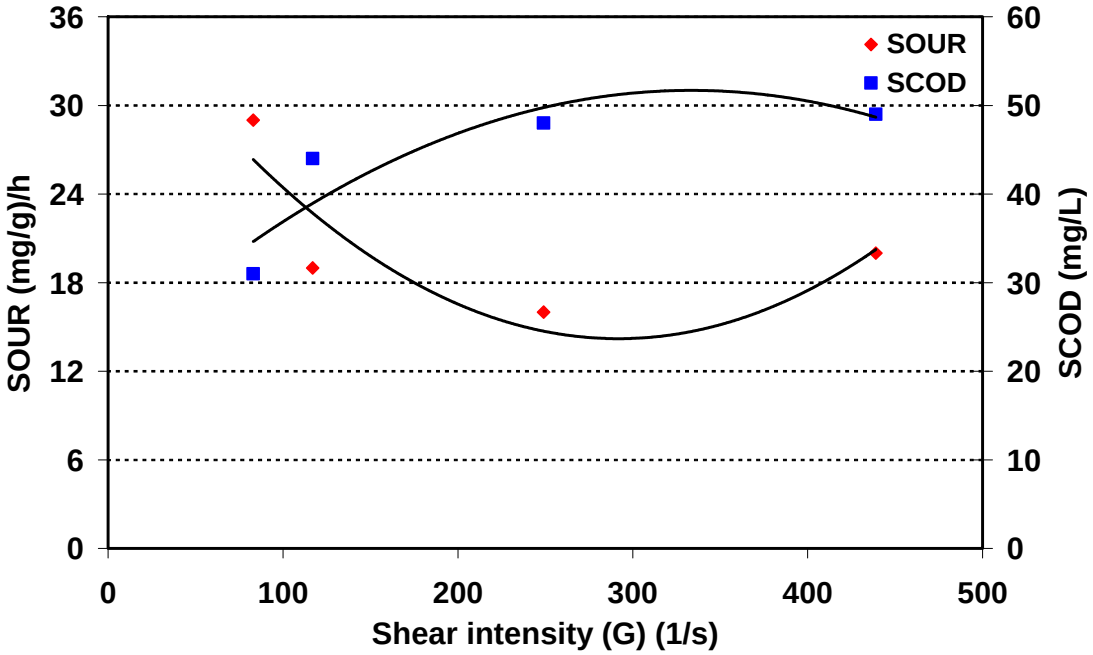

Figure F-4: Relationship between SCOD and SOUR in the MBRs

This relationship depicts that with a decrease in the microbial activity in terms of SOUR due to the increase in the shear intensity, the biodegradation efficiency of organic substrate (SCOD) or control of SMP generation consequently deteriorated. However, this relative increase in SCOD was always compensated by the physical separation by filtration mechanism in the MBRs with overall COD removal efficiency above 95%.

As shown in Figure F-3, the variation in bio-particle size could play an important role in the bioactivity and consequently the biopolymer concentrations within a MBR. In this context, the influence of particle size before floc rupture (MBR_{450} condition) on the SOUR and SCOD was established as shown in Figure F-5.

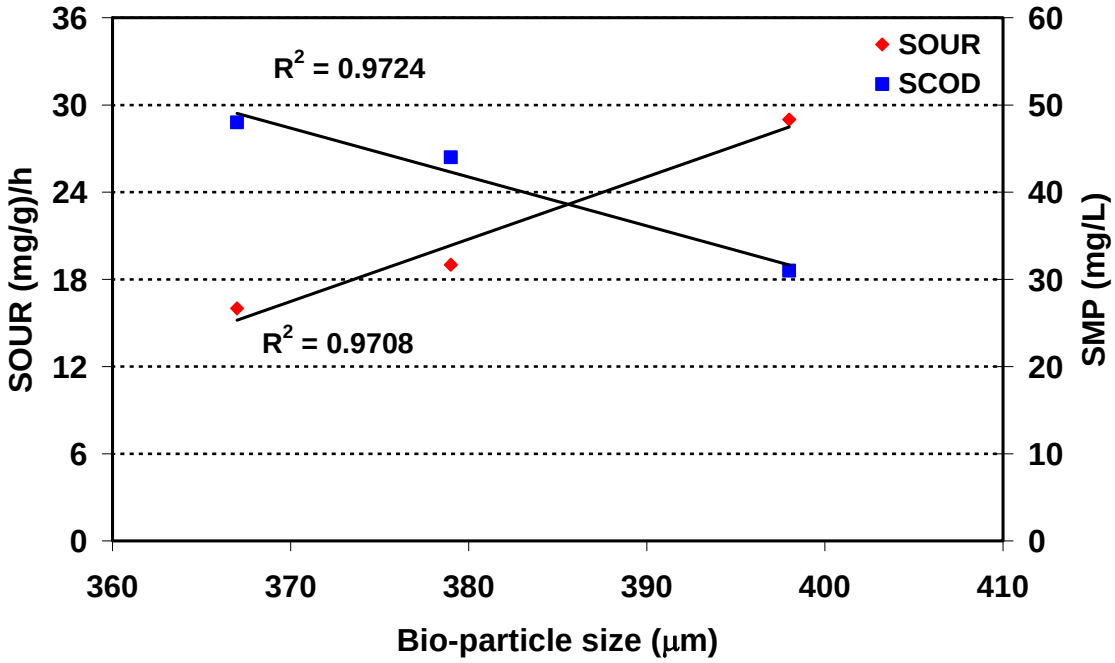

Figure F-5: Influence of bio-particle size on SOUR and SMP before bloc breakage

The SOUR of bio-flocs reduced with the decrease in floc size under increasing shear stress as shown in Figure F-5. The decrease in SOUR could have adversely influenced the biodegradation efficiency with increase in SMP concentration. However, the lower SOUR also resulted in reduced activity within the biofilm developed on the membrane fibers consequently generating lower EPS temporally which was found to be great importance in fouling control in a MBR.

These results suggest that slightly higher EPS or SMP concentration in the bulk solution can be excreted due to relative biofloc breakage or abrasion under higher shear stress conditions provided the threshold shear intensity condition is not exceeded. On the contrary, SMP which also constitutes the soluble organic matter from the influent can also be increased due to lower bioactivity and consequently lower biodegradation efficiency. However, in context of MBR the slight increase in the biopolymer concentration in the bulk solution may not influence the MBR permeate due to its physical retention by membrane filtration mechanism.

The present study revealed that the EPS generation with the thickening of biofilm on the membrane surface was found to be the major cause of severe membrane fouling after certain filtration period. Moreover, it was found that the control of EPS excretion in the thickened biofilm by delaying the cell death rate due to low bioactivity could be an effective fouling mitigation approach.